Analyzing the Effect of Optimizing the Spatial Locations of Green Infrastructure on Land Surface Temperature: The Case of Dire Dawa City

Amanuel Atnafu Jifar

A Thesis Submitted to

The Department of Geomatics Engineering

School of Civil Engineering and Architecture

Presented in Partial Fulfillment of the Requirements for the Degree of Master's in Geo-informatics Engineering

Office of Graduate Studies

Adama Science and Technology University

Adama, Ethiopia

October, 2020

Analyzing the Effect of Optimizing the Spatial Locations of Green Infrastructure on Land Surface Temperature: The Case of Dire Dawa City

Amanuel Atnafu Jifar

Advisor: Daniel Alemayehu (PhD, Asst. Prof.)

Co-Advisor: Tilahun Erduno (PhD, Ir.)

A Thesis Submitted to

The Department of Geomatics Engineering

School of Civil Engineering and Architecture

Presented in Partial Fulfillment of the Requirements for the Degree of Master's in Geo-informatics Engineering

Office of Graduate Studies

Adama Science and Technology University

Adama, Ethiopia

October, 2020

BOARD OF EXAMINERS APPROVAL

We, the undersigned, members of the Board of Examiners of the final open defense by Amanuel Atnafu Jifar have read and evaluated his thesis entitled “Analyzing the Effect of Optimizing the Spatial Locations of Green Infrastructure on Land Surface Temperature: The Case of Dire Dawa City” and examined the candidate. This is, therefore, to certify that the thesis has been accepted in partial fulfillment of the requirement of the Degree of Master’s in Geo-informatics Engineering.

Daniel Alemayehu (PhD, Asst. Prof.) Advisor	Signature	Date
Tilahun Erduno (PhD, Ir.) Co-Advisor	Signature	Date
External Examiner	Signature	Date
Internal Examiner	Signature	Date
Chairperson	Signature	Date
Department Chair	Signature	Date
School Dean	Signature	Date
Post –graduate Dean	Signature	Date

CANDIDATES DECLARATION

I, Amanuel Atnafu Jifar declared that, this MSc Thesis is my original work and that it has not been submitted partially; or in full, by any other person for an award of a degree in any other universities, and all sources of material used for this thesis have been duly acknowledged.

Amanuel Atnafu Jifar	________________	_______________
Name	Signature	Date

Date of submission: ________________

ADVISOR'S APPROVAL

To: Geomatics Engineering Department

Subject: Thesis Submission

This is to certify that the thesis entitled "Analyzing the Effect of Optimizing the Spatial Locations of Green Infrastructure on Land Surface Temperature: The Case of Dire Dawa City" submitted in partial fulfillment of the requirements for the degree of Master's Geo-informatics Engineering, the Graduate program of the department of Geomatics Engineering, and has been carried out by Amanuel Atnafu Jifar, ID. PGR/18063/11 was under our supervision. Therefore, we recommend that the student has fulfilled the requirements and hence he can submit the thesis to the department.

Daniel Alemayehu (PhD, Asst. Prof.) ______________

Name of major Advisor Signature Date

Tilahun Erduno (PhD, Ir.) ______________ ______________

Name of Co-Advisor Signature Date

ACKNOWLEGMENTS

I am so grateful to God, Who is always there for me to strengthen when I was weak, and to lead when I felt hopeless. Without his all rounded help I wouldn't have accomplished any of my achievements.

My acknowledgments also goes to my advisor Daniel Alemayehu (PhD, Asst. Prof.) and my co-advisor Tilahun Erduno (PhD, Ir.), for their useful, fruitful and cherished comments and guidance throughout this study. And also, for their technical and psychological supports from the beginning to the end of this study. I would also like to pass my gratitude to the different organizations and the managers, and different levels staffs of the organizations' that has been the sources of the data for the accomplishment of this study.

Finally, my dearest family and friends especially my lovely friend, Kuleni Asefa thanks all for your care, support and motivation.

TABLE OF CONTENTS

Contents **Page**

LIST OF TABLES

Table Number and Title **Page**

LIST OF FIGURES

Figure Number and Title **Page**

LIST OF ACRONYMS AND ABBREVIATIONS

BLHI	Boundary Layer Heat Island
BT	Brightness Temperature
CLHI	Canopy Layer Heat Island
FCC	False Color Composites
GI	Green Infrastructure
GPS	Global Positioning System
IDW	Inverse Distance Weighted
LCC	Low Carbon Cities
LST	Land Surface Temperature
LULC	Land Use Land Cover
MLST	Mean Land Surface Temperature
NDVI	Normalized Difference Vegetation Index
OLI	Operational Land Imager`
SUHI	Surface Urban Heat Island
TIRS	Thermal Infrared Sensor
TM	Thematic Mapper
TOA	Top of Atmosphere
UHI	Urban Heat Island
USGS	United States Geological Survey

ABSTRACT

The urban heat island (UHI) refers to the phenomenon of higher atmospheric and surface temperatures occurring in urban areas than in the surrounding rural areas. Green infrastructure (GI) can mitigates warming, providing cooling benefits important to reducing energy consumption and improving human health. Lack of proper identifications of the most critical area or temperature hotspot location and the arrangement of GI is one of the most important problems in Dire Dawa City Administration, especially considering the spatial location of urban heat island effects. Surprisingly, methods of identifying the hotspot location that support the strategic placement of green infrastructure in the context of identified urban heat island locations are lacking. In order to overcome these problems, the integrations of remote sensing and geographic information systems were developed as framework to identify the hotspot areas, examines the relationship between the urban GI and LST and finally proposing the optimal locations of new GI with respect to cooling benefits. To achieve the objective of the study, Land-use/land-cover, LST and NDVI were extracted from Landsat 5 TM (1999) and Landsat 8 OLI/TIRS (2019). The result of LU/LC change indicated for the last 20 years there has been a radical increase in areal coverage of settlements by more than 6% and on the other side, sparse vegetation was decreased by more than 4%. The study indicated that most areas having lower LST in 1999 were changed to higher LST in 2019. The results show that average LST in Dire Dawa City was increased from 24.61°C to 28.77°C. This due to the increased in settlements LU/LC, especially attributed to the decreasing of vegetation cover in the study area. This shows that, the correlation between LST and NDVI for both study years (1999 and 2019) have strong negative correlation with the R^2 values of 0.88 and 0.94, respectively. The study also found that, more than 13% of LU/LC was identified as hotspot location with mean LST more than 33°C. As a result of optimal GI placement, significant cooling benefits can be achieved. The results showed that, the distance from the park was positively correlated with the LST. The mean LST increased by 0.53°C, as the distance increases by 500m from the park. Also, this study found that, increasing the GI rate on this hotspot area by 13%, the mean LST drops approximately by 0.79°C, from the local hotspots area and 1.55 –1.64°C regionally, this can be achieved by the addition of new GI. The study conclude that, optimizing the spatial locations of GI in the proximity of most heat load or hotspot areas such as built-up areas and bare lands should receive primary attention in the process of planning and designing. The optimization based framework can effectively inform planning decisions with regard to GI allocation to improve excessive heat. This study showed that geospatial tools and techniques can give fast and reliable results of LST variability and its impact on the environment in a shorter analysis and evaluation.

Keywords: LST; NDVI; GI

CHAPTER 1. INTRODUCTION

1.1. Background of the study

Urban climate change and rapid urbanization are two challenges and fundamental considerations in 21st century urban planning (Simonds J.O, 2007). According to the United Nation in 2018, over half of the world's population (55%) lives in urban areas, and this number is expected to increase to 68% by 2050 as a result of rapid urbanization (Chaobin,2017 & UN., 2018). As result, more people will suffer from urban heat island (UHI) effects, which are caused by dramatic changes in land use and land cover, energy use and natural ecosystems increasingly being replaced by impervious surfaces. Therefore, urban heat island is an event resulting from rapid urbanization (Amani-Beni; Zhang, 2018) which is described as urban areas with significantly warmer temperatures than its surrounding rural areas.

One of the notorious effects of urbanization is UHI, which can be defined as an increase in the mean air and land surface temperature of built up areas compared to the nearby rural areas (Kanniah *et al.,* 2014). According to the study in Malaysia by Balling (1991), an increase in temperature is mainly the outcome of urbanization which leads to replacement of green infrastructures with impervious surfaces (i.e. buildings, roads and etc.)

As the number of population increases, urban land cover will be changed and architecture coupled with intensifying human activities will led to a modified thermal climate, forming UHI (Yujia *et al*., 2018). This effect has significant implications for sustainability, with consequences for energy and water consumption, emissions of air pollutants and greenhouse gases and the emergence of regional heat islands (Arnfield, 2003).

Dire Dawa City has critical functions as a center of community activities. This is closely related to the characteristics of urban areas as a center of government and economic activities (DDCA, 2018). The economic activities of the City caused community movement from suburbs and villages. The number of population in Dire Dawa City was increasing from 188,000 in 1999 to 391,000 in 2019 (DDAS, 2019). Increasing population leads to increase settlements and other impervious surfaces which give rises to urban surface temperatures. During that period there was an increase in average annual temperature from 24.6°C in 1999 to 25.9°C in 2019 (NMA, 2019), so that the comfort zone of the City decreased. Increasing activity that concentrated in an urban or industrial area will form characteristic of a typical microclimate. This microclimate characteristic is one of the occurrences of urban heat island.

In Dire Dawa City, the effect of UHI has been increasing from time to time; due to minimum number of green infrastructures with respect to land use land cover compositions and the number of population in the City, resulting temperature increase (Matiwos, 2018). According to Ethiopian National Meteorological Agency (2019), for the last 20 years, the mean minimum temperature has been increasing by 0.4°C, the annual maximum temperature has been increasing by about 0.49°C and average annual temperature has been increasing by 0.6°C per decade, particularly during the cool months, throughout the City.

From available data, annual maximum temperatures, over the last 30 year, showed upward trend at the meteorological stations located in Dire Dawa City Administration. Summers in Dire Dawa are characterized by peaks in energy use and increased residential water consumption as well as the emergence of extreme hot environments. Lack of strategic placement of Green infrastructures (GI) and considering the role of GI during planning and designing period can enhance this problem (Muluneh *et al*., 2018). One of the strategies to make Cities a livable place and cool environment is the integration of the GI into the development and planning of new urban areas (Kanniah *et al*., 2014).

According to Alan *et al*. (2018), recognizing the potential to mitigate UHI, the City of Phoenix has launched a master plan that aims to increase the amount of green space. Consequently, an important question is where to site new green space in order to best realize potential cooling benefits. Improvements in measuring and modeling cooling benefits of green spaces are required, however, to make informed decisions. However, previous studies have mainly focused on the cooling effect of greeneries inside parks; few reports are available on the extension of the cooling effect in the surrounding area of green patches, and it has come out with different conclusions. For example, Hamada and Ohta (2010) suggested that, the cooling effect of the urban park is to extend for several hundred meters (Hamada and Ohta, 2010) ; however, according to Honjo *et al*., (1990), the cooling benefit of an urban park can be extended in the surrounding area with a distance similar to the length of the park . On the other side, air temperature based studies have found that green space can be 1°C to 3°C, and sometimes even 5°C to 7°C, cooler than surrounding built-up areas, with cooling impacts extending as much as several hundred meters beyond green space boundaries (Chow *et al*., 2011).

According to Maheng and Dikman (2019) study in Sri Lanka show that, increasing green space up to 30% in urban areas can decrease the average air temperature by 0.1-0.7^{0}C. On the other hand, converting entire green areas into urban areas in suburban areas increases the average temperature from 27.75°C to 29.78°C in Colombo. This demonstrates the sensitivity of UHI to vegetation cover in both urban and suburban areas. Study in the Manchester (Kanniah *et al*., 2014), found that increasing green cover by 10% in the built up areas could decrease maximum surface temperatures by 2.4°C to 2.5°C. This can be done via creating new green spaces, increasing street tree planting, and designing of green roofs and walls. Similar strategies can be adopted in Malaysia by increasing the tree cover in "hot spots" such as town and City centers, transport hubs, tourist destinations, to reduce urban heat load. According to Voogt *et al*. (2002), a 10% increase in vegetation cover (as a general rule) reduces the temperature by about 3°C.

Currently, different cities in the world have been focused on the development of green infrastructure, in order to reduce the environmental temperature. For example, the study by (Spronken *et al*. 2001; Ruddell, D. *et al*., 2010 and Klok *et al*., 2012), concluded that, to reducing vulnerability and exposure to present climate variability, identifications of hot spots spatial location and strategic placements of GI is the first step towards adaptation to future climate change. Strategies such as GI that include actions with co-benefits for other objectives can increase resilience across a range of possible future climates while helping to improve human health, social and economic wellbeing, and environmental quality.

Urban GI, such as open parks, forests, and grasslands, have been increasingly recognized as key components of urban planning (Santamouris,2001; Chaobin, 2017). They forms cool islands and improve outdoor thermal comfort throughout warm seasons, as well as significantly reduce environmental stress produced by heat island (Chang and Akpina,2014; Kun , 2017). They can also provide critical ecosystem services that could improve residents' health and wellbeing.

Currently, numerous studies have been conducted to deal with the spatial characteristics, changing trends and impact factors of UHI effect based on remote sensing data and Geographic Information Systems (GIS) technology (Fortuniak, 2009) and (Gandhi and Christy, 2015). Among the above, the relationships between LST and related indicators become a hot topic that attracts wide-ranging research because these related findings have great significance to formulate urban planning policies to relieve UHI effect. Traditionally, some important indicators such as NDVI and Fractional Vegetation Cover have been commonly applied to examine the spatial variations of LST (Liu,2011; and Hongbo, 2018).

Extensive research has explored relationships between SUHI and urban land cover, especially with regard to vegetation (Weng 2009; Huang, G. *et al.,* 2011; Feyisa, G *et al.*, 2014). Studies have suggested that land cover composition and configuration of the GI's are strong predictors of its cooling benefit (Doan *et al*., 2010).

Furthermore, land use land covers, distance and density of existing adjacent green space also have impacts on cooling (Chang *et al.,* 2015). Explicit linkages between cooling benefits and the locations of green infrastructures are missing, however, causing difficulties for location model construction. On the modeling side, micro-climate numerical models deal with surface energy balance, simulating thermodynamic processes for canopy layer UHI assessment (Connors, *et al*. 2011; and Yuan, 2013). Results from such models are rich in temporal scale but are limited in spatial extent, thus fail to capture intra-urban temperature variations.

Combining broader scale spatial data, multi-objective optimization models have been applied recently to determine green infrastructures locations in the City, balancing various kinds of environmental benefits. The study by (Neema and Ohiga, 2013) also developed a multi-objective empirical technique for optimizing the configuration of parks and open space with respect to air and water quality improvement as well as noise and temperature reduction. Zhang and Huang (2014) sought to minimize LST in the allocation of land uses within a multi-objective heuristic, where temperature is a regressed function of land use intensities. As yet, however, no current mathematical model has attempted to account for the agglomeration of cooling resulting from green infrastructures, which greatly affects their spatial allocation.

The above mentioned measuring and modeling gaps are addressed in this research using an integrated framework that combines remote sensing and GIS. The remote sensing data can greatly improve method reality, allowing better representation of the LST intensities. Incorporated with GIS, statistical and mathematical optimization methods facilitate practical location decision making to enhance green infrastructures locations. The study first identifies the hotspot zones and then, quantifies cooling benefits of existing green infrastructures using LST, LULC and NDVI. Finally, linking hotspot zones with green infrastructures, the cooling benefits of proposed GI location can be predicted.

The purpose of the study is to propose the potential locations of green infrastructures (GI) in Dire Dawa City through identifying the hotspot location. The developments of this infrastructure could reduce the severity of the temperature in the environment. And also for building academic knowledge and provide base for further career improvement. Keeping in view, the detailed LULC map of the City will further helps municipal land use information demand in the planning and arrangement of GI requirements. The result also helps, for improving the capacity of Dire Dawa City Administration, to implement sound plans at local level for improvement of strategic placements of green infrastructures.

1.2. Statement of the Problem

Urbanization is the main driver of UHIs, as it leads to massive land use land cover (LULC) change, transforming natural urban landscapes from green into grey areas to accommodate housing and public infrastructure (Arrau and Pena, 2010). As urban areas develop, changes occur in the landscape. Buildings, roads, and other infrastructure replace open land, vegetation and other green infrastructures (Ipek *et al*. 2010). Surfaces that were once permeable and moist generally become impermeable and dry. The climate warming trend and City growth contribute to excessive heat in urban areas (Ahmed, 2015).

The climatic condition of Dire Dawa City is characterized by warm and dry climate with a relatively low level of precipitation. This is due to urbanization which leads to decreasing of GI in the City therefore; solar energy is directly converted to sensible heat. This increase the surface temperature, resulting in higher urban temperatures during the evenings and nights compared to those in surrounding non-urban areas with high vegetation covers.

Increasing temperature due to urbanization has been observed in Dire Dawa City Administration. Also land degradation, lack of appropriate land use policies and regulations, lack of more green infrastructures development during planning's the serious problems in Dire Dawa City Administration. Due to these problems the temperature of the environment increases from time to time.

The serious problem that initiated to do this study is the increasing temperature of City due lack of proper identifications of the most critical area or temperature hotspot location and the arrangement of green infrastructures to gain the full potential of cooling benefits, especially considering the spatial location of urban heat island effects is one of the most important problems in Dire Dawa City. Lack of considering the role of green infrastructure during planning and designing period can aggravate this problem. Surprisingly, methods of identifying the hotspot location is that support the strategic placement of green infrastructure in the context of identified urban heat island locations is not developed.

This study focused on the identified LST hotspot location based on indicators such as; LULC change, change in temperature and existing GI's and finally propose GI locations based on identified hotspot which reduce LST effects by introducing vegetation in urban design.

1.3. Objectives

1.3.1. General Objective

The general objective of this study is to investigate hotspot location for optimizing green infrastructure which reduces land surface temperature effects in Dire Dawa City.

1.3.2. Specific Objectives

The specific objectives of this study are to:

1. Identifies the surface temperature hotspot areas / maximum heat load area.
2. Test the interactions between land surface temperature (LST) and green infrastructure (GI), through NDVI.
3. Evaluate the cooling benefits of green infrastructure.

1.4. Research Questions

1. Where is the location of temperature hotspot in Dire Dawa City?
2. Is the existing green infrastructure good enough to reduce temperature of Dire Dawa City?
3. How much is the degree of cooling benefits from the introduction of green infrastructure development in Dire Dawa City?

1.5. Significance

Identifying the spatial distribution of urban heat island particularly, the location of LST hotspots with their magnitudes can be used as the basic information for minimizing the risk and improving safety of the environment by allocating resources in high priority areas. If the critical areas with the highest heat load location will identified, urban planning measures could be optimized through targeted and combined implementation. The output of study is used as basis to give more detail information about the spatial distributions of surface temperature, the clue for further investigation in preparation of a planning and designing. And also helps as an indication for Dire Dawa City Administration, for planning the urban green infrastructure.

At the end of the study the society and different stakeholders get the following benefit: optimizing the locations of green infrastructure has produce multiple benefits including decreasing the erosion by keeping the soil in place with the roots and reduces air pollution by filtering pollution and reducing air temperatures, energy demand, greenhouse gas emissions, increasing urban biodiversity and improving air quality in case of urban vegetation and generally, the aesthetics of Dire Dawa City. It also help as an input for government policy makers, urban land management, natural resources managers, environmental experts and other concerned bodies for their decision making processes related to how LST changes through time.

1.6. Scope of the Study

The spatial scope of study was limited to Dire Dawa City Administration, which is characterized by warm and dry climate with a relatively low level of precipitation (NMA, Ethiopian National Meteorological Agency, 2019). The study was focused on the identifications of temperature hotspot areas, the spatial variations of LST and its correlation with GI in the City and analyzes the cooling benefits of green infrastructure. Finally recommend potential green infrastructure sites in Dire Dawa City.

1.7. Limitations of the Study

The framework, however, is a first-generation effort and as such has a number of limitations that require attention in future research. For example, distance decay patterns of the cooling benefit and the effect of the landscape configuration of green infrastructure were simplified to an “all or nothing” coverage assumption based on a fixed cooling extent. In addition, an isotropic surface temperature distribution was employed, in which the temperature is represented by its mean value within a given area. In reality, the cooling effect varies spatially in different directions, which would potentially affect the extent and the interactions of cooling among adjacent green areas (see Lin *et al*., 2015). Further study requires more adjacent green infrastructure samples to better quantify indirect cooling.

Also, the study only used daytime remotely sensed data to study the land surface temperature, while seasonal and nighttime data is also necessary to comprehensively understand the mechanisms of the cooling benefits of urban green infrastructures. In addition, new spatial structures of urban green infrastructure such as, green walls, green roofs and blue infrastructures are not taken into account in this study and should be addressed in the process of urban planning and green infrastructure design.

CHAPTER 2. LITERATURE REVIEW

A literature review was performed on the effect of optimizing GI on the land surface temperature. This chapter explores both theoretical and conceptual frameworks. A Comprehensive review of green infrastructure concepts, exploring the impacts of UHI and role of green infrastructure in reducing temperature which was studied by different scholars in different countries were covered under theoretical framework. The choice of these frameworks is based on the perception that theories are fundamental tools in research problems, which facilitate the choice of methodological approaches to be used in studies as well as interpreting the findings (Elvik, 2002). And finally the conceptual framework was developed based on the objectives and statement of the problems of the study.

2.1. Introduction

The current rate of global urbanization is accelerating dramatically, with nearly 70% of the world's population projected to be living in urban areas by 2050 (Andrew, 2012). At the same time we have climate changes which are expected to be present for at least 30 to 40 years into the future, due in part to the long shelf-life of carbon dioxide (Kalkstein, 1991). Moreover, the effects of climate change are expected to be amplified in urban areas due to their distinctive biophysical features (Gill and Pauleit, 2007).

Urban green infrastructure (GI) is a network of nature based features situated in built-up areas that form part of the urban landscape. These features are based on vegetation (green); including grassed areas, trees and parks are all examples of this type of architecture. Green infrastructure is important as a climate change mitigation and adaptation measure, and has a host of wider benefits to people and wildlife (Kathry and Dr.Ana, 2019).

2.2. Theoretical Framework.

2.2.1. The Urban Heat Island Phenomenon

The UHI phenomenon describes the excess warmness of the urban environment as compared to its rural surroundings. This heat discrepancy is due to differences in the relative surface cooling rates between urban and rural areas (Akbari, 2005). Thus, the term

‘UHI’ has been described as the relative elevated temperatures found over urban areas (Voogt, 2002), appearing as an “island” in the pattern of isotherms on a map (Geer, 1996). Atmospheric and surface temperatures within urban environments are generally warmer than their peripheries. This is due to the replacement of natural green surfaces with non-evaporative and non-porous urban materials with high heat capacity and low solar reflectivity, such as concrete masses, asphalt roads and metal surfaces. These materials exhibit a high degree of thermal inertia (Arrau and Pena, 2010) and are characterized by a high level of absorption of solar radiation, with a greater capacity for thermal conductivity as compared to natural surfaces (Rose and Devada, 2009). Such surface materials cause a reduction in potential cooling rates within urban areas, as compared to their surroundings (Quattrochi and Luvall,1997; Rose and Devada, 2009). This difference in cooling rates is what produces the UHI.

i. Spatial Characteristics of the Urban Heat Islands (UHI): The spatial characteristics of UHI are contingent upon the configuration and topographic setting of the urban area, however, the spatial pattern of UHI isotherms are typically aligned with the urban-rural boundary (Voogt, 2002). Moreover, the increased temperatures associated with the UHI phenomenon are not uniform across the urban area as whole, as intra-urban thermal patterns are generally influenced by urban surface features (Santana, 2007).

ii. Hotspots (UHI Intensity): Hotspots are the result of two interrelated factors: the magnitude of average weather changes at the local level; and the relationship between weather and living standards in that location. This is due to their high thermal inertia. By the time most rural surfaces have already experienced cooling after sunset; most urban materials will have only partially cooled, releasing heat at a much slower rate (Amani-Beni; Zhang, 2018). The result is a modified urban climate, much warmer than its non-urbanized surroundings (Rose and Devada, 2009). Moreover, the differential cooling rates between urban areas and their rural peripheries are usually most distinct on calm and clear nights. It has been found that cities with populations of up to one million or more, the average hotspots zones are 1°C to 3°C warmer in atmospheric temperature as compared to their rural surroundings LST (EPA, 2010). However, in some cases this temperature discrepancy has been measured to be as much as a 4°C - 12°C difference (University of Manchester, 2007) depending on the LULC and topographical location.

The magnitude of an UHI is known as hotspot, which can be defined as the air temperature difference between urban and rural areas. According to (Andrew, 2012), UHI intensity is identified by considering the exposure and sensitive areas that, influenced by climate region, local topography, industrial development of City size and density, LULC characteristics, population density areas and vegetation abundance (Fortuniak, 2009).

Meteorological conditions especially wind speed, temperature change and sun intensity also another indictors of hotspot (EPA, 2010) . Of all the indicators mentioned above, LULC characteristics, mean temperature change and the abundance of urban vegetation are the two factors which are considered to have the most significant effect on UHI intensity, as well as on intra-urban thermal patterns (Xian and Crane,2006; Arrau and Pena, 2010).

2.2.2. Types of Urban Heat Islands (UHIs)

i. Atmospheric Urban Heat Islands: Atmospheric urban heat islands can be divided into two different categories: canopy layer heat island (CLHI) and boundary layer heat island (BLHI). The CLHI refers to the layer of air closest to the surface which extends to approximately building height. The BLHI is located above the canopy layer and may be up to 1Km or more in thickness by day and a few 100m in thickness at night (Voogt, 2002). Of the two types of atmospheric heat islands, CLHIs are the ones most commonly observed and referred to in the majority of UHI research.

ii. Surface Urban Heat Island (LST): The Surface Urban Heat Island (SUHI) refers to the relative warmth of urban surfaces compared to surrounding non-urbanized surfaces. While the atmospheric UHI can be detected by ground based air temperature measurements, the SUHI is typically characterized as a measurement of land surface temperature (LST), based on the use of thermal remote sensing (Rose *et al*., 2009). SUHIs are generally strongest during the day but are usually present during the night as well. Similar to UHIs, the magnitude of LST is influenced by sun intensity, LULC characteristics and vegetation abundance. LSTs are typically largest during the summer and their intensity tends to vary much more than that of UHIs (Arnfield, 2003). The difference in daytime surface temperatures between urban and rural areas is on average 10°C to 15°C, however, at night the difference is between about 5°C to 10°C (Oke *et al*., 2003).

2.2.3 Environmental and Social Impacts of UHI

Although there may be certain positive impacts attributable to the increased temperatures associated with UHIs (including the melting of ice on roads during the winter, reductions in energy required for heating, and longer plant-growing season), such potential benefits are largely outweighed by the substantial detrimental environmental and social aspects discussed below (EPA, 2010).

The UHI phenomenon is known to reduce the stability of the urban atmosphere at night which, under certain meteorological conditions, may intensify the explosion of convective clouds. Thus, the effect of rainfall events (which according to the intergovernmental panel on climate change are expected to increase in magnitude and frequency due to climate change) may be amplified in urban areas, resulting in economic losses and extra costs due to, among other things, the need for improvements in storm-water drainage (Parry and Hanson, 2007)

2.2.4. UHI Mitigation through Optimizing Urban Green Infrastructure locations

There is widespread evidence that communities would be better able to adapt if they were able to work with natural processes and systems (Kovats and Osborn, 2016). Green infrastructure provides a host of different benefits to people and wildlife. Its presence can improve air and water quality, enhance flood and temperature regulation, reduce noise (Kathry and Dr.Ana, 2019). Green infrastructure approaches help to achieve sustainability and resilience goals over a range of outcomes in addition to climate adaptation. The climate adaptation benefits of green infrastructure are generally related to their ability to moderate the impacts of extreme precipitation or temperature (Maksimovic *et al*., 2017).

I. Methods of optimizing Green Infrastructures

An optimization approach involves mathematical representation of a problems (modeling); specifications objective function, decision variables and constraints; and determination of solution methods (Gilbert *et al.,* 1985). In optimization, a problem is fully represented by mathematical terms. The mathematical representation is in terms of objective functions to be maximized or minimized subject to set of constraints.

Some of the earlier applications of optimization to land-use allocation are single land-use allocation models. A model by Wright *et al.,* (1983) is one of the single land-use allocation models. The main issue addressed on this model is the problem of land acquisition for the construction of any structure such as real state, parks etc. This model has three objectives: maximization of acquired area, maximization of benefit and minimization of risks

The general form of a multi-objective optimization model can further be explained by considering specific land-use allocation problem as an example. Land-use allocation is defined as the problem of determining a land-use map that identifies locations for specific land-use types. The objectives can be minimization of environmental impacts. The decision variables will, therefore, be the determination of whether a particular land-use type is applied to particular location or not. The final solution of these kinds of optimization models is a land use map with every land-use type allocated to the best possible land-use unit within the study area.

Combining broader scale spatial data, multi-objective optimization models have been applied recently to determine green infrastructures locations in the City, balancing various kinds of environmental benefits. The study by (UN-Habitat, 2015; CSA, 2017) also developed a multi-objective empirical technique for optimizing the configuration of parks and open space with respect to air and water quality improvement as well as noise and temperature reduction.

Zhang and Huang (2014) sought to minimize LST in the allocation of land uses within a multi-objective heuristic, where temperature is a regressed function of land use intensities. As yet, however, no current model has attempted to account for the agglomeration of cooling resulting from green infrastructures, which greatly affects their spatial allocation.

2.2.5. The Cooling Benefits of Green Infrastructures

The abundance of urban vegetation is known to greatly influence the urban thermal environment and the development of the UHI. Vegetation can reduce LSTs and atmospheric temperatures through evapotranspiration (Hamada, S. and Ohta, T. , 2010), a process by which heat from the air results in the evaporation of water (Gill and Pauleit, 2007). Evapotranspiration is believed to be able to cause a reduction in peak summer temperatures within urban environments by as much as 1°C up to 5°C (EPA *et al*., 2010).

As study by (Bozovic *et al*. 2017) indicates in the city of Manchester; trees positioned next to buildings lowered internal summer temperatures by 4°C and raised winter temperatures by 6°C compared to a 'no tree' scenario, with a corresponding decrease in energy consumption of 26%. He also concluded that increasing the current area of green infrastructure in greater Manchester by 10% (in areas with little or no green cover) could result in a cooling of up to 2.5°C under a high emissions world compared with a 'no action' scenario (Gill *et al*., 2007). Green roofs buildings can reduce surface temperatures on roofs by around 20°C in one study (Charlesworth, 2010). Green walls in the UK were found to reduce indoor temperatures by 4°C up to 6°C in the summer (Ipek *et al.,* 2010). Optimizing green space could result in a cooling benefits of up to 1–7°C (Chow *et al.,* 2011), with cooling impacts extending as much as 100m beyond green spaces (Bowler *et al*., 2010).

2.2.6. Measuring the Urban Thermal Environment:

There are a variety of approaches to the measurement of the urban thermal environment including mobile sampling of air and surface kinetic temperatures from ground and airborne vehicles, sampling of air and surface kinetic temperatures at fixed locations, and the remote measurement of LSTs from space-borne platforms (Andrew, 2012). However, remote sensing is considered to be one of the most useful tools for detecting thermal variations within urban settings due to the ability of this tool to collect scores of spatially contiguous samples over large areas instantaneously (Yue, 2007).

Moreover, the remote sensing method can provide measurements regarding the spatial extent of surface heat island effects for metropolitan areas as well as regarding the magnitude of surface temperatures (Yuan and Bauer, 2007). According to the study of Yue (2007), in Shanghai, remote sensing is also a valuable tool to use in studying urban vegetation and LST as it can obtain data which can be used to quantify the extent and condition of vegetation.

Remotely sensed thermal infrared data are extensively used for retrieval of LST and urban heat islands (Weng *et al*., 2004). Moreover, remote sensing in combination with geospatial information system (GIS) can be used in large number of studies (Youssef *et al.,* 2011; Wakode *et al*., 2013). Yujia, Z et *al.,* 2017 used the integrations of GIS and remote sensing, spatial statistics and spatial optimization to identify the best locations of new green space.

And he found that, optimizing new green space can provides approximately 1–2°C locally and 0.5°C regionally cooling benefits can be achieved in Phoenix, Arizona.

2.2.7. LST Zoning (Classification) methods

LST data is time-synchronized and grid based for a considerable areal extent (Nichol 1996). So far, various remote sensing sensors have been used to estimate LST zones with thermal infrared bands from coarse to fine spatial resolution.

(Peng, Xie *et al.* 2016) was adopted "Distribution Index" (DI) method to explore the contribution of LCZs to SUHI phenomenon. He particularly focused on "high" LST pixels as a direct indicator of the SUHI phenomena. To quantify "high" LST level, the original LSTs were normalized and categorized by five levels from "very cool/low" to "very hot/high" with Jenks natural breaks classification scheme (Weng, Liu *et al*. 2008).

Hotspots can be categorized into six classification schemes: equal interval, defined interval, quartile, natural breaks, geometric interval and standard deviation. In the natural breaks scheme, the classes are based on natural categories inherent in the data and based on Jenks algorithm (Deepthi and Ganesh, 2010). This algorithm is a common method of classifying data in a choropleth map, a type of thematic map that uses shading to represent classes of a feature associated with specific areas.

Jenks algorithm generates a series of values that best represent the actual breaks observed in the data, as opposed to some arbitrary classification scheme; thus, it preserves true clustering of data values. Further, the algorithm creates *k* classes so that the variance within categories is minimized (Manepalli and Bham, 2011). The break points are identified by the class breaks that best group similar values and maximize the differences between the classes. The features are divided into classes and create boundaries that correspond to relatively big jumps in the data values (Esri, 2016). This classification scheme is best suited in which the output of the classified zones is a raster file displaying the areas of low, medium, medium-high and high LST zones. Lighter shades represent locations with lower LST zones or cold spot, while darker shades represent the locations with highest LST zones (Nyoni, 2017).

2.2.8. The Relationship between NDVI and LST

Vegetation abundance is also known to influence LSTs and UHI conditions through the process of evapotranspiration. Therefore, investigation into the relationship between NDVI and LST becomes informative and meaningful, especially in regards to areas where the UHI phenomenon is more pronounced and where mitigation measures are needed (Honjo, T. and Takakura, T, 1990). Given that vegetation abundance is known to reduce LSTs through the transfer of latent heat from the surface to atmosphere via evapotranspiration, NDVI can be used to investigate this relationship and thereby, provide insight into how this natural cooling mechanism of vegetation might be employed to improve urban thermal environments. In general, areas with high NDVI will typically have lower LSTs; however, this correlation may be influenced by soil moisture conditions and evapotranspiration of the surface (Amani-Beni; Zhang, 2018).

2.2.9. LULC and Urban Thermal Environment

LULC characteristics are known to have a significant influence on intra-urban thermal conditions (Xian and Crane,2006; Arrau and Pena, 2010). For example, (Roth, 2008), found a strong correlation between LULC and intra-urban thermal patterns with industrial areas being the warmest and vegetated and coastal areas being the coolest. As different LULC characteristics can modify thermal conditions in cities, an enhanced understanding of the interrelationship between LULC and LST can be employed in order to improve urban planning decisions aimed at UHI mitigation (Santana, 2007).

2.3. Empirical Review

Urban heat islands (UHIs) are meteorological impacts of urbanization that cause the air temperature in urban areas to be higher compared to their surrounding non-urban areas. (Andrew, 2012). Increasing urban temperature due to urbanization has been studied in cities around the world such as Atlanta (Weng, 2017), Dhaka (Ahmed, 2015), Ho Chi Minh City (Doan and Kusaka, 2016), Jakarta (Sofyan *et al*., 2010), and (Matsumoto *et al.,* 2017) in Tokyo. According to (Tong and XuCheng , 2018), UHIs may adversely affect physical and mental health, as well as promote cardiovascular disease and chronic kidney disease. They also have significant effects on energy consumption for cooling of urban buildings.

Presently, most cities in the world are greening their cities. For example, the city of Rotterdam in the Netherlands implements the greening concept in city planning and development (Bolund, 2015). Cities can reduce the heat island effect by using green space that provides shadings and open wind-flow paths, which can eliminate the accumulation of heat (Hunhammar, 1999). This can be practically done by increasing the percentage of green space in urban areas.

Many studies have looked at the relationship between the intensity of UHIs and urban green space with regard to its composition and configuration (Forman,1995;Zhou,2011 and Dikman, 2019). Composition refers to vegetation density and variety of land cover types, green space size, as well as spatial distribution. In Hanoi, Vietnam, the transformation of agricultural land into the impervious (built-up) surface due to urbanization and industrialization between 2003 and 2015 has increased the mean land surface temperature (MLST).

The developed multi-objective model is applied to evaluate the diurnal cooling trade-offs in Phoenix, a reduction of land surface temperature of approximately 1°C up to 2°C locally and 0.5°C regionally can be achieved by the addition of new green space (Brazel *et al.,* 2000). Sun and Chen (2017) revealed that 108.86km^2 of the green space in Beijing was lost, which increased LST between 1.6°C and 2.2°C, while 92.5km^2 of the green space expansion had reduced the LST within the range of 0.67°C up to 1.1°C. These results indicate that changing the levels of green space influence air temperature changes and generate various temperature patterns.

In general, the UHI described in the term of air temperatures by the direct in-situ measurement and surface temperature from thermal remote sensing data(Zhao *et al*., 2018). With the development of remote sensing technology, satellite based estimation of land surface temperature (LST) derived from thermal infrared remote sensing imagery (Juntao Tan and Hung, 2018) becomes effective in interpreting UHI effect because it provides a relatively rapid and low-cost data information on landscape scale.

2.4. Conceptual Framework

The theoretical framework presented the review of literature on different theories related to the effects of optimizing the spatial location of green infrastructure on UHI specially the role of identifying LST hotspots zones to mitigate UHI effects. Also different methods of measuring LST, classifying LST to identifying LST hotspot zones and analyzing the correlation between GI and LST; to determine the cooling benefits of GI.

UHI studies can be performed using several methods, including field observations, remote sensing (Li *et al*., 2018) and numerical modeling (Oke *et al*., 2017). Field observations are normally made by comparing records from meteorological stations inside and outside of the urban area or using mobile monitoring cars moving between rural fringe and the city center (Hidalgo *et al.,* 2008). In addition, advanced computer technology along with high spatial and temporal resolution of satellite imagery has been used to measure UHIs in more detail (Weng *et al.,* 2009). The UHI phenomenon can also be studied by using numerical atmospheric simulation (climate) models (Dikman *et al*., 2019).

Identifying LST hotspot locations using GIS-aided technique can highlight contributory factors that can assist the government and its agencies to implement corrective measures at such spots and reduce the effect of UHI on the environments. To quantify LST levels as “high” LST zones, the original LSTs were normalized and categorized by five levels from “very cool/low” to “very hot/high” with Jenks natural breaks classification scheme (Weng, Liu *et al*., 2008; Manepalli and Bham, 2011 and Nyoni, 2017).

Remote sensing techniques previously used in research, such as (Ahmed, 2015), study on the “identification of environmental changes with NDVI and LST Parameters in Bharin”. Correlations between NDVI and LST have been done by (USGS, 2018). And also the study by (Lestari *et al*., 2018), used statistical analysis (regression) and buffer analysis to analyze changing of radius temperature. And results, the higher value of NDVI give impact of LST value in the same location will tend to be low with average value of temperature rise of 0.122^{o}C per 30m. (Sara *et al.,* 2013; Aakriti and Ram,2015; Nedun, 2019), uses regression technique and obtain the correlation between LST and NDVI. They concluded that, the correlation between NDVI and LST is negative. (Xian *et al.,* 2006), used spatial statistics to identify the best locations of new green space with respect to cooling benefits.

The above mentioned measuring and modeling gaps are addressed in this research using an integrated framework that combines remote sensing and GIS. The remote sensing data can greatly improve method reality, allowing better representation of the LST intensities. Incorporated with GIS, statistical and optimization methods facilitate practical location decision making to enhance green infrastructures locations. The study first quantifies and predicts cooling benefits of existing green infrastructures using LST and land use land cover classes, linking cooling benefits with green infrastructures locations. The exact formulation and solution for green infrastructures allocation is developed next and explicitly accounts for agglomeration based cooling. The comprehensive related literature reviewed can be summarized by table 2.1 below.

Table: 2.0.1. The conceptual framework developed from related literature reviewed

1. Extractions of LST		
Author Name	**Methods**	**Descriptions**
• Ahmed, *et al.*, 2015 • Alexandra, S. *et al.*, 2018	• Used Integrated frame work of Remote Sensing and GIS Technology and validate using Meteorological Interpolation	• "Identification of environmental changes with NDVI and LST" • The potential of local climate Hotspot zones map.
• Dikman *et al.*, 2019; Oke *et al.*, 2017;	• Numerical atmospheric simulation (climate) models	• UHI phenomenon and Simulation of LST.
• Li *et al.*, 2018 • Weng *et al.*, 2004 and Deepthi, 2010;	• Field observations and Remote Sensing data and validate using NOAA data. • Remote sensing and GIS and Jenks natural breaks classification	• Analyze Temporal and spatial variations of LST • Retrieval of LST and identify urban heat islands zones by classifying LST zones into 5
•Manepalli, 2011; Nyoni, 2017.	•classification method, Meteorological stations Data and Remote sensing data	•To categorize or classify LST zones and determine the best arrangement of values into different classes based on
• Hongbo Zhao *et al.*, 2018; Sundara K. *et al.*, 2011	• Remote sensing , GIS and Meteorological stations Data	• Identify the most UHI areas and measurers LST effects from thermal RS data
2. Correlations between NDVI and LST		

• USGS, 2018; Lestari *et al.*, 2018; Sara *et al.*, 2013; Aakriti and Ram, 2015 • Belete T., 2016	• Statistical analysis (regression technique) • Using geospatial tools and verified by field data and regression technique	• They concluded that, the correlation between NDVI and LST is negative. • Impact of LULC changes on LST. And he found that, LST has negative relationship with vegetation cover (NDVI)
3. Cooling Benefits Analysis		
• Yujia, Z. et al.,2017 • Fei Zhang *et al.,* 2016,	• Integrating GIS, Remote sensing, spatial statistics and spatial optimization. • RS thermal infrared data and meteorological data	• Identifies the best locations of new green space and about 1–2 °C locally cooling benefits can be achieved in Phoenix, Arizona. • Dynamics of LST in response to LULC and Identifies cold island area which is 1-3.5°C cooler than other areas in China.
• Chow *et al.,* 2011; Spronken, S. & Oke, 1998; Wang, & Yuan, 2012. • Majid A. et al.,2019	• Micro-climate numerical models deal with surface energy balance, simulating thermodynamic processes. • Remotely sensed thermal infrared data and meteorological data	• Concluded that, green space can be 1–3°C, and sometimes even 5–7 °C, cooler than surrounding built-up areas. • Found that, for every 10% increase in the green space, the LST drops by 0.4°C, and increase in the distance from the park, LST increases by 0.15 °C.

CHAPTER 3. MATERIALS AND METHODS

3.1. Description of the Study Area

Dire Dawa, in eastern Ethiopia, was established in 1902 as a relatively lowland with elevation of 1200m above sea level. The City is about 515km from Addis Ababa (capital of Ethiopia) and 300km from the international port of Djibouti, with a latitude and longitude of 9°36’N and 41°52’E respectively(UN-Habitat, 2015; CSA, 2017). The map that describe of the location of study area is shown in figure 3.1 as follows.

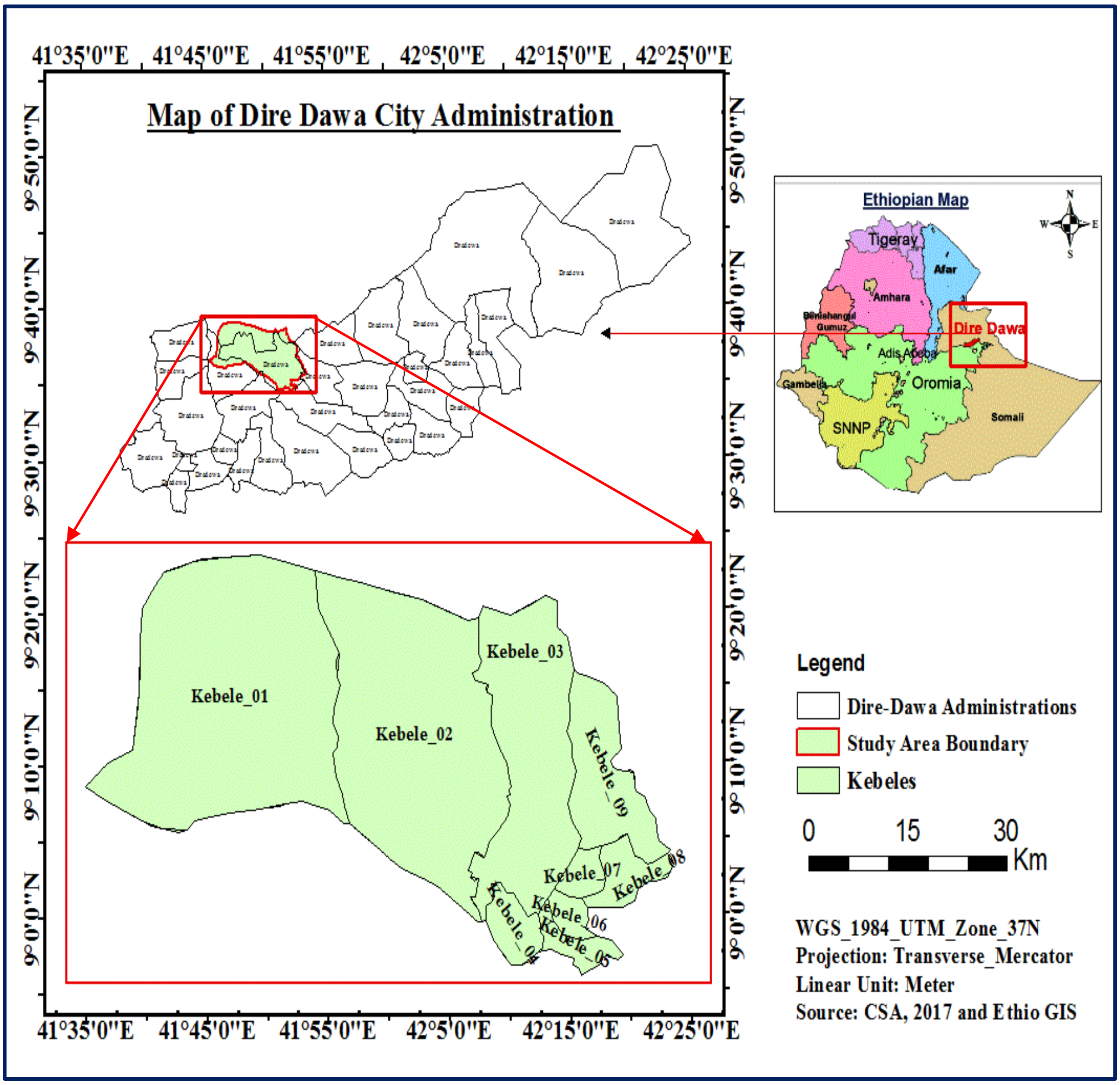

Figure: 3. 1. Location of the study area

i. Land Size and Composition: The Dire Dawa Administration is a chartered City Administration that consists of 9 urban and 38 rural kebeles. In all, the Administration has a total land size of 1,300 square kilometer or 130,000 hectares, of which 94.65% accounts for the size of the rural area, while the remaining 5.34% covers the land size of the urban areas found in the Administration (D.D.E.P.A, 2019). With this economic slump, growth has been more organic and dense; unplanned (informal) settlements can be seen scattered throughout the City.

ii. Demographic Characteristics: Based on the 2017 Census conducted by the CSA of Ethiopia, Dire Dawa City Administration has a total population of 252,279 which is the second populated city in Ethiopia next to Addis Ababa (UN-Habitat, 2015; CSA, 2017).

iii. Climate: Dire Dawa City has a hot semi-arid climate (koppen climate classification Bsh).The mean annual temperature of the provisional administration is about 25.91°C. The average maximum temperature of the Administration is 33.13°C, while its average minimum temperature is about 19.01 °C. (D.D.E.P.A, 2019). For the last two decades, the average annual temperature of the City was increasing by 0.6°C per decade, especially in the cool months.

The climatic condition of Dire Dawa City Administration seems to be greatly influenced by its topography and urbanization which is characterized by warm and dry climate with a relatively low level of precipitation (NMA, 2019).

Dire Dawa City has two rain seasons; that is, a small rain season from March to April, and a big rain season that extends from August to September (see Appendix 1). The aggregate average annual rainfall that the region gets from these two seasons is about 583.2mm. On the other hand, the region is believed to have an abundant underground water resource (D.D.E.P.A, 2019).

iv. Topography: Topography is the study of the shape and feature of the surface of the earth and other related phenomenon or it is an integral part of the land surface. It includes such as landforms, elevation, latitude, longitude and topographic maps. The Dire Dawa City has a broad flat area. The elevation of the study area is lies up to 1,350m MSL, the elevation map of the study area is indicated in (Fig. 3.2).

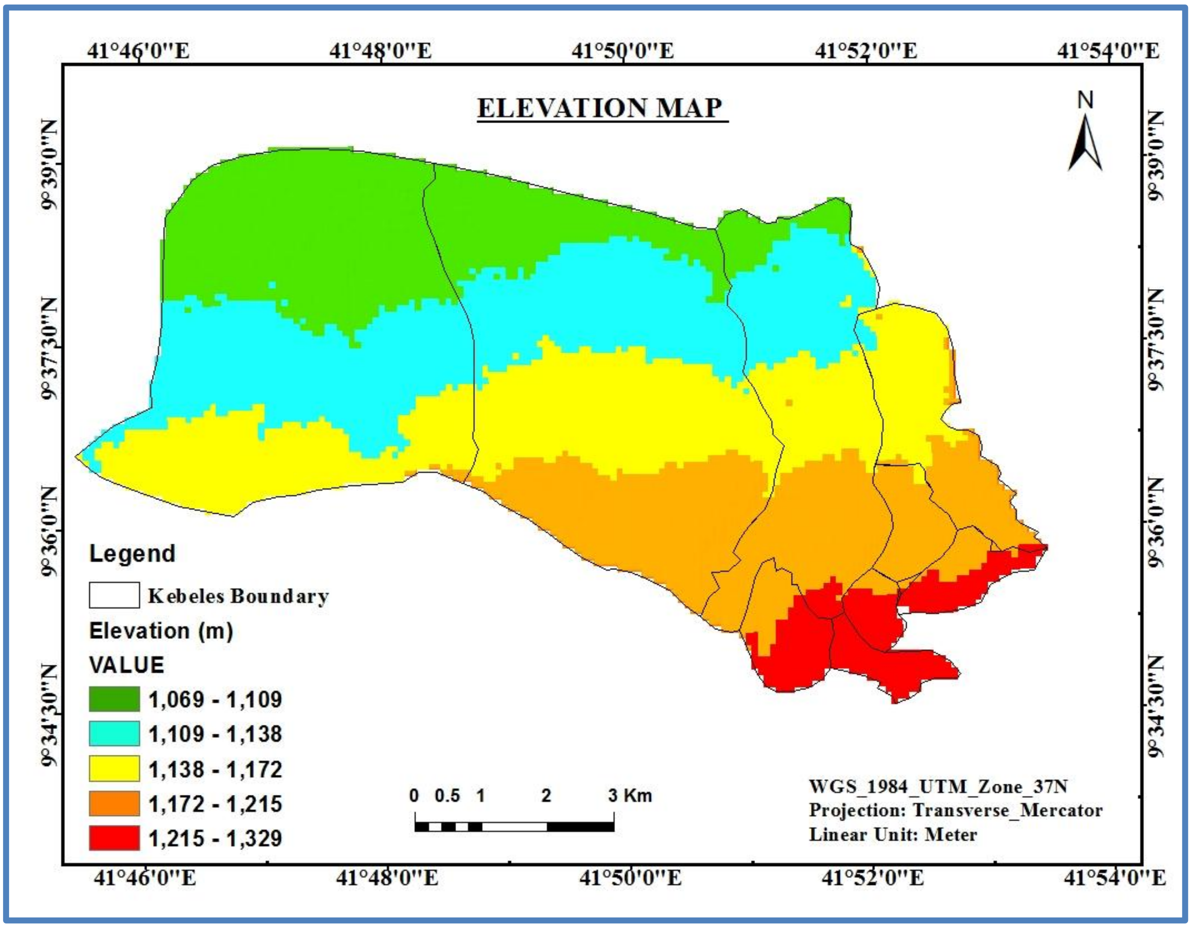

Figure: 3. 2. Elevation range distribution map of study area

The slope was derived from a preprocessed DEM. According to the FAO slope classification which depend on land surface percentage rise (Sheng,1993), the study areas was classified into five slope classes, which extends from nearly level (less than 1%) to Steep sloping (greater than 30%) follows (Table3.1 and Fig.3.3).

Table: 3. 1. Slope Classification of the study area

No.	Slope (%)	Slope Category
1	0-1	Nearly level
2	1-3	Very gentle sloping
3	3-8	Gently sloping
4	8-15	Moderately sloping
5	15-30	Steep sloping

[Source: FAO Slope Classifications, (1999)]

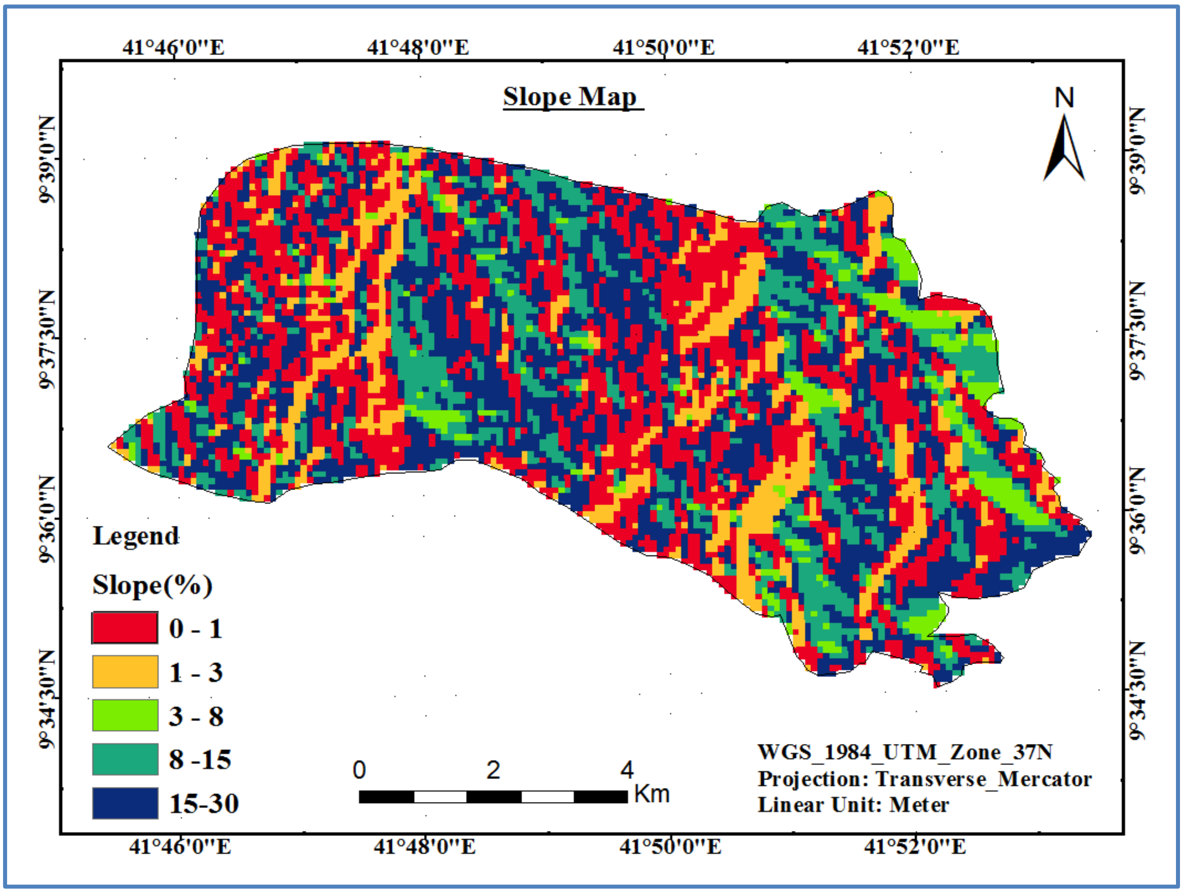

Figure: 3 3. Slope range distribution map of study area

As shown on the above figure the slope range distributions of study area were more dominantly extends from nearly level (less than 1%) up to moderate slope (8 - 15%) and less percentage of steep sloping.

3.2. Data Source

3.2.1. Primary Data

The primary data includes satellite image (Landsat data): Thematic Mapper (TM) 1999 and Operational Land Imager/Thermal Infrared (OLI/TIRS) 2019 obtained from USGS. Digital Elevation Model (DEM) data with the resolution of 30*30 m for mapping the elevation and slope of the area and field data, GPS point of different classes of LULC were used.

3.2.2. Remote Sensing Data Acquisition

One scene of Landsat 5 TM (1999) and Landsat 8 OLI/TIRS (2019) cloud free image of the study area with the path of 166 and row 053 were downloaded from the website of earth explorer. usgs.gov, United States Geological survey (USGS) and Landsat8 from https://libra.developmentseed.org.The-acquired data is world datum (WGS84) projection system. Remote sensing images used to calculate LST, NDVI and LULC in Dire Dawa City were shown in the following (table 3.2).

Table: 3. 2. Specification of Landsat Satellite Images Used in the Study

Date of Acquisition	Sensor	Path	Row	Multispectral Band	Thermal Band	Source
12/05/1999	TM	166	53	1 to 5 and 7	6	USGS
14/05/2019	OLI/TIRS	166	53	1 to 7 and 9	10 and 11	

[Source: Landsat-5and Landsat-8 Meta data, Obtained from USGS, 2019]

A. Landsat Thematic Mapper (TM)

The Landsat Thematic Mapper (TM) sensor was carried on-board four and five from July 1982 to May 2012 with 16-day repeat cycle. Thematic Mapper sensor has seven spectral bands; three in the visible range and four in the infrared range. Band 6 is specifically sensitive to thermal infrared radiation to measure surface temperature. Detailed information is shown in table 3.3.

Table: 3. 3. Landsat 5 Thematic Mapper sensor bands and description

Satellite/ Sensor	Bands	Description	Wavelength (Micrometers)	Spatial Resolution (m)	Repeating time	Source
Land Sat 5 TM	Band 1	Blue	0.452-0.518	30	16 days	USGS
	Band 2	Green	0.528-0.609			
	Band 3	Red	0.626-0.693			
	Band 4	NIR_1	0.776-0.904			
	Band 5	NIR_2	1.567-1.784			
	Band 6	Thermal	10.45-12.45	120		
	Band 7	MIR	2.09-2.34	30		

[Source: Landsat-5 Documentation manual, Obtained from USGS, 2019]

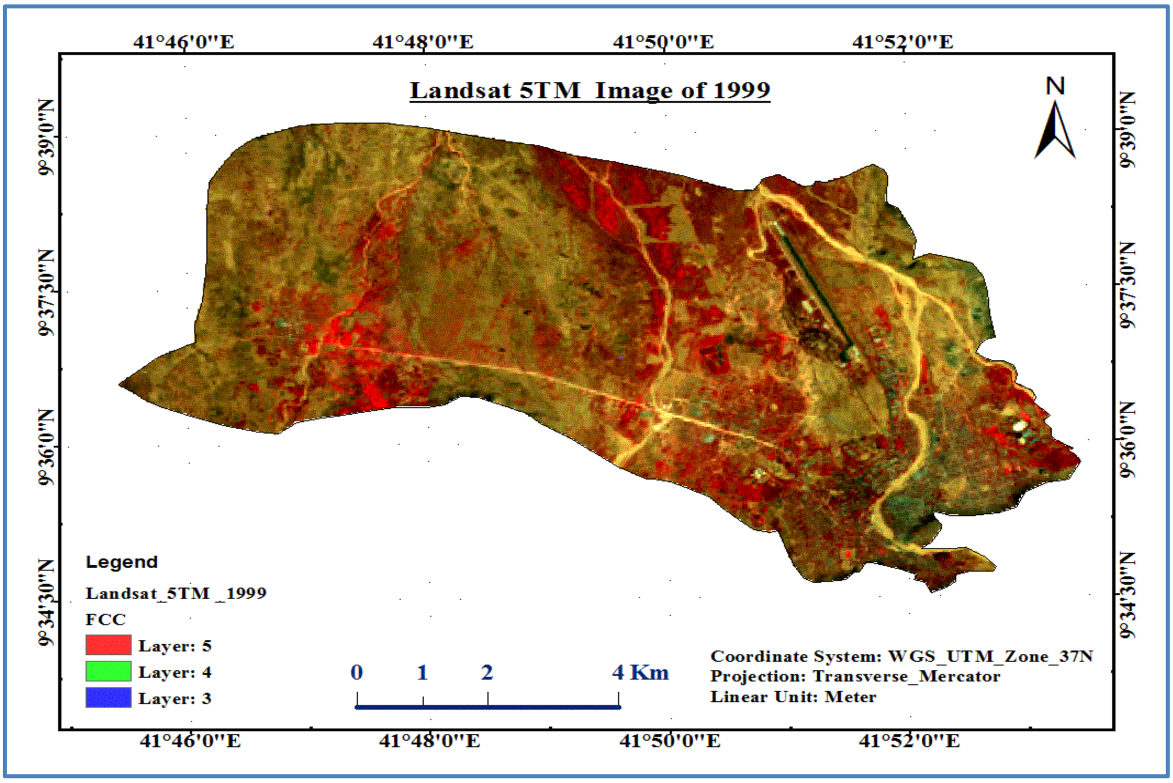

Figure: 3. 4. Landsat Image of 1999 TM of the study area

B. Landsat 8 Operational Land Imager (OLI) and Thermal Infrared Sensor (TIRS)

Images consist of nine spectral bands with a spatial resolution of 30 m for band 1-7, 9, and TIRS with two bands (band 10 and 11). New band 1 (ultra-blue) is useful for coastal and aerosols studies. Another new band 9 is useful for cirrus cloud detection. Landsat 8 was launched in February 11, 2013 (table 3.4).

Table: 3. 4. Landsat 8 OLI/TIRS bands and description

Satellite/ sensor	Bands	Description	Wavelength (micrometers)	Resolution (m)	Repeating time	Source
	Band 1	Coastal aerosol	0.43-0.45			
	Band 2	Blue	0.45-0.51			
Land Sat 8 OLI/TIRS	Band 3	Green	0.53-0.59	30	16 days	USGS
	Band 4	Red	0.64-0.67			
	Band 5	Near Infrared	0.85-0.88			

	Band 6	Short -Wave Infrared IR (SWIR-1)	1.57-1.65	30	16 days	USGS
	Band 7	(SWIR-2)	2.11-2.29			
	Band 8	Panchromatic	0.50-0.68	15		
	Band 9	Cirrus	1.36-1.38	30		
	Band 10	Thermal Infrared (TIRS-1)	10.60-11.19	100		
	Band 11	Thermal Infrared (TIRS-2)	11.50-12.51			

[Source: Landsat-8 Documentation manual, Obtained from USGS, 2019]

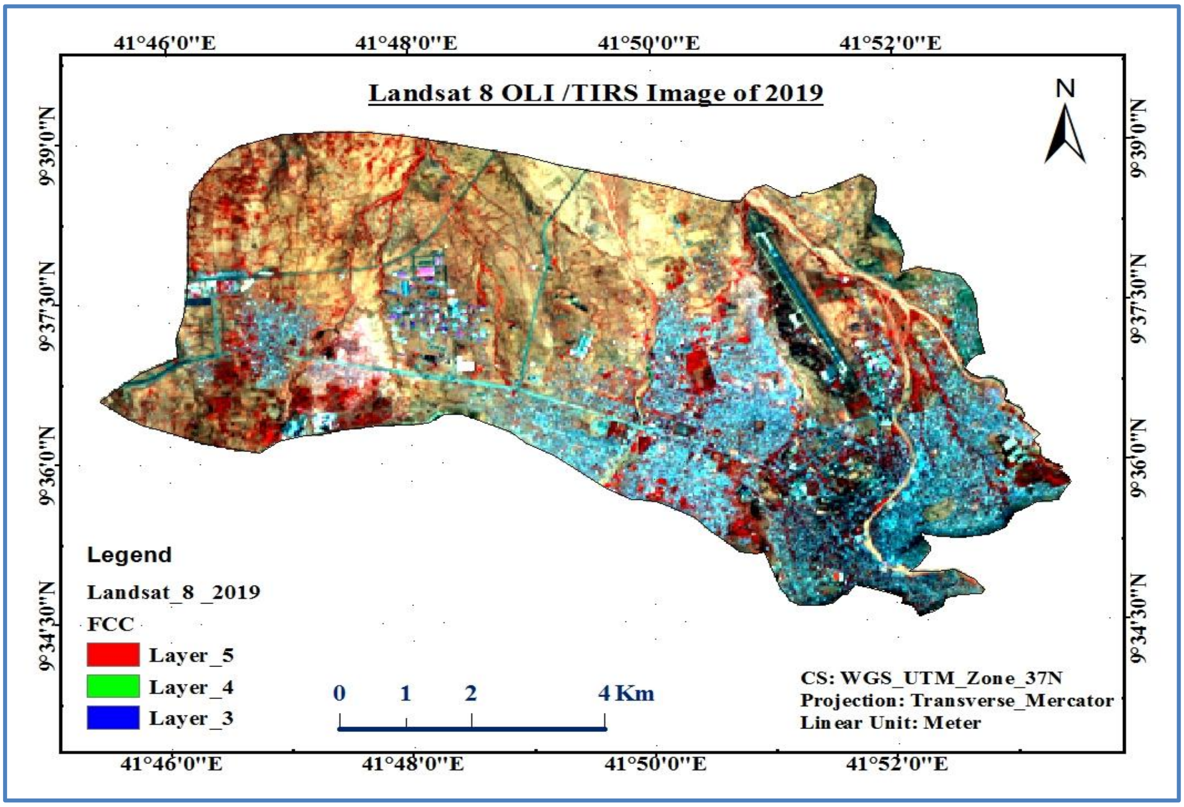

Figure: 3. 5. Landsat Image of 2019 OLI and TIRS of study area

3.2.3. Field Data

A ground truth activity was carried out in the study area, in which different LU/LC classes were validated. The observed LU/LC includes: shrubs, spares vegetation, bare land, settlement and dry rivers were identified. The training data sets (samples) used for image classification were developed. During this ground truthing activities, the coordinates from sampled LU/LC classes were collected from the field. Using hand held Global Positioning System (GPS) instrument, the field survey was conducted and about 50 points were collected. After Random point, generated GPS point was collected and pictures showing different LU/LC classes were also captured.

3.2.4. Secondary Data

Secondary data used in this study comprises meteorological data such as average monthly temperature (1999–2019) and average monthly rainfall (1999–2019).These meteorological data was used for evaluation and validation. In addition to this, the other data used in this study were Google earth, aerial photo of Dire Dawa City and population data from CSA to realize the status of the population of the study area.

3.2.5. Data Description and Source

Primary and ancillary data that used in this study was collected from different sources as indicated in table 3.5.

Table: 3. 5. Source of Data and Description of Data used in the Study

GIS Data layer	Data Description	Data source
Vector (polygon)	kebeles Boundary	CSA, 2017
Vector (line)	River and Roads	CSA, 2017
Vector (point)	Major Town	Ethio-GIS
Raster	Elevation and Slope	DEM 30 m SRTM
Attribute table	Rainfall and Temperature	National Metrological Agency
Attribute table	Population	CSA, 2017
Ground point	Ground truth for LU/LC	Field survey
Raster	*Satellite Image:* 1999 Landsat 5 TM 2019 Landsat 8 OLI &TIRS	USGS 1999 and 2019

3.2.6. Software Packages Used

Software packages used for this study were ArcGIS 10.3 for image analysis; calculate LST, NDVI and map preparation, ERDAS (Earth Resources Data Analysis System) Imagine 2014 for Remote Sensing application in order to process satellite images including image enhancement, preprocessing and for LU/LC classification. Google earth also used to check and compare results with ground truth, especially for the year 1999 and 2019 LU/LC verification. In addition to ERDAS Imagine Software, ENVI software was used for classification to compare and contrast the results. Microsoft Office, Microsoft Excel and Microsoft Power Point was used to create word documents, analyze spreadsheets, to do graphs, manage databases and for presentation. The lists of data, materials, software and equipment used for the study are tabulated as follows in table 3.6 shown below.

Table: 3. 6. List of data, materials, software packages and equipment used for the study

A. Data Used		**Purpose**		**Sources**
1	Landsat 5 and 8 image	Land use land covers classification, extractions of LST and NDVI and show the changes.		http://earthexplorer.usgs.gov (USGS)
2	Rectified google-earth image	To get updated information this may not exist on Map.		Google Earth Explorer
3	Geographic coordinates of land use locations	LU/LC-locations identification and obtain ground truth		From Field Survey
4	Meteorological data 1999 to 2019 (monthly)	To show temperature difference.		Dire Dawa City Meteorological stations and NMA.
B. Software Used				
	Name	**Version**	**Purpose**	
1	ArcGIS	10.3	Database creation and LST extraction. Integration and management of spatial information, LST hotspot analysis.	

2	ERDAS IMAGINE	2014	Land use land cover classification and radiometric correction,
C. Equipment Used			
1	Hand held GPS	Garmin64	• Collection of geographic coordinates of LU/LC location.

3.3. Methods

In this study, the method used to achieve the objectives, the research was begun with acquisition of Landsat imagery for the year 1999 and 2019 from website of earth explorer (USGS). The reason behind that these years chosen were because of the availability of the data. The image acquired or downloaded was during the dry season and cloud free image. Radiometric correction was performed for adjusting the brightness value of the image, and then the image was geometrically corrected by registering it on a local land use map.

Maximum likelihood algorithm was used for land use land cover classification because it uses a probability value on every pixel to divided into specific information classes and subsequently, image was processed in ArcMap using raster calculator and obtained : top of atmosphere (TOA) using reflectance rescaling coefficients provided in the land sat metadata file (Zaitunah *et al*., 2018), conversion of spectral radiance to temperature in Kelvin using brightness temperature (Landsat Project Science Office, 2001), vegetation density using the normalized difference vegetation index (Andrew, 2012), vegetation proportion, land surface emissivity (LSE) (Sara *et al.*, 2014), and LST was derived from Landsat5 TM using band 6 and Landsat8 OLI /TIRS using band 10 and band 11 based on (Artis and Carnahan , 1982). And finally LST was classified into five LST zones by using Natural Breaks (Jenks) classification and hotspot zones was identified by over laying land surface temperature map, vegetation index map and meteorological data.

Proximity analysis was used to analyze the cooling extents of green infrastructure; to look range area that were influenced by a hotspot i.e. direct cooling benefit to an identified area was derived. Zonal statistics as table and regression analysis were used to examine the correlation between NDVI and LST. Range of buffer that was used 100m interval adjusts to spatial resolution of landsat8 band10 and band11. The data values which have been extracted from proximity analysis were continued and the degree of cooling benefit was determined through mathematical analysis. The activity of collected data and processed data is summarized as follows in figure 3.6 below:

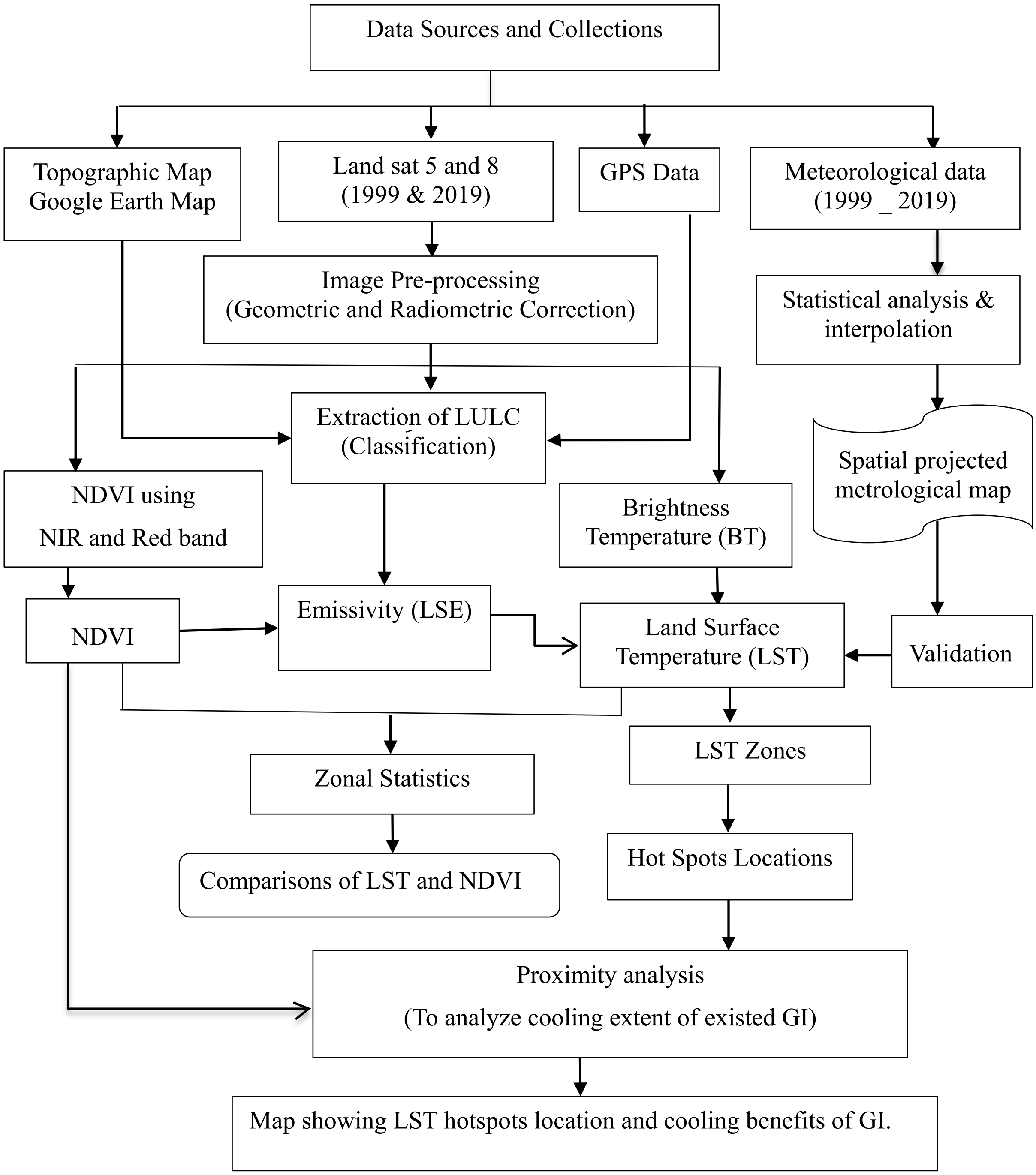

Figure: 3. 6. Technological scheme of the study

3.4. Land Use Land Cover (LU/LC) Extraction

Steps or processes that were followed to classify land-use/land-cover from a Landsat image were presented in fig. 3.7 below and the detail data process is discussed in chapter four.

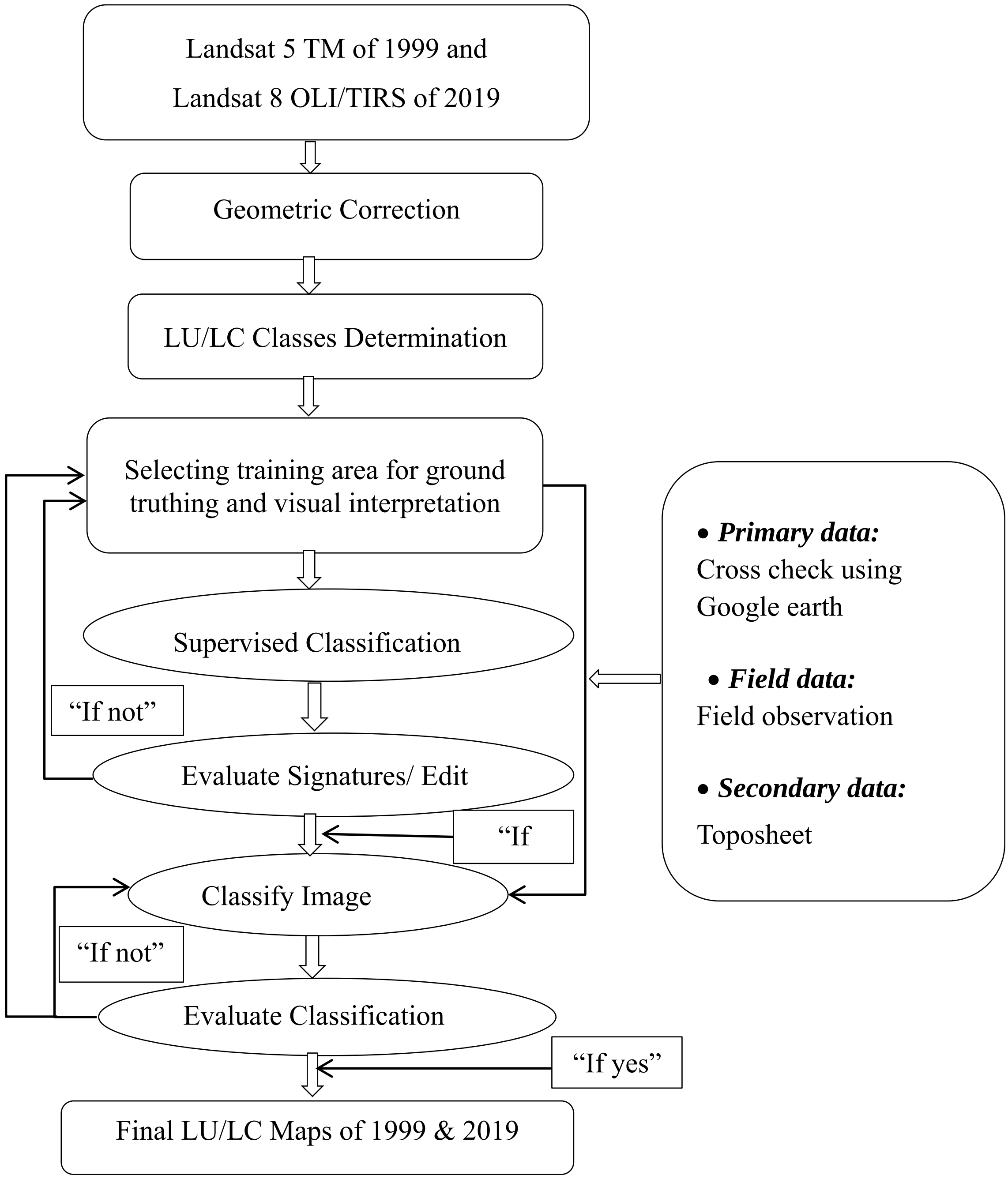

Figure: 3. 7. Steps followed to classify land-use/land-cover from a Landsat image.

3.5 Derivation of Land Surface Temperature

The activity of extracting Land Surface Temperature (LST) data from Landsat image is summarized as follows in figure 3.8 below and the detail data process of this flow chat is discussed in chapter four.

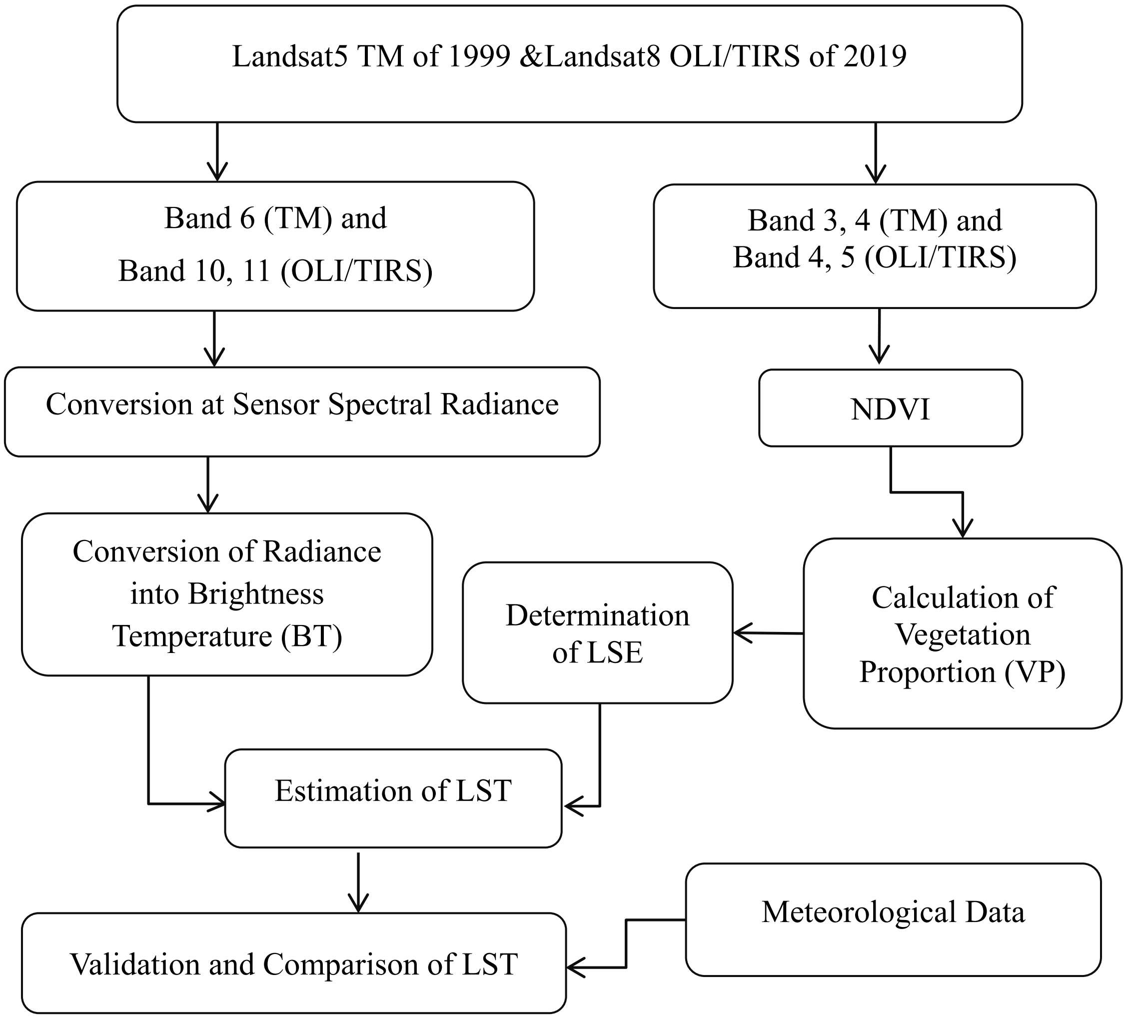

Figure: 3.8. Steps followed to retrieve LST from Landsat data

3.6. Zonal Statistics

A zone is defined as all areas in the input that have the same value. Zonal statistics function summarizes the value of a raster within the zones of another dataset (either raster or vector) and reports the results as a table and figure. Maps of LU/LC, NDVI and LST were prepared for the year 1999 and 2019. To examine the spatial difference of LST according to varies land classes; the result was summarized using the zonal statistics tool of the Arc

GIS10.3.Subsequently, summarized LU/LC, NDVI and LST map data were analyzed using excel. Zonal statistics as table and figure is one of important methods that used to examine the correlation between LU/LC, NDVI and LST.

3.7. Spatial Interpolation

Spatial interpolation is the procedure of using points with known values to evaluate values at other unknown points. For instance, to map rainfall and temperature of given area based up on nearby weather station. In present study, meteorological data was used to interpolate and see the result and compare with the LST values that were done from Landsat thermal infrared bands.

To interpolate rainfall and temperature data Inverse Distance Weighted (IDW) interpolation method was used. Inverse distance weighted is one of the interpolation methods in which the sample points are weighted during interpolation such that the impact of one point to another with distance declines from the unknown point. Inverse Distance Weighted is the simplest interpolation method and deterministic models. Deterministic models include IDW, rectangular, natural neighbors and spine. Interpolation uses vector points with known values to estimate unknown locations to create raster surface covering an entire area (Legates and Wilmont, 1990).

The reason why IDW interpolation method was used is that, in IDW interpolations different distances are integrated in the estimation; the distance weighting is able to precisely regulate the impact of the distances and it allows very fast and simple calculation. The output value for a cell using inverse distance weighting (IDW) is limited to the range of the values used to interpolate. Because IDW is a weighted distance average, the average cannot be greater than the highest or less than the lowest input. Therefore, it cannot create ridges or valleys if these extremes have not already been sampled. The influence of an input point on an interpolated value is isotropic. Since the influence of an input point on an interpolated value is distance related, IDW is not ridge preserving (Philip and Watson 1982). Therefore, in the present study rainfall and temperature data was interpolated using sample points in ArcGIS 10.3 environment and finally the interpolated maps were used for validation.

CHAPTER 4. DATA ANALYSIS, RESULTS AND DISCUSSIONS

4.1. Introduction

Landsat 5 TM and Landsat 8 OLI/TIRS image was acquired on May 12th 1999 and May 14th 2019 respectively. This Remote Sensing Data was used to derive LST, LU/LC and NDVI over the study area. The image, which was acquired from the United States Geological Survey (USGS), was captured under clear atmospheric conditions. At the time of image capture (May, 1999) the maximum temperature recorded in Dire Dawa City Administration was approximately 32.8°C and the minimum temperature recorded was 21.3°C. And also the maximum and minimum temperature recorded in May, 2019 was 33.1°C and 22.2°C respectively (NMA,2019).

It should be noted that when studying the LSTs contrasts, the SUHI intensities are at their greatest during the afternoon, at least during the warm season. This is the opposite of UHI results based on the measurement of air temperatures where the anomaly will typically reach its greatest intensity during the nighttime (Weng *et al*., 2004). Therefore, the selection of Spring or Tseday sesson (May) image, which was the best image available given that it was captured in the afternoon, is suitable.

The May 12th and 14th image was also selected for the reason that it falls within the early part of the warm season when green vegetation is likely to be in abundance. The presence of green vegetation is paramount to a study concerned with the association between LSTs and NDVI, as NDVI is an indicator of biomass production and is therefore impacted by seasonal changes (Yuan and Bauer, 2007). Another reason why this particular image was chosen has to do with the fact that for semi arid region, such as Dire Dawa City, UHI intensities are often strongest during the warm season (Voogt *et al*., 2004). Thus, a study which attempts to establish an understanding of how biological solutions might help to alleviate UHI's through the analysis of intra-urban relationships between LST and GI (the values of which are likely to vary significantly between seasons), becomes much more meaningful if the data used to derive these variables are captured during a time of year when heat island intensity is most extreme and poses the greatest risk to society.

4.1.1. Data Processing

i. Image Preprocessing: Satellite image by its nature have some distortion, noise, haze and others. Therefore, before processing the data, image pre-processing activities were done (Fei, Z., 2016). Preprocessing includes importing, layer stacking, and sub setting of the image based on the boundary of Dire Dawa City Administration, geometric correction, radiometric correction, and pan sharpening and other image enhancement techniques. Radiometric correction is a removal of atmospheric noise to make more representatives of the ground truth conditions based on the sensors. These all previously mentioned activities done were to improve visible interpretability of an image by increasing apparent distinction between the features in the scene. In addition, the image was also geo-referenced using boundary of the Dire Dawa City Administration. During geo-referencing and re-projecting process, WGS1984, UTM Zone 37N coordinate system was followed for raster and vector data in the study to maintain uniformity.

ii. Image Enhancement: The main purpose of image enhancement is to improve the interpretability of information in images for viewers, or to provide better input for other automated image processing techniques. Image enhancement is a procedure applied to image data in order to make more effective display or record the data for subsequent visual interpretation. Normally, image enhancement involves techniques for increasing the visual distinction between features in the scene (Billah, M., and Rahman, G., 2004).

iii. Image Classification: Digital image classification techniques assemble pixels to represent LU/LC classes. Image classification uses the reflectance statistics for individual pixels. Pixels were grouped based on the reflectance properties of pixels called clusters (Chen, X., 2000). The users identify the number of clusters to generate and which bands to use. With this information, the image classification software generates clusters.

In this study, multispectral band from band 1 to 5 and 7 of Landst5TM of 1999 and band 1 to 7 Landsat8 (OLI /TIRS) of 2019 are used. And land-use/ land-cover pattern was mapped using supervised classification with the maximum likelihood classification (MLC) algorithm in ERDAS Imagine 2014 software (Asubonteng, K. , 2007). The advantage of the supervised classification was development of information classes, self-assessment using training sites and training sites reusable. However, information classes may not match spectral classes, the signature homogeneity, uniformity of information classes may be varies and also, MLC is one of the most known methods of classification in remote sensing, in which a pixel with the MLC is classified into the matching classes (Pansi, O., 2013 and Yang, L., 2015). It is a statistical decision measure to assist in the classification of overlapping signatures; pixels are assigned to the class of the highest probability and considered as more accurate than parallelepiped classification (Coppin and Bauer, 1996).

Table: 4. 1. Land-use/land-cover classes and description of the study area

No.	**LU/LC Classes**	**Descriptions LU/LC Classes**
1	Shrubs Land	• Areas covered with shrubs, bushes and small trees, with little useful wood, mixed with some grasses and less dense than forests.
2	Sparse Vegetation	• Lands with a mosaic of forests, woody plants, trees, natural vegetation, gardens, parks and vegetated lands, agricultural lands, and crop fields.
3	Settlement	• Area occupied by houses buildings including road network residential, commercial, industrial, transportation, roads, mixed urban and other facilities.
4	Dry Water Body (Rivers)	• Areas previously covered by natural and manmade small dams, like pond and river and currently not existed or dried.
5	Bare Land	• Areas which are characterized by thin soil, sand/rocks including deserts, dry Salt flats, beaches, sand dunes, exposed rocks, stripe mines, queries and gravel pits/non-vegetated area dominated by rock out crops, roads, eroded and degraded lands.

[Dire Dawa Administrative Council and Office (2012)]

According to Dire Dawa Administrative Council and Office (2012), the land use/land cover types have been grouped into four major classes. They are designated as urban built up, physiognomic vegetation types, cultivated land, and bare land. In line with the major class identified by the office, the study adopts five major classes, which comprise bare land, settlement, shrub land, spares vegetation and dry rivers (Matiwos, B., 2018).

The supervised classification image of each year involves pixel categorizations by taking training area for each class of LU/LC. After the training area assigned for each classes, the classification activity was performed (Mohan, M. and Pathan, S., 2011). For bare land and spares vegetation LU/LC types taken 11 training site, shrub land and settlement LU/LC types taken 10 training site, where as for dry river was taken 8 training areas as sample. Areas in digital images were marked as signature of individual identity and the field truth verification was adapted to represent LU/LC classes.

iv. Post Classification: After all classification activity has been completed, the accuracy of the classification was checked. The classification accuracy requires the collection of some original data or a prior knowledge about some parts of the terrain, which can then be compared with classified map (Belete, T., 2017). Shortly, accuracy assessment is performed by comparing the created by RS analysis to a reference map based on a different information sources. The field survey and Google Earth were used as a ground for evaluation the LU/LC classification accuracy. The final output of classification accuracy was calculated for the years 1999 and 2019 LU/LC map.

Land-Use-Land-Cover change detection was continued after the classification accuracy was completed. The LU/LC change was done by involving images of 1999 and 2019. Using GIS techniques thematic image was compared. The cross operation process of mapping LU/LC over time began with mapping the recent 2019 satellite imagery, then looking back in time to map of 1999 imagery. Post classification is among the most widely used approach for change detection purpose (Chen, 2000; and Belete, T., 2017). The analysis of LU/LC maps involved technical procedures of integration ERDAS IMAGINE and ArcMap Software techniques. The first task was to develop a table indicating the area coverage in square kilometers and the percentage change for each year 1999 and 2019 measured against each LU/LC classes. Therefore, to calculate LU/LC in percentage equation (eq. 1) were used (Lambin *et al*., 2001).

$$\text{Percentage Change} = \frac{\text{Observed Change}}{\text{Sum of Area}} * 100 \qquad \text{Eq. (1)}$$

v. Green Infrastructure Data Extraction: According to Farooq (2012), the reason NDVI relates to vegetation is that, the one which is well vegetated reflects better in the near infrared part of the spectrum. Green leaves have a reflectance of 20% or less in the 0.5 to 0.7 range and about 60% in the 0.7 to 1.0 micrometer range. The value of NDVI is between -1 and 1. NDVI was acquired from spectral reflectance measurements in the visible (Red) and near infrared regions (NIR) in the ArcGIS environment. Equation 2 was used to calculate NDVI for the sensor TM 1999 and OLI/TIRS 2019. But in case of Landsat 8 NIR is band 5 and the red band is a band 4 (Weng *et al.*, 2004).

$$\mathrm{NDVI} = \frac{\mathrm{NIR} - \mathrm{R}}{\mathrm{NIR} + \mathrm{R}} \ldots\ldots\ldots\ldots \text{Eq. (2)}$$

Where, NDVI: Normalized Difference Vegetation Index NIR: is the near infrared band 4, R: is the red band3.

Proportion of Vegetation: Proportion of vegetation that helps in calculating Landsat 8 land surface emissivity (LSE). Based on the result obtained from NDVI values; the proportions of vegetation was determined by using the following equation 3 (Voogt, J. *et al*, 2000).

$$\mathrm{PV} = \left(\frac{\mathrm{NDVI}-\mathrm{NDVImin}}{\mathrm{NDVImax}+\mathrm{NDVI\ min}}\right)^2 \ldots\ldots\ldots\ldots \text{Eq. (3)}$$

Where, PV is proportion of vegetation, NDVImin and NDVI.max: normalized difference vegetation index minimum and maximum value respectively.

vi. Derivation of Land Surface Temperature

Radiometric Correction: Radiometric correction requires converting a remote sensing digital number to spectral radiance values. Image processing procedures that are used to correct errors, converting digital number (DN) values to radiance and then reflectance was categorized as a radiometric correction (Prata .A, 1999).

Conversion at Sensor Spectral Radiance: In radiometric calibration, pixel values, which were represented by Q in remote sensing raw data and unprocessed image data, were changed into absolute radiance values. The equation 4 was used to perform the conversion at sensor spectral radiance or satellite data scaled into 8 bits (Belete, T., 2017).

$$\mathbf{L\lambda} = (\mathrm{Lmax}\lambda - \mathrm{Lmin}\lambda) / (\mathrm{Qcalmax} - \mathrm{Qcalmin}) * (\mathrm{Qcal} - \mathrm{Qcalmin}) + \mathrm{Lmin}\lambda \ldots\ldots\ldots\ldots \text{Eq. (4)}$$

where; $L\lambda$: Spectral radiance at sensors aperture or the calculated radiance associated to the ground area enclosed in the pixel and referred to the λ wavelength range of specific band. Lminλ and Lmaxλ: spectral at sensor radiance minimum and maximum that is scaled to Qcalmin and Qcalmax respectively. Qcalmin and Qcalmax are minimum and maximum Quantized Calibrated Pixel values. Qcal: Quantized Calibration Pixel value (DN).

Conversion of Radiance into Brightness Temperature: Thermal infrared data can be converted from atmosphere reflectance (Lλ) to effective sensor brightness temperature (TB) using thermal constants provided in the Meta data file (Zhao, W. and Oke, J., 2014). Remote sensing data (Landsat imagery) thermal band that is band 6 on thematic mapper and band10 and band11 of OLI/TIRS were used from a sensor spectral radiance to effective at sensor brightness temperature. Brightness temperature is the radiance travelling upward from the top of earth atmosphere. To covert Lλ (spectral radiance) to TB equation 5 was used (Landsat Project Science Office, 2001).

$$\mathrm{BT} = \frac{\mathrm{K2}}{\ln(\frac{\mathrm{K1}}{\mathrm{L\lambda} + 1})} - 273.15 \text{..........} \text{Eq. (5)}$$

Where; TB: effective at satellite brightness temperature (unit in Kelvin) K2: calibration constant, Ln: natural logarithm K1: calibration constant, $L\lambda$: spectral radiance at sensors aperture.

Generally, to calculate LST for the sensor subtracting 273.15 from the existed result that is performed from effective at satellite temperature formula in Kelvin. Landsat 8 has two thermal bands (band 10 and band 11) and landsat5 TM has one thermal band (band 6). Table 4.2 and table 4.3 shows the calibration constant used during performing the formula for brightness temperature.

Table: 4. 2. Thermal Band Calibration Constant of Landsat 5 TM of 1999

Satellite	**Sensors**	**Categories**	**Band 6**
		K1	607.76
		K2	1260.56

Landsat 5 TM	Radiance_maximum_band	15.153
	Radiance_minimum_band	1.238
	Quantize_cal_max	255
	Quantize_cal_min	1
	Map_projection	"UTM"
	Ellipsoid	"WGS84"
	Utm_zone	38
	Grid_cell_size_reflective	30

[Source: Landsat-5 Metadata, Obtained from USGS, 1999]

Table: 4. 3. Thermal Band Calibration Constant of Landsat 8 OLI/TIRS of 2019

Satellite	Sensors	Categories	Band 10	Band 11
Landsat 8	OLI/TIRS	K1	777.8853	480.8883
		K2	1321.0789	1201.1442
		Radiance_maximum	22.0018	22.0018
		Radiance_minimum	0.10033	0.10033
		Quantize_cal_max	65535	65535
		Quantize_cal_min	1	1
		Resolution	100 * (30)	100 * (30)

[Source: Landsat-8 Metadata, Obtained from USGS, 2019]

Land Surface Emissivity (LSE): Emissivity is a ratio which compares the spectral radiant remittance of a surface to that of a blackbody at the same temperature (Artis and Carnahan, 1982). Land surface emissivity is an important parameter when deriving land surface temperature as the emissivity of a surface will influence the amount of thermal radiation that it emits. Land surface emissivity is determined by several factors including the chemical composition, roughness and moisture content of a surface. The emissivity of a surface can have values between 0 and 1; however, for most objects spectral emissivity is very close to 1. Equation6 below was used to determine emissivity (Sara *et al*. 2014).

LSE = 0.004Pv + 0.986................……….. …………………...……......................... Eq. (6)

Where, LSE is land surface emissivity and PV is the vegetation proportion.

Land Surface Temperature (LST): The spatial distribution of LST of the study area was extracted and quantified using Landsat5 TM of 1999 and Landsat8 OLI/TIRS thermal bands of 2019. LST was derived from Landsat TM band 6 and OLI/TIRS using band 10 and band 11 based on the following equation (Artis and Carnahan , 1982).

$$\mathrm{LST} = \frac{\mathrm{TB}}{1 + \left(\lambda * \frac{\mathrm{TB}}{\rho}\right) Ln\ \varepsilon} \ldots\ldots\ldots\ldots\ldots\ldots\ldots\ldots\ldots \mathrm{Eq.}\ (7)$$

Where; TB is brightness temperature, λ is wavelength of emitted radiance, ρ is h×c/σ (1.438×10^{-2} m K), σ is Boltzmann constant (1.38×10^{-23} J/K), h is Planck's constant (6.626×10^{-34}Js), c is velocity of light (2.998×10^{8} m / sec), ε is the surface emissivity.

Vii. Cooling Benefit Analysis

Proximity to Existing Green Infrastructure (GI): The Millennium Park, with the area of 8 hectare, has been constructed in 2000.EC, and become a recreational center. It is covered with trees, grasses, shrubs and other man-made infrastructures. The buffer zone of the park mainly includes green and grey spaces, where grey spaces refer to buildings, roads, etc.

The purpose of identifying the existing GI and evaluating the current cooling benefits is an important indication for proposing the green infrastructure on the identified hotspot locations. Therefore, evaluating the proximity of existing green infrastructure was used to predict the direct cooling benefits from optimizing the potential green infrastructures on identified hotspot area.

Determination of the buffer interval is adjusted to the map scale used that can determine the minimum mapping unit (Suryandari and Widyatmant, 2018). At the scale used for 1: 100,000 even though the buffer display results are made on a scale of 1: 50,000 but the scale used refers to the scale used to map the land surface temperature and NDVI, then the minimum mapping unit to do is 10mm which is equivalent to 100m (spatial resolutions of band 10 and 11) in the field, so that 100m interval for LST can be used.

Although LST is routinely derived by satellite OLI/TIRS observations, currently, there is no space borne sensor capable of providing frequent thermal imagery at the spatial resolution needed in urban studies (local scale). Landsat series of satellites retrieve

OLI/TIRS data at a resolution between 60m and 120m, with the recently launched Landsat 8 that measures radiation in two thermal bands (bands10 and 11) of 100m spatial resolution (Roy; Becker F & Anderson, 2014).

Millennium Park in study area was selected to analyze the cooling benefits of the existing green infrastructure. For a detailed study on the gradient changes of the green infrastructure and its surface temperature, the 500m buffer zone of the Millennium Park was used. Firstly, the area was delineated at 500m and divided to five rings in increments of 100m, which the first ring had a 100m distance from the edge of the park, and finally, LST and land covers types of each section as well as the entire study area were studied. The result obtained from this analysis will be used to propose the local and regional cooling benefits for optimizing the spatial locations of green infrastructure on identified hotspot locations.

Mathematical optimization model was structured to identify the best locations for new green infrastructure (GI) in order to realize the greatest overall benefits. The approach taken from model of (Church and Re Velle, 1974) and also from (Murray, 2009); (Tong & Kim, 2010) in a number of ways especially, the nature of benefits differs, where βi accounts for direct cooling benefits. These basic types of cooling benefits can be characterized mathematically. For a given area *i* (cell, hotspot land zone), let βi represent the temperature reduction possible if it is GI. The cooling benefit is location dependent, affected by the surrounding land cover as well (Cheng *et al.*, 2015). Given the temperature for an area as it currently exists (Ti) and the anticipated temperature if it will be converted to GI, Ti', then the direct cooling benefit to area *i* derived as follows: (Yujia *et al*. 2018).

$$\beta_i = T_i - T_i' \quad \text{Eq. (8)}$$

Where, β_i *is* cooling benefit, T_i *is* temperature for an area as it currently exists, T_i' is expected temperature if area i is converted to green infrastructures.

In general, expected temperature is a function of temperature for an area as it currently existing (T_i) and land use land cover classes of observed characteristics for each area and *i* is index of potential GI areas:

$$X_i = \begin{cases} 1 \text{ if area } \boldsymbol{i} \text{ converted to GI} & \text{Eq. (9)} \\ 0 \text{ otherwise;} \end{cases}$$

Maximize $\Sigma\, \beta_i\, X_i$ ....Eq. (10)

The objective of Eq. (11) is to maximize the total sum of cooling benefits

$\Sigma\, X_i = p$..Eq. (11)

Objective 11 specifies that p areas are to be converted to GI. The value of p is predetermined base on the goals associated with the City's plan (Tendayi, G., 2014; and DDCA, 2015). But in this study, the identified hotspot area was used.

4.2. Data Analysis and Results

4.2.1 Land-Use/Land-Cover Analysis

Based on the land use/land cover class type adopted from Dire Dawa Agriculture Bureau, five major classes were classified for both study years (1999 and 2019). The classification was intended to produce land use land cover change for 20 years and compare against land surface temperature change. Land use land cover map of Dire Dawa City for 1999 and 2019 study years with five major categories namely settlements, bare land, shrub land, sparse vegetation and dry rivers were generated. The supervised maximum likelihood algorithm was applied and total area with its percentage was calculated, as table 4.4 below.

Table: 4.4. Land-Use/Land-Cover classes and area coverage of 1999 and 2019

		1999		**2019**		**Net changing (km²)**
No.	**Class name**	**Area (km²)**	**Percentage (%)**	**Area (km²)**	**Percentage (%)**	
1	Sparse Vegetation	13.33	19.37	10.07	14.63	-3.26
2	Shrub Land	16.53	24.02	17.61	25.59	+1.08
3	Settlements	15.1	21.94	19.62	28.50	+4.52
4	Bare Land	23.41	34.01	21.19	30.79	-2.22
5	Dry River	0.46	0.67	0.34	0.49	-0.12
Total		68.83	100.00	68.83	100.00	

According to table 4.4 and figures 4.1, in 1999, LULC of bare land (23.4km²) and shrub land (16.53km²) takes the largest portion followed by settlements area (15.1km²) and sparse vegetation (13.33km²). The least share of LULC category was dry rivers with a total area of 0.46km².

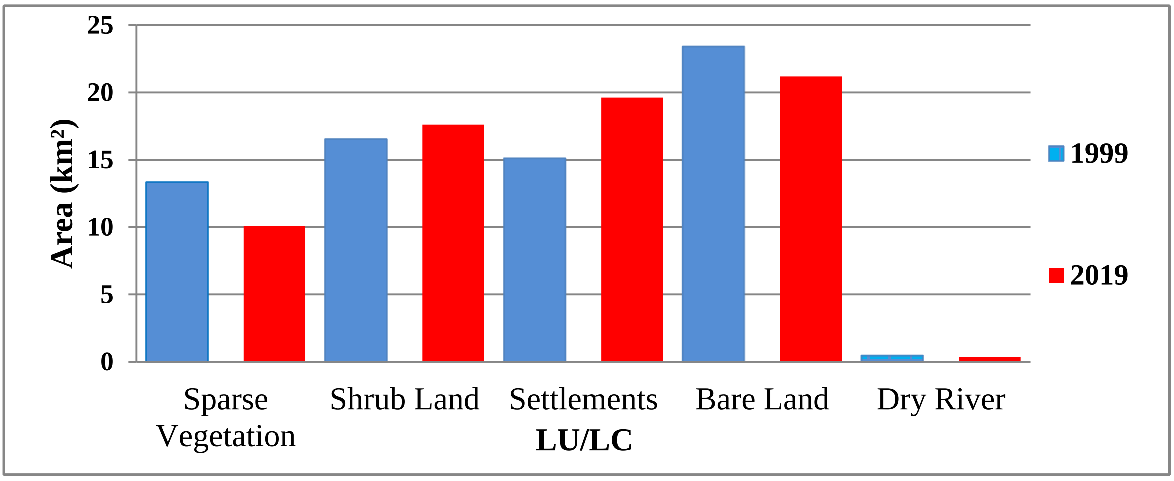

Figure: 4.1. Land Use Land Cover Classes during 1999 and 2019

In 2019 or after 20 years, the total area of bare land is grater (21.19km²) and followed settlements (19.62km²). Shrub land area had also grown having a total area of 17.61km² and dry rivers (0.34km²). Therefore, in both years the dominant class of LULC was bare land. However, the extent of settlements in 2019 increased by 4.52km² (28.5%) from 1999 than shrub land which is increased by 1.08km² (25.59%). On the other hand, the above table 4.4 and figure 4.1 also depicts that, the least dominant type of LULC was dry rivers.

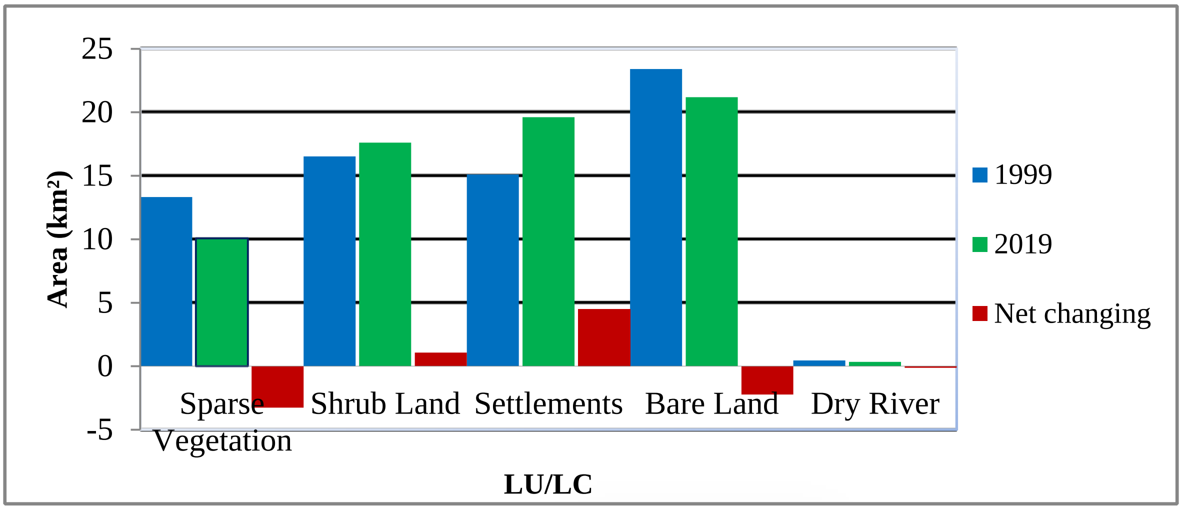

Figure: 4.2. Land Use Land Cover Changes during 1999 and 2019 in Dire Dawa City

LU/LC changes of 20 years were calculated using change detection matrix to point out the rate of change and conversion. Evidently, Table 4.1 and figure 4.2 shows, for the last 20 years there has been a radical increase in areal extent and coverage of settlements from 15.1km^2 (21.94%) to 19.62km^2 (28.50%) which is about 4.52km^2 (increased by 6.56%) area and followed by shrub land area 16.53km^2 (24.02%) to 17.61km^2 (25.59%) which is about 1.08km^2 (increased by 1.57%).

In contrary to settlements and shrub land, bare land has shown a considerable decrease in areal extent from 23.41km^2 (34.01%) in 1999 to 21.19km^2 (30.79%) in 2019. Thus, a total area of 2.22km^2 has been converted in to other LULC classes. In addition, sparse vegetation has been steadily decline from 13.33km^2 (19.37%) in 1999 to 10.07km^2 (14.63%) in 2019 which is about 3.26km^2. Consequently, 3.26km^2 sparse vegetated areas were converted in to shrub lands and settlement area. Even though it is minimum in comparison with sparse vegetation, dry rivers has been shown a slight reduction from 0.46km^2 (0.67%) in 1999 to 0.34km^2 (0.49%) in 2019 with a total area of 0.12km^2.

Settlements area shows rapid expansion than other LULC. It is parenting that, the expansion of settlement is due to high population growth and rural urban migration which accompanied with informal settlement (Mohan, M. and Pathan, S., 2011).

In the first census 1984, the total population of the City was 99,980 and in the second census 1994, it was grown to 173,000 and also increased to 188,000 in 1999 by 2.73%. In the third census the population number was increased to 274, 292 in 2015. The total population of the City in 2019 was 391,000 growth rates of 4.27% from 2018 (Dire Dawa Finance Economy Development Bureau, 2019).

Therefore, population size have been increasing from time to time hence, due to the growth of Dire Dawa City, settlements area has been considerably grown and barren land and sparse vegetated has been converted in to settlements area.

Shrub land area was the second LULC class that shows rapid expansion next to settlements area. With regard to shrub land, for the last three decades it has been expanded rapidly.

Particularly, alien plant species named Prosopis juliflora scores fast rate of expansion. Prosopis juliflora is a permanent dry land tree or shrub, fast growing, often ever green and drought resistant plant of desert and semi desert areas and it is now a serious topic in Ethiopia especially in Dire Dawa City (Tessema, 2012 and Zeray, 2017). The rate of expansion of Prosopis juliflora species is alarming and fast in nature (FAO, 2006).

According to Dire Dawa City municipal office, the most dominant tree species identified include Prosopis juliflora, Tamarix aphylla, Calotropis procera, Parkinsonia aculeata, Balanites aegyptica, Dodonaea, Acacia species, Combratum molle and Azadirachta indica (Pansi, O., 2013 and Yang, L., 2015). From those identified tree species, Prosopis juliflora is the most common and rapidly invading tree. From invasive plant, Prosopis juliflora has a characteristic of vigorous growth, which helps them to compete with indigenous plant species to cover huge areas of land in a relatively short period.

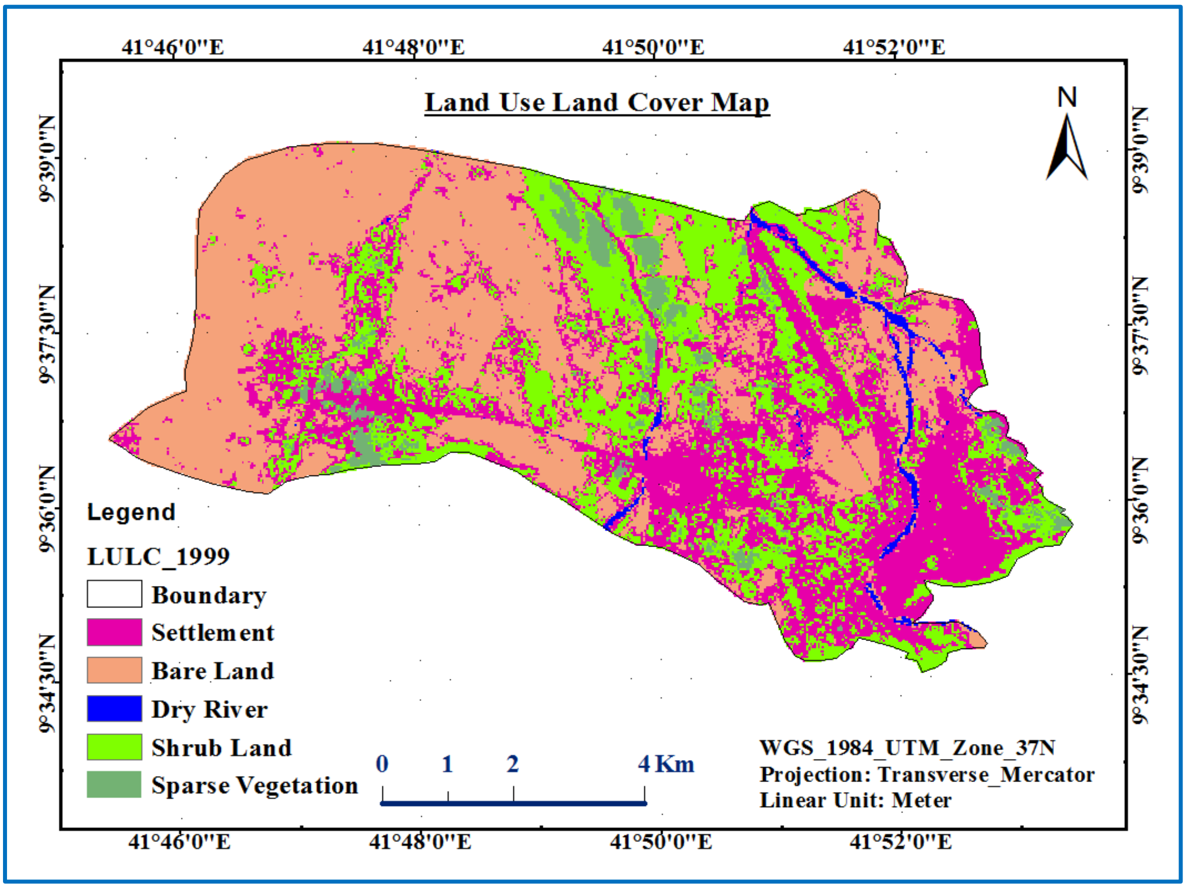

Figure: 4.3. Land Use Land Cover Maps of the Study Area of the year of 1999

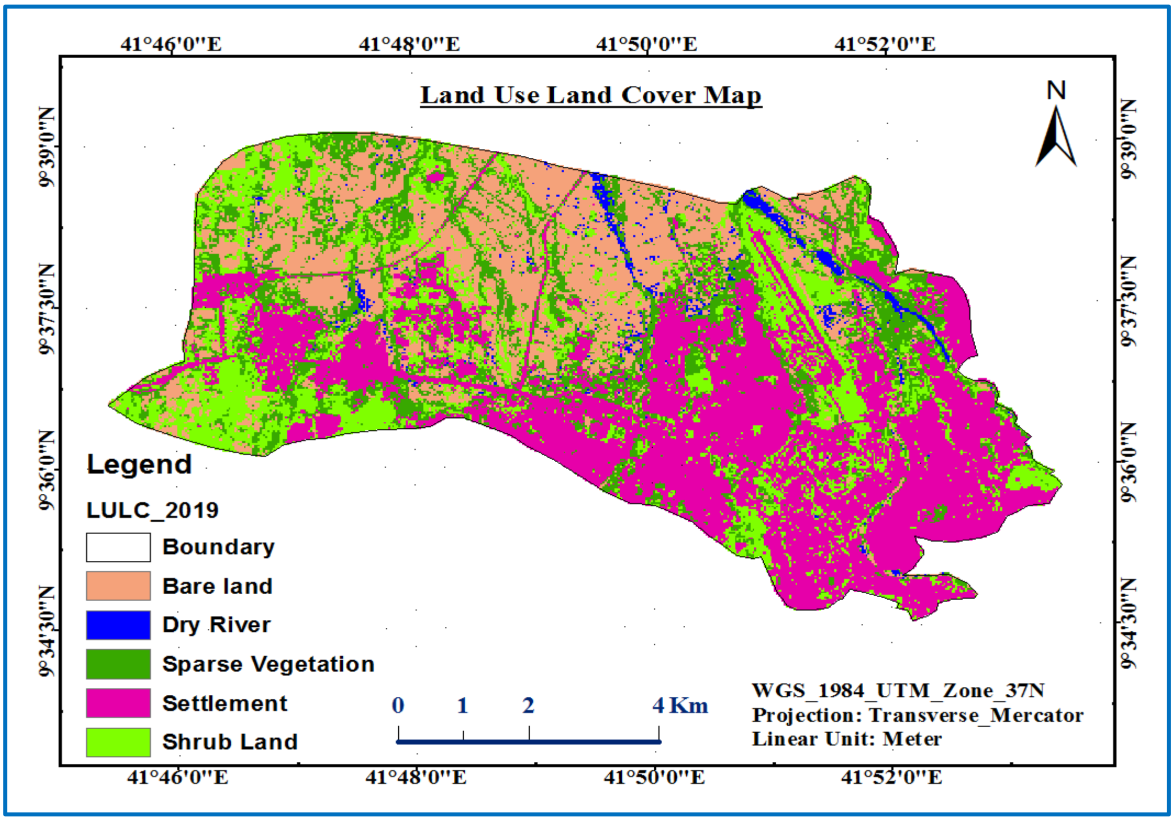

Figure: 4.4. Land Use Land Cover Maps of the Study Area of the year of 2019

The accuracy assessment of LU/LC for the years 1999 and 2019 recorded the overall classification accuracy of 88.00% and 90.00% respectively. The classification Kappa statistics for the year 1999 and 2019 values are 0.8575% and 0.8897% respectively. The detailed information of producers and users accuracy is indicated in (Appendix 2A & B) and table 4.5 below.

Table: 4.5. Statistical information of accuracy assessment for the year 1999 and 2019

Class Name	1999		2019	
	Producers Accuracy	**Users Accuracy**	**Producers Accuracy**	**Users Accuracy**
Settlement	90.00%	90.00%	100.00%	93.33%
Bare Land	90.90%	90.90%	77.78%	87.50%
Dry Rivers	87.50%	87.50%	100.00%	100.00%
Shrub Land	90.00%	81.82%	90.00%	81.81%
Sparse Vegetation	81.82%	90.00%	84.62%	91.67%
Over all Classification Accuracy	88.00%		90.00%	
Overall Kappa Statistics	0.8575%		0.8789%	

4.2.2. Normalized Difference Vegetation Index (NDVI) Analysis

The vegetation cover of Dire Dawa City is quantified and extracted from remotely sensed images of 1999 and 2019. The value of NDVI ranges from +1 to -1 where positive value indicates high vegetation cover and negative value indicates less vegetated area. Very low value of NDVI (0.1 and below) correspond to barren areas of rock, sand, or snow. Moderate values represent shrub and grassland (0.2 to 0.3), while high value corresponds to dense vegetation (0.6 to 0.8). Bare soil is represented with NDVI values, which are closest to 0 (zero) and water bodies, are represented with negative NDVI values (Gandhi and Christy , 2015).

Table: 4.6. Normalized Difference Vegetation Index 1999-2019

No.	Class Name	1999 NDVI				2019 NDVI			
		Min	Max	Mean	STD	Min	Max	Mean	STD
1	Bare Land	0.120	0.267	0.193	0.271	0.02	0.27	0.125	0.018
2	Settlement	-0.38	0.541	0.086	0.424	-0.12	0.37	0.145	0.032
3	Sparse Vegetation	0.195	0.674	0.4345	0.239	0.23	0.53	0.38	0.038
4	Shrub Land	0.097	0.565	0.331	0.234	0.15	0.48	0.315	0.037
5	Dry River	0.015	0.098	0.055	0.039	0.05	0.073	0.062	0.023

Table 4.6, figures 4.5 and 4.6 reveal that, the highest NDVI value for 1999 was 0.67 and lowest negative value of -0.38 was recorded. In 2019, highest NDVI was 0.53 and lowest was -0.12. In comparison to each LULC class in 1999, dry rivers have shown lowest mean value of NDVI 0.055 followed by settlement 0.086 and bare lands 0.193. And also sparse vegetation recorded highest NDVI mean value of 0.43 followed by shrub land 0.33. In 2019, the NDVI mean value of sparse vegetation was high 0.38 and shrub land 0.31. The least NDVI mean value was recorded for dry rivers 0.03 and bare land 0.12 respectively. The negative NDVI value which is recorded at settlement area is shows the existing artificial water (swimming pool) around built up area and recreational places in the City.

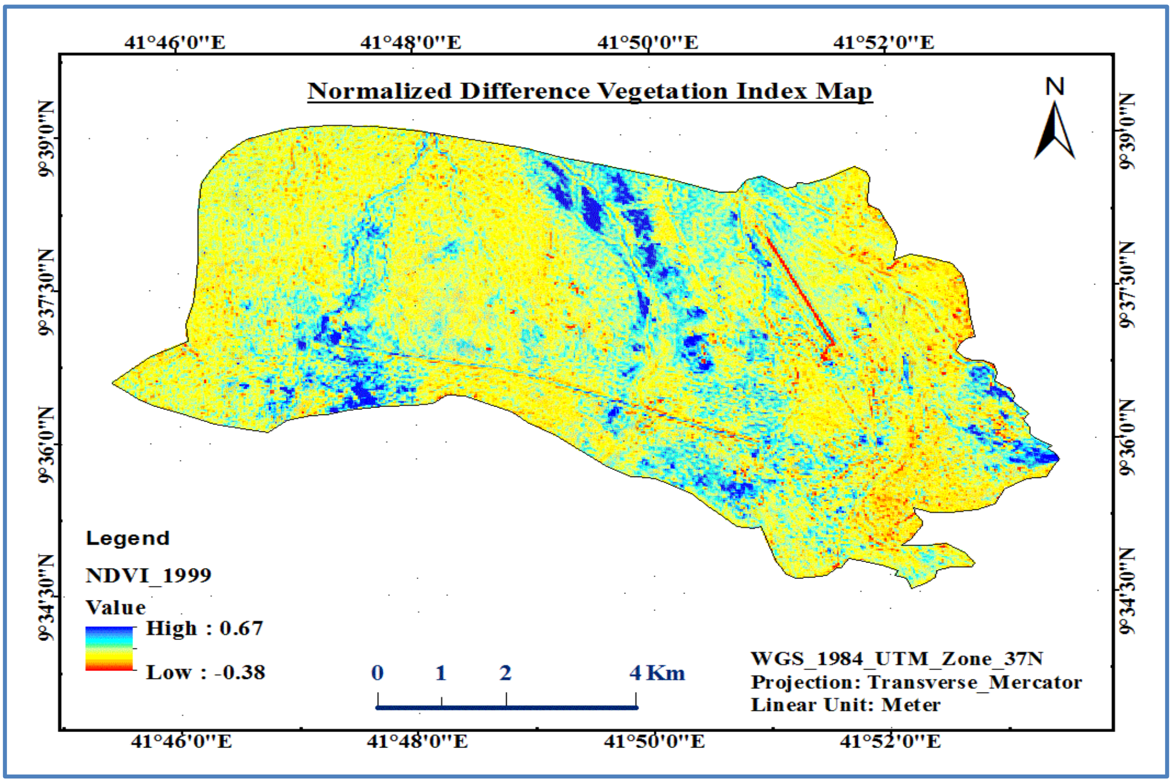

Figure: 4.5. NDVI maps of the study area of the year of 1999

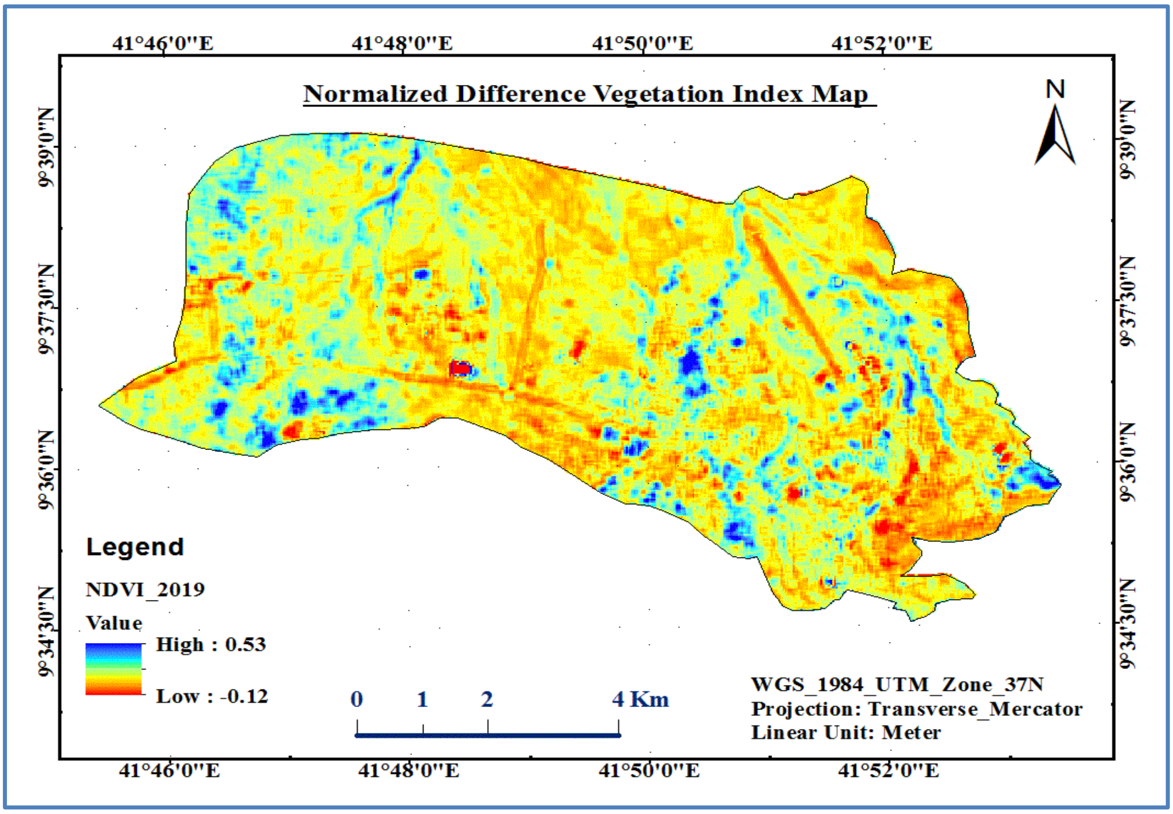

Figure: 4.6. NDVI maps of the study area of the year of 2019

4.2.3. Analysis of Spatial Pattern of LST in the Study Area

The spatial distribution of LST of the study area was extracted and quantified using Landsat5 TM of 1999 and Landsat 8 of 2019 OLI/TIRS thermal bands. The analysis from such images indicated that the LST value of year 1999 ranged from 16.19°C to 33.03°C and ranged from 20.66°C to 36.89°C in 2019.

Table: 4. 7. Land Surface Temperatures of 1999-2019

		1999 LST (°C)				2019 LST (°C)			
No.	**Class Name**	**Min**	**Max**	**Mean**	**STD**	**Min**	**Max**	**Mean**	**STD**
1	Bare Land	24.89	33.03	28.96	0.211	28.11	36.39	32.25	0.37
2	Settlement	21.19	31.47	26.33	0.063	23.67	33.89	28.78	0.91
3	Sparse Vegetation	19.74	27.84	23.79	0.034	21.51	27.29	24.39	0.69
4	Shrub Land	16.19	29.04	22.62	0.071	20.66	27.04	23.51	0.88
5	Dry River	25.31	31.66	28.485	0.825	26.75	34.15	30.45	0.34

Table 4.7 shows the estimated value of five major LULC categories. In 1999, the maximum temperature was recorded 33.03°C with minimum temperature value of 16.19°C. On the other hand, on 2019, the highest temperature recorded was 36.89°C and the lowest temperature was 20.66°C. Therefore, the average LST of overall area for the two observation years has increase from 24.61°C to 28.77°C. Accordingly, in 1999 bare land area exhibit the highest LST having mean value of 28.96°C with a standard deviation of 0.211. Dry rivers and settlement has also exhibited high LST with a mean value of 28.485°C and 26.33°C respectively.

On the other side, sparse vegetation and shrub land show lower LST having a mean value of 23.79°C and 22.615°C with a standard deviation of 0.034 and 0.071respectively.In 2019, the estimated LST value of bare land area exceeds other LULC class with a mean value of 32.25°C and standard deviation of 0.37. Settlement and Dry river area has also exhibit the high LST value having mean of 28.78°C and 30.45°C with standard deviation of 0.91 and 0.34 respectively. On the other hand, sparse vegetation and shrub land shows the lower LST value having mean value of 24.39°C and 23.51°C with standard deviation of 0.69 and 0.88 respectively.

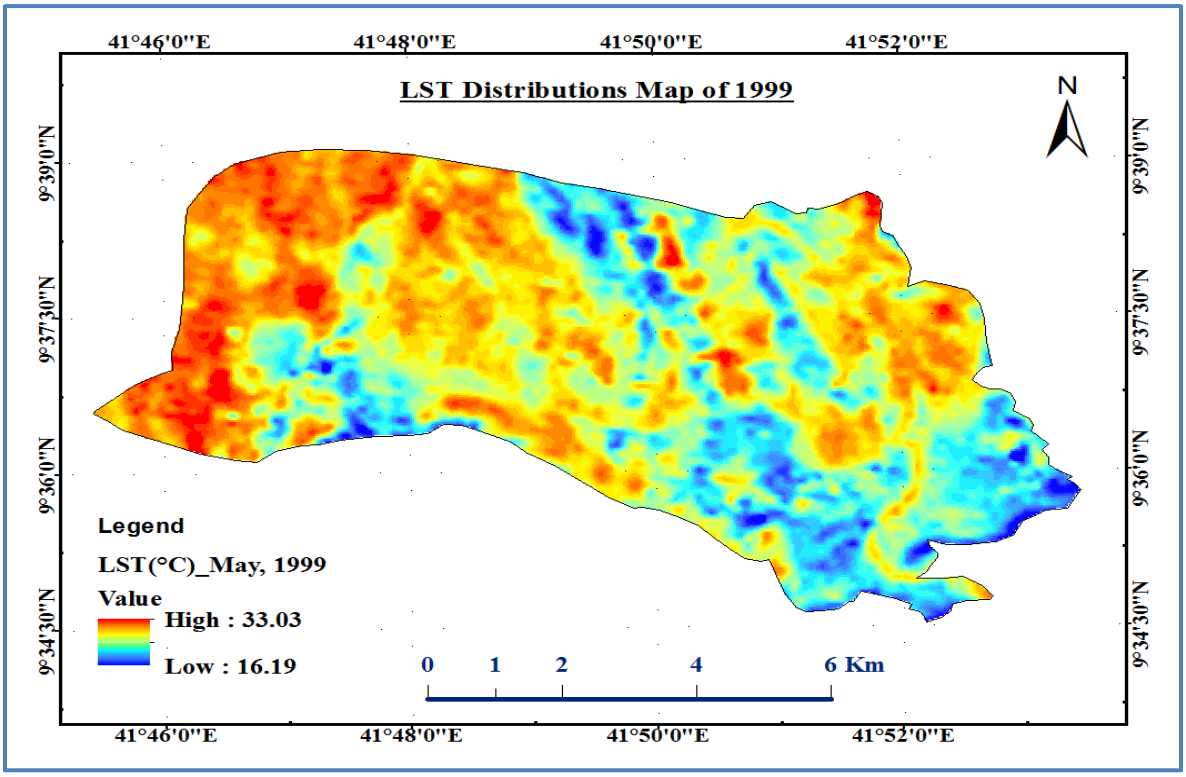

Figure: 4.7. Reclassified LST maps of the study area May, 1999

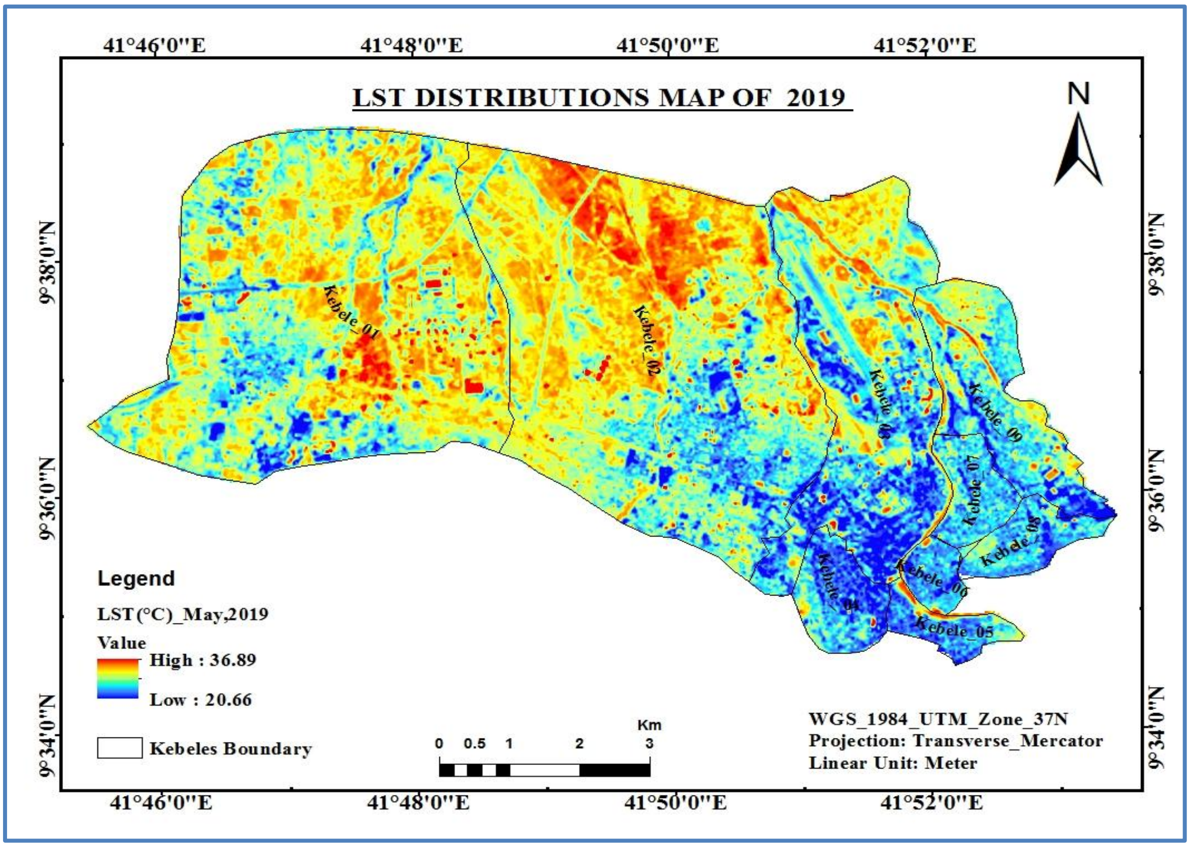

Figure: 4.8. Reclassified LST maps of the study area, May, 2019

The spatial pattern of LST in the study was further quantitatively investigated using Global Moran's I statistic for spatial autocorrelation. The spatial autocorrelation analysis parameters/conceptualization used here are a fixed distance conceptualization, with a distance threshold / bandwidth of 500 meters, and the Euclidean distance method was applied.

The result of the Moran's I spatial autocorrelation analysis is shown in (Appendix_4B). The result of spatial autocorrelation analysis for both years show positive Moran's I index values of greater than 0.6, z-scores of greater than 220 at $p < 0.001$. This suggests that there is a significant clustering of LST values in the study area. The observed positive spatial autocorrelation is for all the years in the study area. The result of the spatial autocorrelation analysis suggests that LST in the area may be driven by a certain underlying geographic process such as land cover type, etc.

4.2.4. Hot Spot Analysis

Hotspots are the result of two interrelated factors: the magnitude of changes in average weather at the local level; and the relationship between weather and living standards in that location. Identifying hotspots is finding the regions where vulnerability to changes in average weather is projected to be the largest. Based on the climate vulnerability assessment method, exposure layer and sensitivity layers were used (see Appendix 5A) as an indicators of hotspot location.

i. Land use Land cover: In order to identify the LST hotspot area in different LULC, the study was classified in to five classes based on the criteria set by different authors and literature and in relation with the objectives of the study. These classes were analyzes the effects of LULC changes in terms of population density, the surface type, and vegetation covers. Similar indicators have been used for sensitivity analyses by (Gebreegziabher *et al*., 2016; Zurovec *et al*., 2017).

As shown in table 4.4, for the last 20 year the LULC change was mainly due to increasing the number of population in the City. On average the number of population was increased by growth rates of 4.27%. High population density was at Sabian (31,215/km^2) and sparsely populated at Addis ketema (18,032/km^2) in 2019 as projected by Central Statistical Authority.

Based on this indicators, the distributions of LST in different LULC classes from Landsat image, the image was categorized into five zones by using Natural break (Jenks) classification method (Nyoni *et at,* 2017), and also standard deviation classification method was used to check the accuracy of classes, based on their pixels (Fei, Z., 2016). And to be more representative of the relationship between temperature variations in the pixels, the number of pixel versus LST frequency histograms was analyzed as shown in (Appendix 3).

As shows on (Appendix 3), majority of the pixels are above 23°C which are settlements, bare land in the northwestern part of the study area, where bare soils and the dry rivers are located. The land use and land cover types, such as settlements land, bare land and dry rivers had temperature between 28°C and 36°C. These LULC types are asphalt road, saline-alkali soil and the desert features in the City.

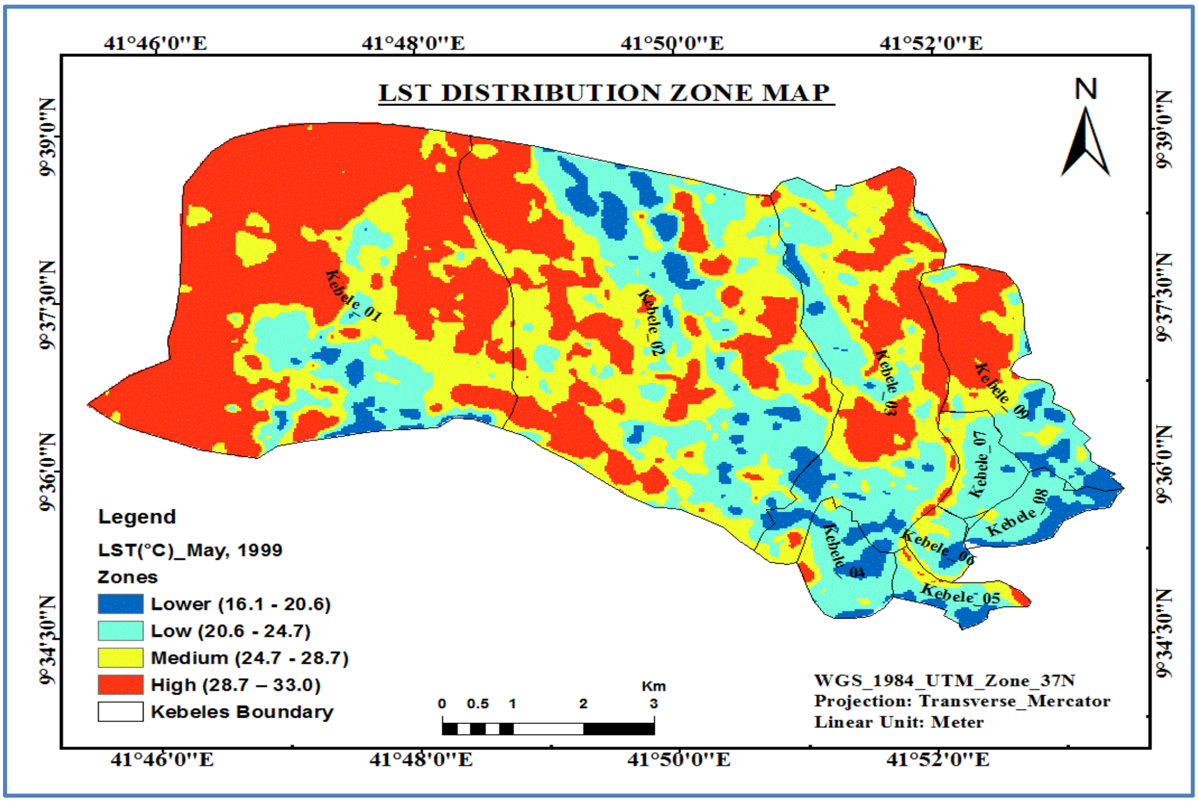

Figure: 4.9. The distributions of LST zones in to different LULC types in 1999

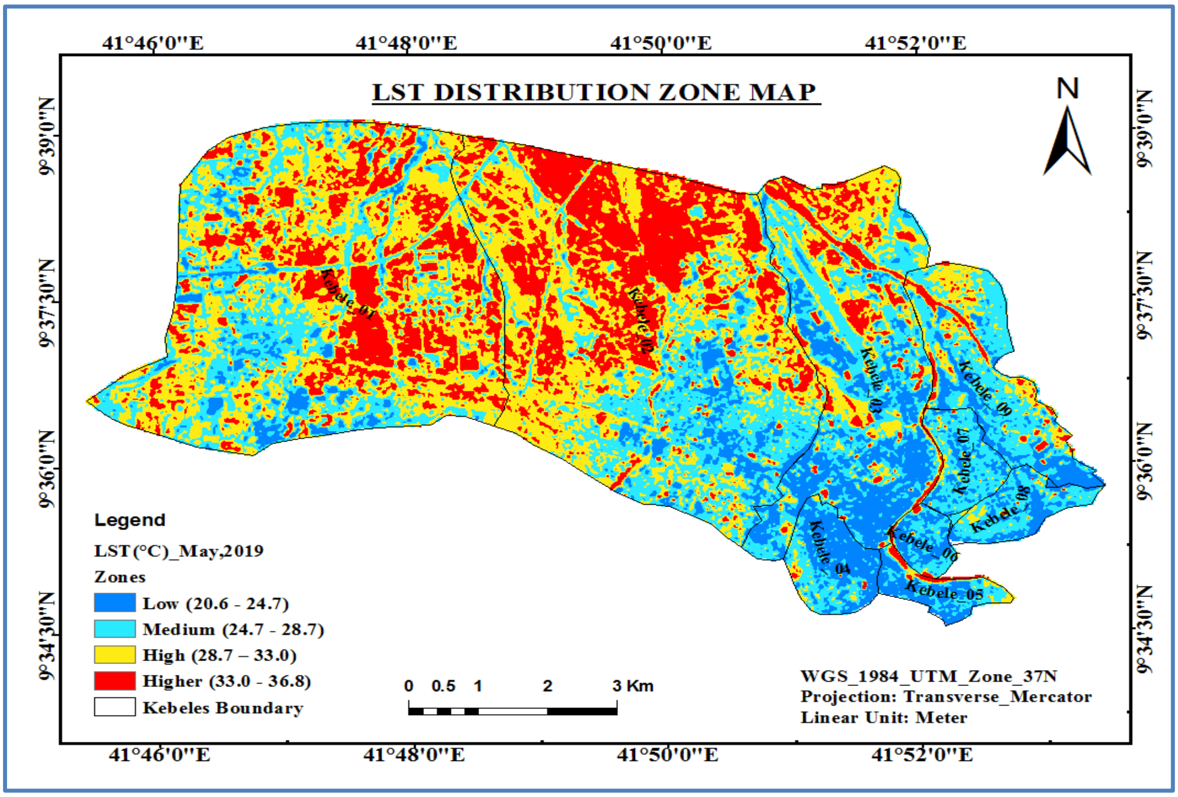

Figure: 4.10. The distributions of LST zones in to different LULC types in 2019

In the both year (figure.4.9 and 4.10), sparse vegetation and shrub land had a low temperature compare to other LULC types. In 2019, the LST distribution was compatible with the LULC types, indicating that a single type of LULC which relatively concentrated and caused large changes in temperature between every land type. Dry rivers and bare land had categorized under high and higher LST zones respectively. Settlements were found in both medium and high LST zone. In 1999, sparse vegetation land and Shrub land were in both LST zone, lower LST zone and low LST zone**.** And also, Dry Rivers and bare land surrounding the study area was in the high LST zone and the higher LST zone, respectively. Settlements were found in both medium and high LST zone this is because of vegetation's around the built up area.

ii. Land Surface Temperature (LST): The mean temperature changes are widely used in climate change exposure analyses. Under temperature change layers two sub-layers have been prepared. One is air temperature change layer, which obtained from direct measurement of meteorological stations from Dire Dawa City and the other is the LST change layer, which were derived from consecutive Landsat satellite images.

As shown previously in (figure.4.7 and 4.8), the LST images between 1999 and 2019 had changed. The temperature in the southeast of the City was lower than the surrounding temperature. The highest temperature distributions were located along the north, central and northwest direction in 2019, but in 1999, the temperature distribution was oriented in to northwest directions. This phenomenon is known as the hotspots or hot island.

Table: 4. 8. The area and percentage of the different land surface temperature zones

Grade	1999 LST (°C)	Area (km^2)	Percentage (%)	2019 LST (°C)	Area (km^2)	Percentage (%)
Lower LST Zone	16.1 - 20.6	8.19	11.90	_	_	_
Low LST Zone	20.6 - 24.7	13.43	19.50	20.6 - 24.7	13.14	19.74
Medium LST Zone	24.7 - 28.7	24.82	36.05	24.7 - 28.7	24.15	35.07
High LST Zone	28.7 – 33.0	22.41	32.55	28.7 - 33.7	22.12	32.13
Higher LST Zone	_	_	_	33.7 - 36.8	9.44	13.06
Total	_	68.83	100	_	68.83	100

As a whole, the temperature in 1999 is lower than in 2019. By using Jenks natural breaks classification adopted from (Weng, Liu *et al*. 2008), LST was classified into five zones: lower zone (16.1~20.4°C), low zone (20.4~24.7°C), medium zone (24.7~ 29.4°C), high zone (29.4 ~33.5°C) and the higher zone (33.5~36.8°C).

In 1999, there were four temperature categories, i.e., the lower LST zone, the low LST zone, the medium LST zone, and the high LST zone. The medium LST zone had the largest area at about 36.05% of the total area, and the high LST zone was the second largest at about 32.55%. But in 2019, the medium LST zone composed the largest area up to 35.07% of the total area. The high LST zone was the second largest area at up to 32.13%.

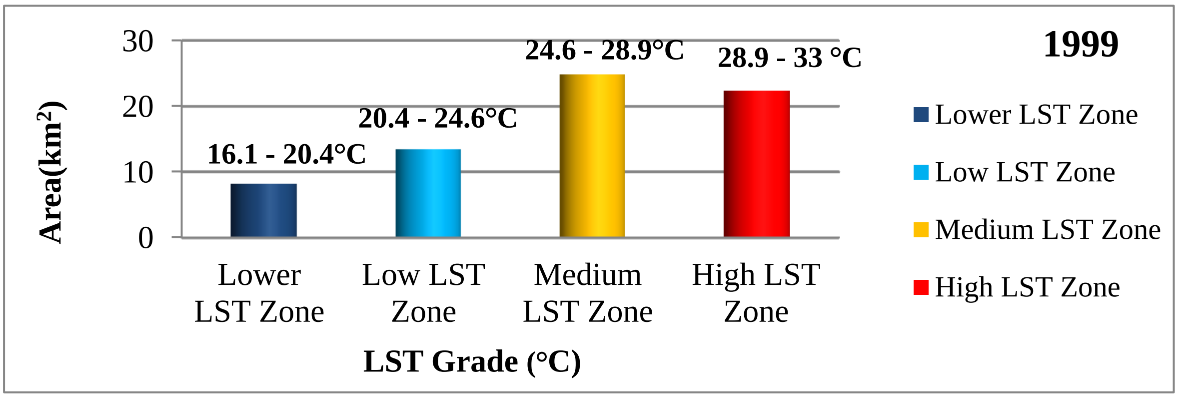

Figure: 4.11. Different land surface temperature zones and its area coverage’s in 1999

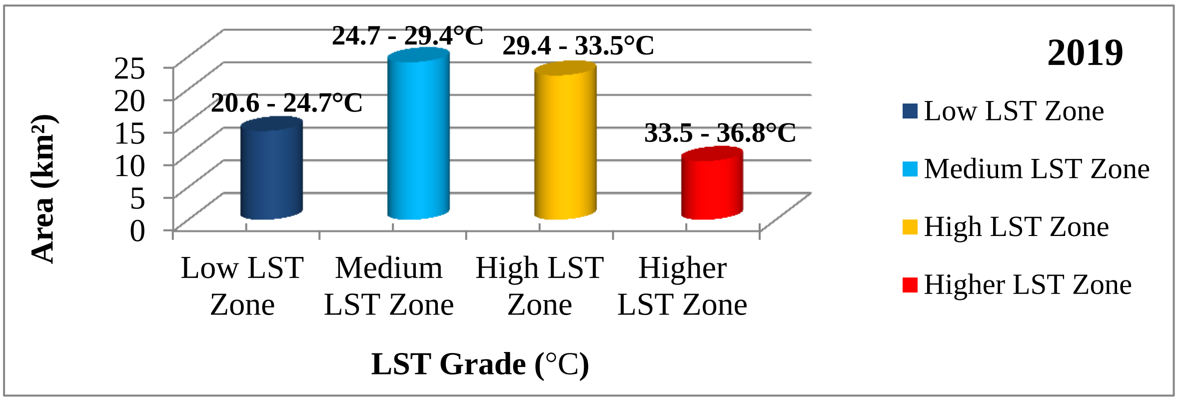

Figure: 4.12. Different land surface temperature zones and its area coverage's in 2019

In 1999 as shown in figure 4.11, there was a lower LST zone (16.1~20.4°C), but not in 2019. Furthermore, there was a higher LST zone (33.5~36.8°C) in 2019. From 1999 to 2019, lower LST zone, high LST zone, and higher LST zone had the greatest change in total area. However, there was no higher LST zone in 1999, and there was no lower LST zone in 2019. Thus, this change indicates the existence of the build-up retrieval that occurred from 1999 to 2019. Based on the above analysis to validate the location of the higher LST/hotspot zones, the meteorological sample was used based on identified LULC types (see Appendix 1-B).

The meteorological sample obtained from study area. The average temperature recorded for this LULC classes were 30.8 ± 2.25°C. The mean LST obtained from Landsat image was 28.66°C. Within the LULC types, the mean temperature recorded for settlements were approximately 31.77 ± 2.25°C, for GI (both Shrub and Sparse Vegetation land) were 25.26 ± 2.17°C and Bare land including Dry Rivers were 37.77 ± 2.2.67°C. Among the sample locations, the highest temperature (39.3 ± 3.46°C) was recorded at bare land and dry river having 37.8 ± 2.26°C, followed by Settlement LULC type such as Cotton Factory (35.8 ± 2.56°C), Taiwan Market (36.7 ± 2.57°C) and 34.4 ± 2.51°C recorded from Cement Factory area, whereas the mean lowest temperature (25.26 ± 2.17°C) was recorded within sparse vegetation and shrub land classes, such as the premises of the Dire Dawa University (Toni Agriculture, 25.2 ± 2.41°C) and at Millennium Park (24.9 ± 1.75°C) and Gendegara mountain (24.1 ± 1.29°C). The study is located on lowland along the East African rift valley, with relatively flat topography. The sample locations are at a mean elevation value of 1198.44m a.s.l and average humidity of 38.8%.

The mean difference of LST ranges from 3.29°C in bare land to 0.6°C in sparse vegetation. The metrological sample shows the same result with that of LST zones extracted from Landsat image. Both results from air and LST change indicates that high rate of change is found in the northern and northwestern parts of the study area, while the high vegetation parts of the City have low magnitude of change in temperature as shown in table 4.9.

Table: 4. 9. Mean changes of LST over LU/LC types during 1999−2019

No.	LU/LC Classes	Mean 1999 LST(°C)	Mean2019 LST(°C)	Temperature Mean (°C)	Change LST (°C)
1	Bare Land	28.96	32.25	33.42	+3.29
2	Settlement	26.33	28.78	30.14	+2.45
3	Sparse Vegetation	23.79	24.39	24.45	+0.60
4	Shrub Land	22.62	23.51	23.27	+0.89
5	Dry River	28.49	30.45	31.65	+1.96

General the result indicates that the highest exposure and sensitive area were in bare land (3.29°C), settlement (2.45°C) and some part dry rivers (1.96°C). Others areas have low exposure to hotspot. The least exposure was green areas such as shrub land (0.89°C) and sparse vegetation (0.6°C) around Millennium Park and Gendegara Mountain.

Therefore, by overlaying the average LST extracted from Landsat and the average temperature obtained from meteorological samples of each LU/LC classes, about eight main hotspot areas were identified. The assumption was that the places with the highest temperature change are more vulnerable to hotspot. Identified exposure and sensitive layers to hotspots are presented in table 4.10 bellow.

Table: 4.10. Identified hotspot location of the study area

FID	Name of hotspot locations	LST(°C) 2019	Air Temperature (°C)	Area_(km²)
1	Industrial Condominium Area	32.89	31.92	0.776
2	Ture Cement Factory	32.06	31.89	0.786
3	Taiwan Market	34.82	34.13	0.776

4	Sabean Area	31.43	31.54	2.359
5	Outskirt	35.39	35.54	0.786
6	Cotton Factory	33.89	33.24	0.786
7	Bare Land	36.69	35.84	1.581
8	Dry River	34.35	33.91	1.567
TOTAL AREA				9.440

In this study the approximately 13% area (9.44km²) were affected by UHI effects this phenomenon is also known as hotspot area. This area were characterized with LST above 32.5°C and classified in different LU/LC classes. According to Arnfield, (2003), the difference in daytime LST hotspot zones from other areas were on average 5°C to 10°C, however, at night the difference is between about 2.5°C to 5°C (Oke *et al*., 2003). The result from the study also shows that, the LST hotspot areas were about 4°C warmer than the average temperature of the study area.

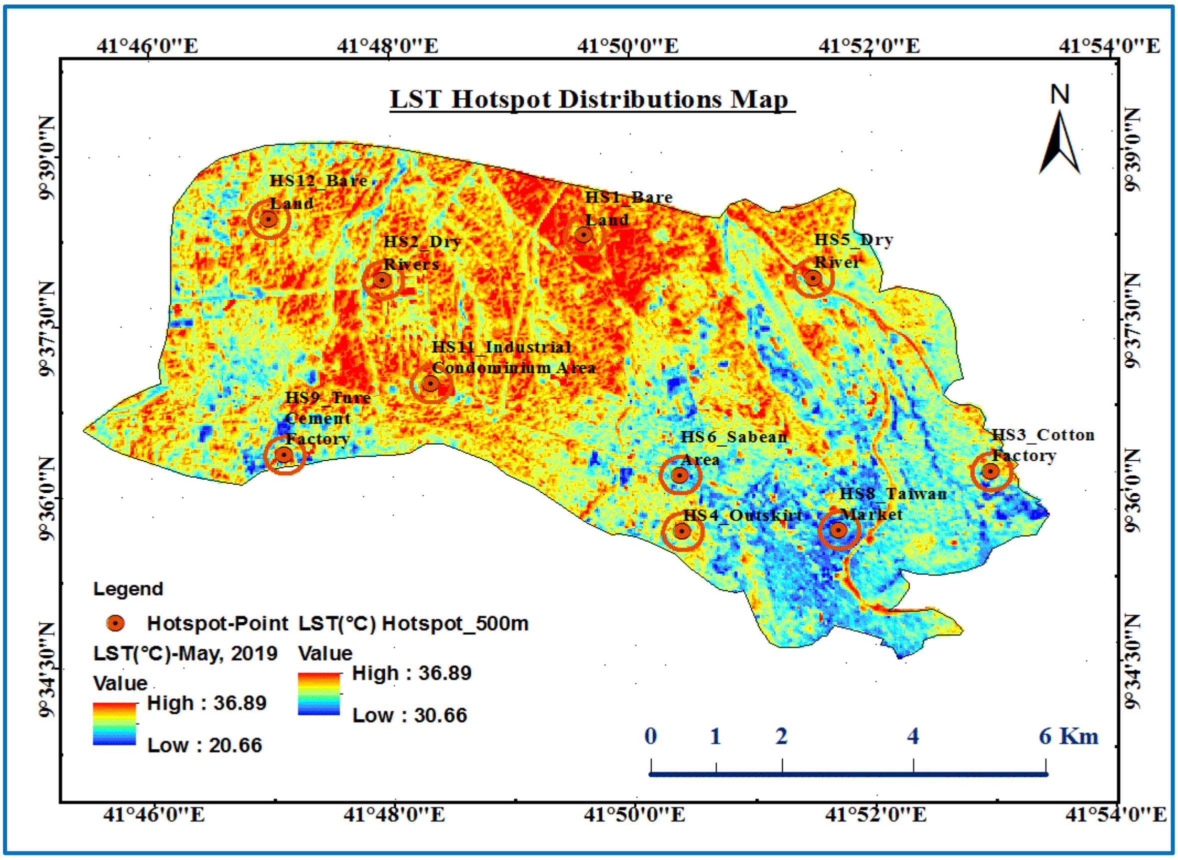

Figure: 4.13. Identified Hotspot Locations of Study Area

4.2.5. Spatial Correlation Analysis

I. Land Surface Temperature and Land Use/Land Cover

LST map and Land use/land cover classes of the study area revealed how the categories and corresponding land surface temperature have changed during the study period. Land use land cover categories that recorded minimum temperature were shrub land and sparse vegetation. Shrub land and sparse vegetation area played crucial role in minimizing the LST. Vegetated area and eucalyptus trees in different part of the City provides shade, which helps to reduce LST effects and minimize air temperature through evapotranspiration, in which plant release water to the surrounding air. Relatively, the higher LST value was recorded from bare land, dry river area and settlement.

From 1999 to 2019, the mean LST was increased by 4.11°C. As shown on table 4.10, the all LU/LC classes have different mean LST over the study period. The highest mean LST was recorded in bare land, settlement and dry river area. Whereas, the lowest mean LST was recorded in shrub land and sparse vegetation area. Comparisons of mean LST with LU/LC classes for the study period are indicated in figure 4.14 below.

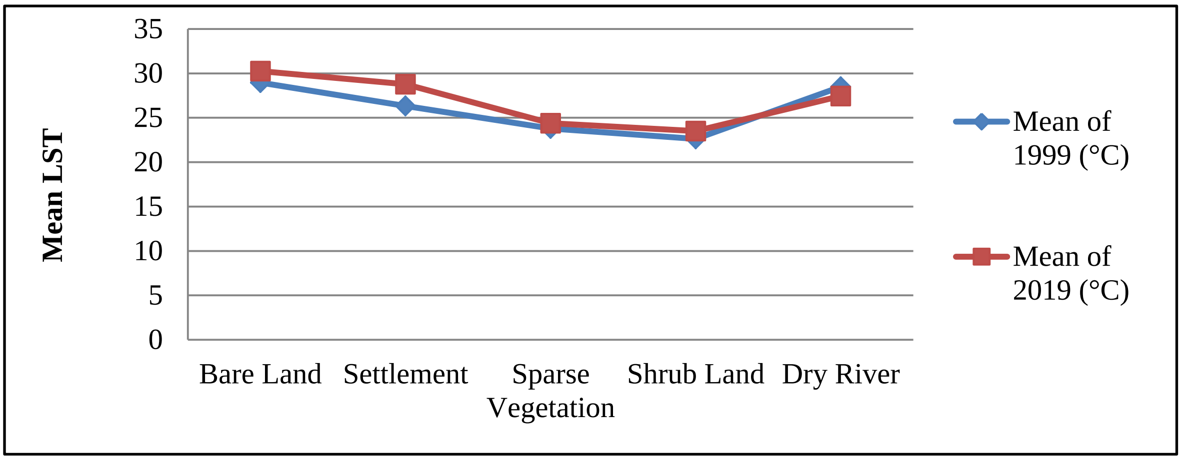

Figure: 4.14. Correlation between mean LST and LU/LC classes

II. LST and Existing Green Infrastructure (GI)

The area and proportion of green coverage in the study area in 1999 were 29.89km^2 (43.86%) but then decreased to 27.68km^2 (40.22 %) in 2019. On the whole, the area of the green spaces from 1999 to 2019 has been reduced by 2.18km^2 which shows 3.17% of the green coverage has been replaced by grey spaces. From this green space types, sparse vegetation within the study area have been reduced by $3.26km^2$ from 1999 to 2019, while shrub land have increased by $1.08km^2$. As shown in Appendix 4, some pixels were between 16.19°C and 23.62°C. This area is mainly shrub lands, sparse vegetation lands. Also in 2019 the number of pixels below 23°C is fewer than those in 1999. The main reason for few pixels is sparse vegetation where temperature between 24°C and 28°C.

Table: 4. 11. Types of GI and mean LST in the study area from 1999 to 2019

		1999			2019		
No.	**Green Space (GI)**	**Area (km^2)**	**(%)**	**Mean LST(°C)**	**Area (km^2)**	**(%)**	**Mean LST(°C)**
1	Sparse Vegetation	13.33	19.37	23.79	10.07	14.63	24.39
2	Shrub Land	16.53	24.02	22.62	17.61	25.59	23.51
Total		29.86	43.39	23.205	27.68	40.22	23.95

LST and NDVI Correlation: In March and April, relatively less temperature was observed during the initial stages this is due to vegetation abundance. After this, temperature increased between the months of May and June, similarly the NDVI values were also increased in these months. The analyzed land sat images of 1999 and 2019 indicated that NDVI and LST have indirect relationships. A low NDVI value has high LST and high NDVI values have low LST. However, the relationship between NDVI and LST were direct/positive relationship for the case of water body, because both NDVI and LST value was less for water body, but there is no water body in the study area.R^2 value shows how much variable X will influence variable Y, it has mean how much vegetation index influence temperature around GI.

The R^2 values of the study period between NDVI and LST correlations indicated 0.94 or (94.9%), and 0.88 or (88.96%), respectively. These results show that, in 1999, about 88.96% value of LST variability was due to the difference in NDVI value, the coefficient variation values are also the same for 1999 and 2019. Generally, LST has strongly and negatively correlated with NDVI values.

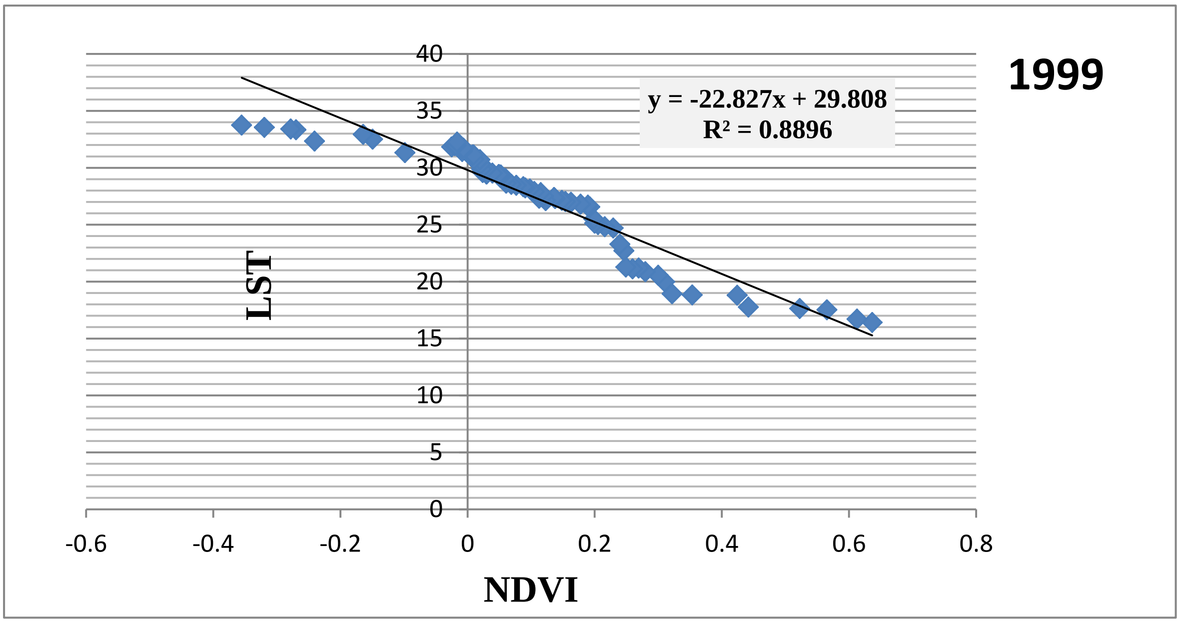

Figure: 4.15. LST and NDVI Correlation for the years 1999 of the Study Area

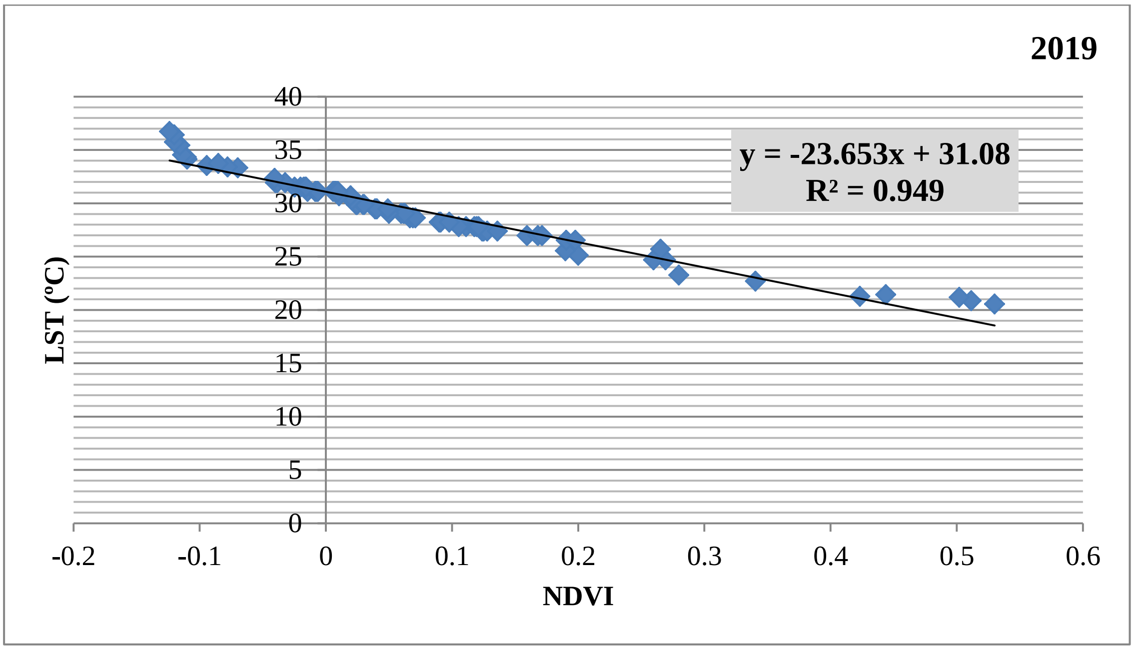

Figure: 4.16. LST and NDVI Correlation for the years 2019 for the Study Area

4.2.6. Cooling Benefit Analysis

I. Proximity to Existing Green Infrastructure (GI):

Urban GI's provide cool islands which extend to the surrounding area. The existing green infrastructure area in the study area was limited to 40%, of this shrub lands are more dominant and there is only one urban park. In this study, the Millennium Park which is located at the center of study area was used to analyze the cooling benefits of existing GI. Since it was located in the center of the City, we analyzed the extension of its cooling effect on the surrounding area based the scale of land sat image and size of the park.

The diameter of the buffer zone was determined to be slightly bigger than the biggest diameter of the park, since the objectives of the study was to analyze the cooling benefits of the park into the surrounding area, and according to Honjo *et al.* (1990), the cooling benefits of an urban park can be extended with a distance similar to the length of the park. (Honjo, T. and Takakura, T, 1990). Therefore, based on the related literatures and considering the existing data the study used 500m buffer. The buffer radius was based on the spatial resolutions of LST and diameter of the park. Finally the result obtained from this analysis will be continued with mathematical optimization model to quantify aver all cooling benefit from the park.

The result shows that, the LST of the surrounding areas of the park is likely to be affected by the distance to the edge of the park and the ratio of the vegetation. The cooling effect of the park was reduced as the distance to the edge of the park increased, and the areas with a 500m distance from the parks was 0.53°C warmer than the area within park on average.

The study also was show that the ratio of the green space in each zone is another important factor to determine the LST level. As an example, in the area within a 500m distance from the park the lower LST is 20.92°C, an increase in the ratio of the vegetation's affected the increasing trend of the LST and lowered it (figure 4.17 and figure 18). The study by Feyisa *et al*., (2014) revealed that, the LST intensity decreases as distance increasing from the periphery to the center of the vegetation's. In addition, the LST maps of the study area confirmed this finding as it shows that the green space patches generate cool area and that its cooling effect contribute to providing a cool buffer zone in the surrounding area, and increasing the distance from these cores will declines the cooling benefits.

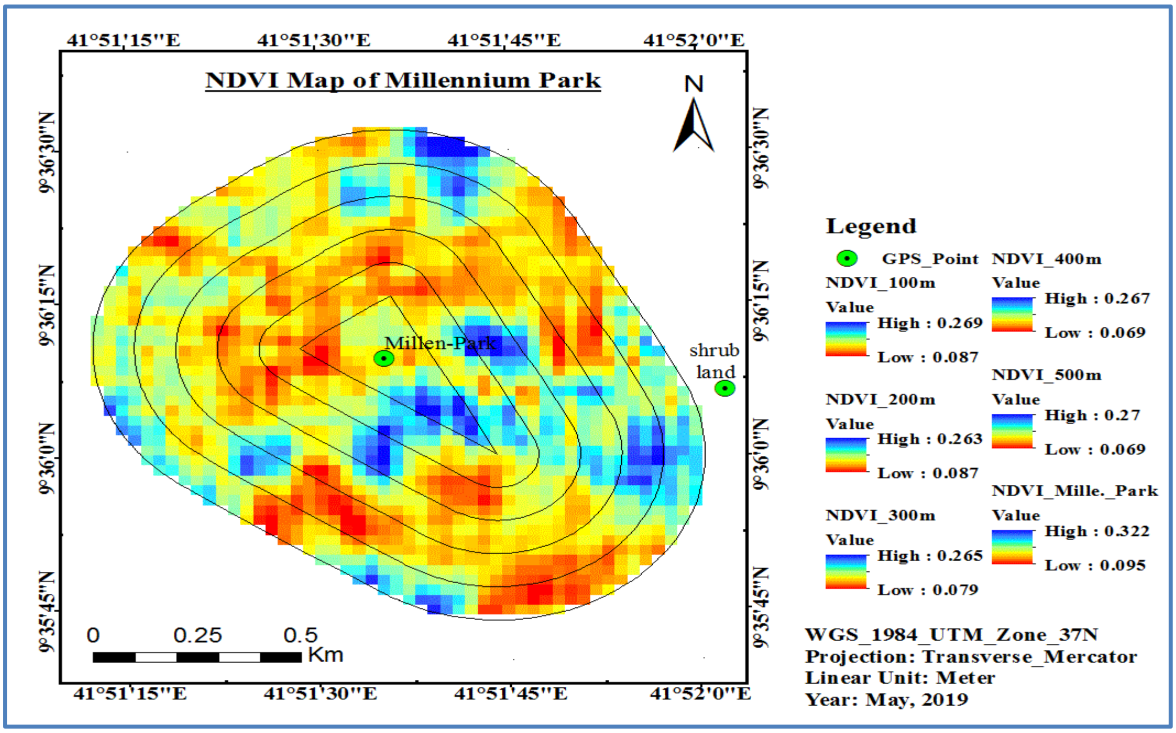

Figure: 4.17. The values of NDVI at 500m buffer distance from Millennium Park

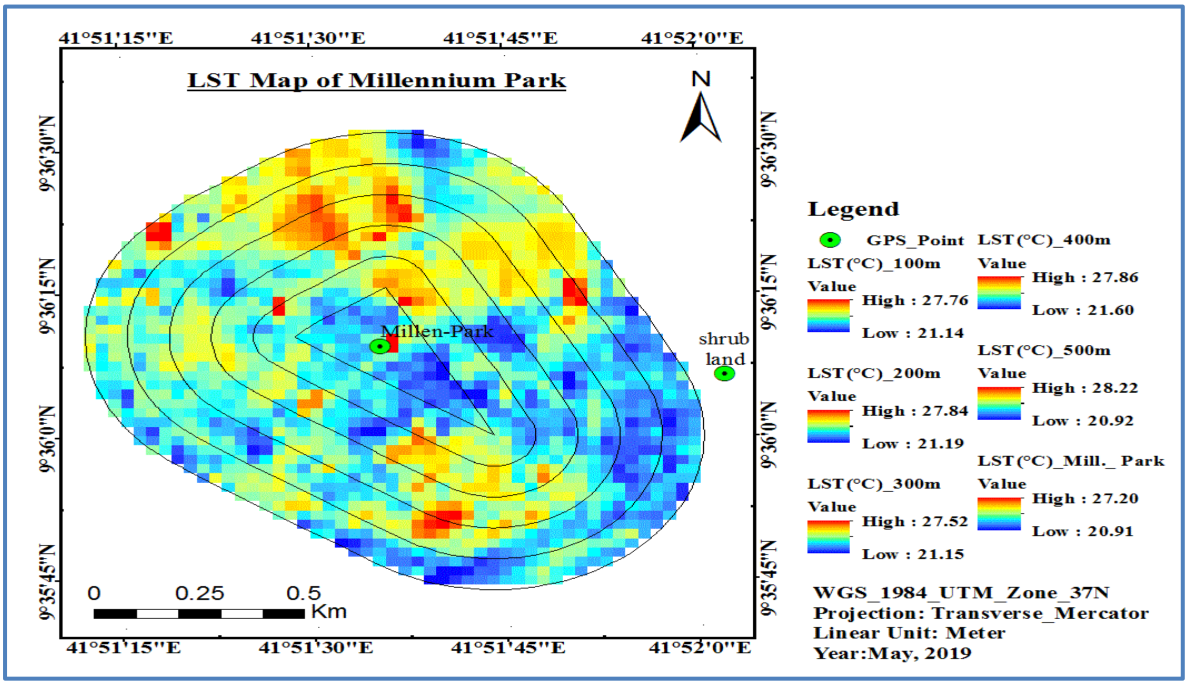

Figure: 4.18. The Variations of LST to Existing Park (GI) and distance from Park

II. Observed Cooling Benefits

The observed cooling benefits from existing GI sample (park) in the Study area was obtained from Eq. (9). Ti' (24.57°C) was estimated using the mean temperature of the local buffers (500m) from Millennium Park (see Appendix, 4B), Ti (24.05°C), the mean LST of Millennium Park as it currently exists and *i* is the existing GI samples (Millennium Park) in the Study area. The direct cooling benefit, βi, was obtained by computing the mean temperature differences between the green infrastructure and its local buffer.

Therefore, $\beta i = Ti - Ti' = -0.52°C$

Based on the above analysis, the mean observed direct cooling benefit was (-0.52°C), which means the mean LST of the existing GI is lower than area outside of the park. At each interval the values of LST was different, this is due to the distributions of vegetation's is not uniform. For example, LST value (27.52°C) at 300m from the edge of the park had lower than LST value (27.84°C) at 200m from the park, this is due to the vegetation density or NDVI value (0.263) at 200m is less than NDVI value at 300m (0.265).

An investigation on the efficiency of parks in reducing urban warming was studied by (Feyisa, G.*et al.,* 2014), the study revealed that the parks cooling intensity is positively related to NDVI. The same study had concluded that cooling effect highly depends on the type of species, cover of the canopy, the shape and size, and distance from the parks.

However, the Pearson analysis suggested that in addition to the distance, LST is more strongly correlated with the GI ratio, which emphases the importance of the construction of more GI at different locations of the Cities to cool down the temperature. And also the existing green infrastructure in the City is not good enough to reduce the current environmental temperature, since there no available water, urban parks and other green space in the study area which mitigates the formations of urban heat island.

III. General implications of LST reduction

The optimal green infrastructure allocations lead to dramatic gains in local cooling benefits. Beyond this, a significant drop in area average temperature across the study area is also observed. The results suggest that optimal GI location may lead to 0.53 - 0.79°C local LST reduction and nearly 1.55 - 1.64°C regional LST reduction, on average, throughout the study area. This is remarkable given that the new green infrastructure was limited to only 13% of the study area. The mean temperature reduction in the study area is shown as table 4.12 below:

Table: 4. 12. The Direct cooling benefit through optimizing GI on identified hotspot zones

$\beta_i = T_i - T_i'$			
***β_i* (hotspot area)**	***Ti* (°C)**	***Ti'* (°C)**	**Cooling Benefit (°C)**
β Industrial Condominium Area	32.89	32.37	0.53
β Ture Cement Factory Area	32.06	31.53	0.53
β Taiwan Market	34.89	34.36	0.53
β Sabean	31.43	29.85	1.58
β Outskirt	35.39	34.86	0.53
β Cotton Factory	33.82	33.29	0.53
β Bare Land	36.29	35.23	1.06
β Dry River	34.35	33.29	1.06
Average	33.89	33.09	0.79

Table 4.12 shows that, the mean observed direct cooling benefits from each of identified hotspot location is 0.53°C. This is true if, the identified area (*i*) will be converted to green infrastructure. The cumulative mean cooling benefit if this all hotspot areas will be converted to green infrastructure can be 0.79°C, which is the expected total cooling benefit obtained from local buffers (500m) from the center of hotspot location.

Also, it was found that, increasing the GI rate on this hotspot area by 13%, the mean LST drops approximately by 0.8°C, from the local hotspots area. This means, the current LST of this Hotspot area drops from 33.89°C to 33.09°C. On the other hand, the average LST of the City will decreased by the mean value of 1.64°C, which means, the current average LST drops from 28.77°C to 27.13°C.

4.2.7. Verification of the result for land surface temperature

The land surface temperature extracted from Landsat thermal band of the study area and the interpolated atmospheric temperature have shown the direct relationships. Considering the existing metrological and acquired time of Landsat, the spatial distribution of the LST was validated. Land surface temperature was verified using meteorological data and LU/LC classes of the study area, which was validated with GPS point collected from field.

Interpolation of rainfall and temperature were done based on the meteorological data collected from three stations within and nearby the study area. These stations were; Dire Dawa, Kersa and Dengego. There is a strong relationship between LST and atmospheric temperature, which was interpolated from these stations. Remotely sensed LST is most valuable in characterization and prediction of spatial temporal patterns of atmospheric temperature. Therefore, LST can atmospheric temperature. Interpolated map of rainfall and atmospheric temperature are given in Figure 4.19 and 4.20 bellows.

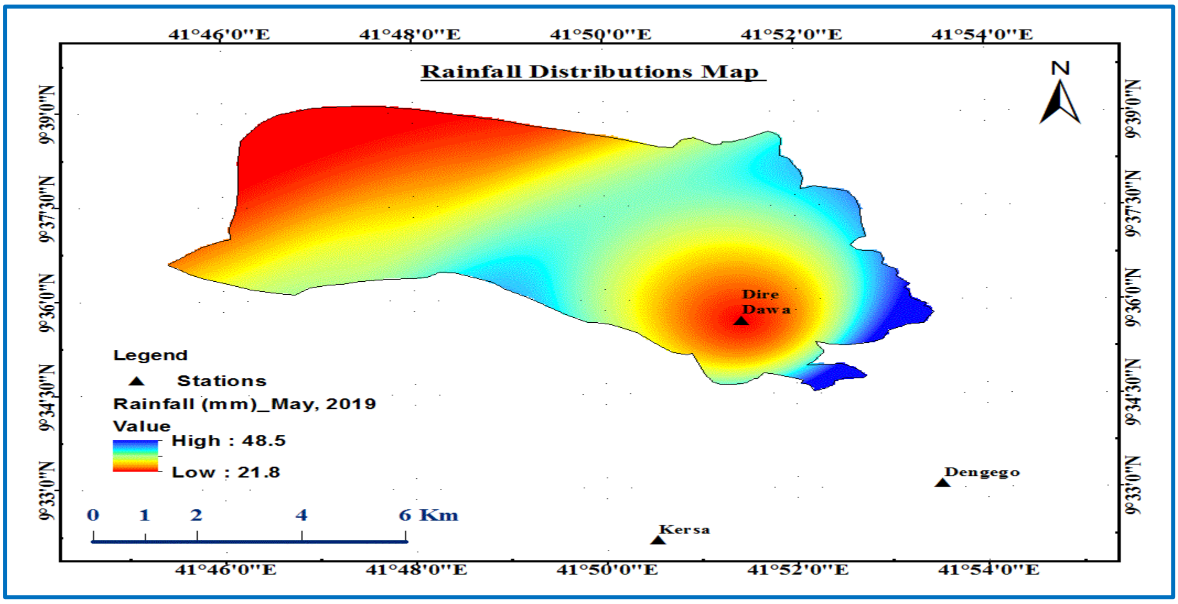

Figure: 4.19. Reclassified Interpolated map of rainfall of Dire Dawa City

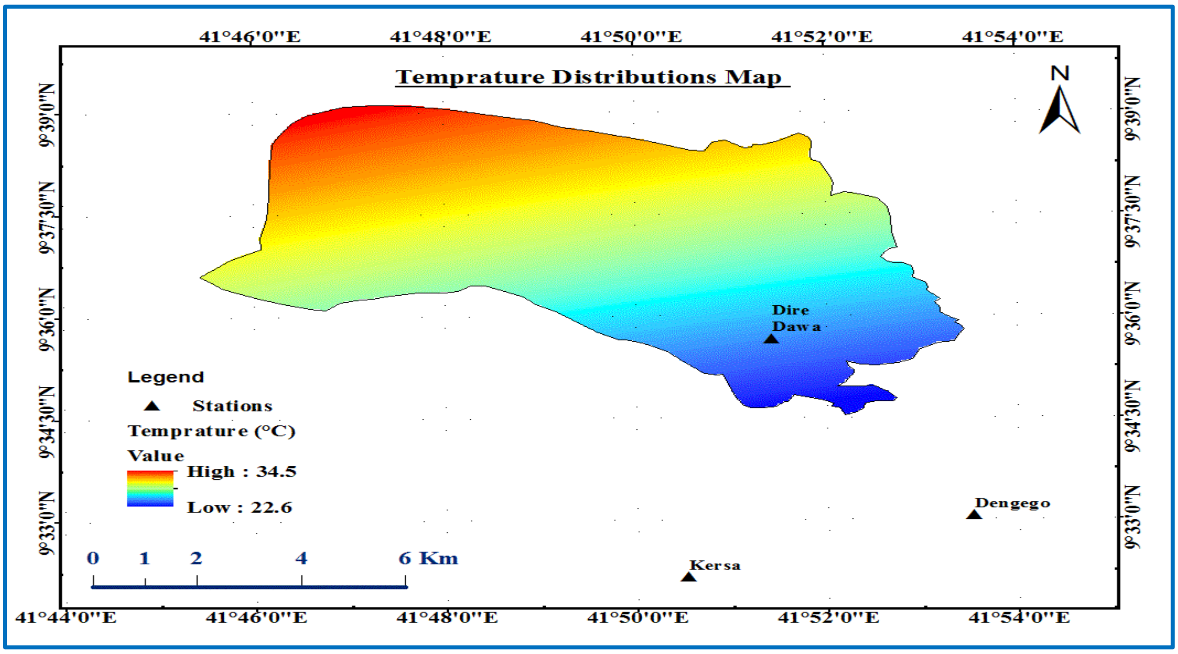

Figure: 4. 20. Reclassified Interpolated map of Temperature of Dire Dawa City

The result of LST extracted from Landsat thermal bands, also revealed that the north, central and some north eastern parts of the study area exhibited relatively high temperature value in each of the study periods, whereas the southeastern parts had low value.

As observed from the interpolated map of the study area, rainfall was higher at the eastern part, but the temperature results were low at the eastern part. However, rainfall map of the northwestern parts have lower values than eastern. Interpolated map of temperature result showed that the southeastern parts have lower temperature value than northwestern parts. For instance, Gendegara is area which characterized as high shrub land had very low LST and also the interpolated map shows low temperature and high rainfall.

On the other hand, both LST map extracted from Landsat thermal bands and interpolated map shows the same result around the central part of the study area; which shows relatively medium temperature. The LST, which was extracted from thermal bands of the study period, was ranged from 20.6ºC to 36.8ºC. Whereas, the interpolated atmospheric temperature map result ranged from 22.6ºC - 34.5ºC.

4.3. Discussions

4.3.1. Extent and Spatial Distribution of Existing Hot Spot Areas

In order to analyze the distributions of LST and identify the hotspot areas from Landsat image, the study was used five LULC classes, five LST zones and NDVI values based on their pixels. The highest temperature distributions were located along the north, central and northwest direction in 2019, but in 1999, the temperature distribution was oriented in to northwest directions. This phenomenon is known as the hotspots or hot island.

In 1999, the maximum temperature was recorded 33.03°C with minimum temperature value of 16.19°C. On the other hand, on 2019, the highest temperature recorded was 36.89°C and the lowest temperature was 20.66°C. Therefore, the average LST of overall area for the two observation years has increase from 24.66°C to 28.77°C. Accordingly, bare land area exhibits the highest LST in both years. Dry rivers and settlement has also exhibited high LST. Increase in LST was due to various types of activities, industrial growth, settlement and reduction of vegetation that causes unexpected changes in climate. On the other side, sparse vegetation and shrub land show lower LST values in both years.

In 2019, the LST distribution was compatible with the LULC types and NDVI values, indicating that a single type of LULC which relatively concentrated and caused large changes in temperature between every land type. Dry Rivers and bare land had categorized under high and higher LST zones respectively. Settlements were found in both medium and high LST zone this is because of vegetation's around the built up area. Sparse vegetation's and Shrubs were in both LST zone, lower and low LST zones. From 1999 to 2019, lower LST zone, high LST zone, and higher LST zone had the greatest change in total area. However, there was no higher LST zone in 1999, and there was no lower LST zone in 2019. Thus, this change indicates the existence of the build-up retrievals.

Based on the result obtained from the analysis, approximately 13% areas (9.44km^2) were considered as hotspot area. This area were characterized with an average LST above 33°C and categorized in different LU/LC classes. Bare lands (Sandy Soil) that surrounding the City and outskirt of the City including; national cement factory and dry rivers, areas were identified as hotspot area. And also, from settlements LULC types, area around cotton factory, Taiwan market, Ture cement factory and some parts of sabian (02 kebeles) around abattoirs were identified as hotspot area. Among the sample locations, the highest temperature (39.3 ± 3.46°C) was recorded at bare land and dry river having 37.8 ± 2.26°C, followed by settlement LU/LC types, such as cotton factory (35.8 ± 2.56°C) and (34.4 ± 2.51°C) was recorded from cement factory.

4.3.2. Interaction of LST and GI

Normalized difference vegetation index play an important role in assessing and investigating of LST. A thermal band of Landsat image was used in quantifying the LST and NDVI of the study area. Different researchers used thermal bands to study LST. (Gebrekidan, W., 2016), used Landsat satellite imagery to investigate the relationship between LST and NDVI. He found negative linkage in NDVI and LST values. Normalized Difference Vegetation Index value is less for bare land, and settlement and dry rivers classes. However, in the case of sparse vegetation and shrub land, the values were relatively high. In both 1999 and 2019, bare land, dry rivers and settlement area exhibit the highest LST mean value. On the other side, sparse vegetation and shrub land show lower

LST mean value. In the present study settlement, bare land and dry rivers have the highest LST (Matiwos, B., 2018).

Basically LST and NDVI were the best applications to know the temperature in study area, and NDVI confirmed the findings of the study. Less GI area reflected increase in LST and vice versa. The outcomes showed the pattern of vegetation and LST changes in Dire Dawa City. NDVI was negative in built-up area and bare land of the City, mainly because of lack of GI such as trees and other vegetation cover.

Other scholar has also witnessed it also shows that, the highest values of LST are in the urban or built-up area and other impervious surfaces while the lower LST values are found around vegetated areas (Honjo, T. *et al*., 1990). Vegetative covers absorb heat during the daytime and release it at night as a result low value of LST is commonly recorded in such LULC type (Kong, F. *et al*., 2014)

The temperature value around industrial shades, road networks, concrete pavements and bare land become considerably higher than area around GI. Nevertheless, urban built up areas geographically proximate to shrub land, parks, sparse vegetation shows relatively low LST value because of coarser spatial resolution of satellite imagery used.

The study showed that the highest LST value due to settlements like buildings, roads and bare soil had an impact on environment. Spatial and temporal distribution of LST and NDVI during 1999 and 2019 revealed that during the study period there were radical changes in the area. This shows that, those LULC classes that have higher LST values have shown lowest NDVI value. This is due to surface radiant temperature value is negatively correlated with NDVI value for all land use type. As a result, the highest NDVI value and lowest LST is observed in land cover with high vegetation (Li, X.; *et al*., 2013).

Therefore, shrub land (22.61°C in 1999 and 23.51°C in 2019) and sparse vegetation (23.79°C in 1999 and 24.39°C in 2019) depict lowest mean LST value and high NDVI mean value for both study years. The highest NDVI and maximum LST values for 1999 was 0.67 and 33ºC respectively and lowest NDVI and minimum LST values was -0.38 and 16ºC respectively. In 2019, highest NDVI and maximum LST values were 0.53 and 36ºC respectively, and lowest and the minimum LST values was -0.12 and 20ºC respectively.

According to Burgan and Hartford (1993), the negative values are indicative of water, soils, snow, clouds, non-reflective surface and other non-vegetated areas while positive values expresses reflective surfaces such as vegetated area. However, it does not mean that all negative values of NDVI have high LST value. LST depends up on the reflective conditions of the surface of the earth. In general, area of non-vegetated and non-reflective surface, have high LST than those of vegetated and water body. Bare soil is represented with NDVI values, which are closest to zero (Burgan, R. E., and Hartford, R. A., 1993).

This shows that, the correlation between LST and NDVI for both study years have strong negative correlation with the R^2 values of 0.88 and 0.94, for study period 1999 and 2019 respectively. These results show that, in 1999, about 94.9% value of LST variability was due to the difference in NDVI value, the coefficient variation values are also the same for 1999 and 2019. Generally, negative correlation was found between NDVI values with LST. In this scenario, it becomes imperative to focus on a stricter implementation of urban planning norms and to stress increasing green cover in the Cities.

4.3.3. Cooling Benefits of Existing GI

Overlaying land cover and LST maps showed that land cover type is an important factor to determine LST. The results showed that, the distance to the park was positively correlated with the LST and with distance increase (500m) from the park, the mean LST also increased by 0.42°C - 0.53°C.

Findings from previous studies have confirmed the extension of the cooling effect in the surrounding area, while they have provided different interpretations for it. Hamada and Ohta (2010) studied an urban park with the size of 147 hectares in Japan and suggested that the cooling effect of the urban park extends for several hundred meters (Hamada, S. and Ohta, T. , 2010). According to Honjo, T. *et al*., (1990), the cooling effect of an urban park can be extended in the surrounding area with a distance similar to the length of the park (Honjo, T. and Takakura, T, 1990). Also, the cooling range of the influenced area by the green space depends on the size of green space (Zhao, W. and Oke, J., 2014).

The farther away from the central point of Green area in generally will increase the temperature with the average value of temperature rise of 0.22°C (Suryandari and

Widyatmant, 2018). However, in some points there is a variance, in the first ring of the buffer or in one of the ring buffer area that is more far from the park has a lower temperature than the center of the park. This occurs, due to several factors described as higher vegetation density. This is possible because the vegetation's around the edge and center of park is one part of the GI represented by a certain area. GI is not only limited to the edge and center of park, so that although visually described to be the same NDVI class but NDVI both can have different values.

The study found that, the availability of GI in the proximity of built-up areas and most heat load or hotspot areas such as bare lands should receive primary attention in the process of planning and designing. Although, the distance is not a prime factor and LST can be affected by the ratio and configuration of the green infrastructures as well. However, further researches are necessary to fully understand the mechanism of the extension of the indirect cooling benefits of green infrastructures in surrounding built areas.

It is well known that increasing GI in urban areas helps to reduce the UHI and LST effects. The research dedicated to this relationship has largely focused on the amount or area of existing GI and hotspot areas (Hondula D. Vanos J. & Gosling S., 2014), although increasing attention has focused on the broader characteristics of the pattern of GI such as concentration and distance between them (Myint, F. *et al.,* 2015). To the knowledge, however, no attempts have been made to determine the optimal locations for GI accounting for diurnal UHI variations, creating an information gap for decision makers confronting the negative impacts of excessive urban temperatures.

The framework of the study were effectively addresses this issue by integrating GIS, remote sensing and spatial statistics with optimization modeling. This framework links the existing GI locations with LULC and enables identification of hotspots location to propose GI allocations that reduce LST and balance cooling benefits.

In general, out of the total area of the study area about 13% or 9.44 km² were identified as Hotspot area. The results suggest that optimal GI arrangement may lead to 1.55 – 1.64°C local LST reduction, on average, throughout the study area. This is remarkable given that the new GI was limited to within (500m) buffer zone and 13% land was used out of the total study area. This may increases the amount of GI in the study area to 53%.

The implication from this observation is that, optimizing the locations of green infrastructure was more important in reducing LST effects, which is consistent with previous findings (Zhou *et al.,* 2011 & Li *et al*., 2012). However, the results also showed that distance from existing park and density of GI together were the most deterministic factors of LST than the unique effects of a single variable.

Many of the results from this study regarding to the relationships between the green space and LST were expected as reported in a number of publications (Weng *et al*., 2004; Ohta, 2010; & Hamada and Connors *et al*., 2013). Traditionally, increasing the green space by planting more trees has been emphasized in urban planning (Rizwan *et al*., 2008a; Zhou, W. *et al*., 2011).

Therefore, based on the result obtained from the analysis, this study revealed that, optimizing the spatial locations of GI can reduce the effect of LST. While confirming the fact that the increase in GI can significantly mitigate LST effects, the results showed that optimizing the locations of GI as expressed by the joint effect of distance and density of GI is the most deterministic metric that affects LST.

CHAPTER 5. CONCLUSIONS AND RECOMMENDATIONS

5.1. Conclusions

The study investigates the effects of optimizing the spatial locations of green infrastructure on land surface temperature. This study analyzed the cooling benefits of GI, through identifying hotspot location, by integrating GIS, remote sensing and spatial statistics for Dire Dawa City. The result indicates that, the study area experienced LST effect as result of urbanization. According to the result of the study, all hotspot areas were recorded from impervious surfaces and sandy soils such as, built up area/ settlement, bare land and dry rivers. The result shows that, more vegetated area like sparse vegetation and shrub land shows lowest LST value and high NDVI. This shows due to the conversion of land from vegetated area to built-up area, LST depicts highest value in the City. Therefore, the result concluded that, LST has strong negative correlation with NDVI.

The integrated framework of the study demonstrates significant cooling benefits can be gained through optimizing the spatial location of GI, especially on the most heat load areas in City. By concentrating the parks in the City, the cooling benefit could be amplified as compared to hotspot areas. The study also identifies the potential of green infrastructure areas to mitigate the heat load. This heat load mitigation measures should be applied extensively in order to reach substantial reduction of urban hotspots area in a City scale. If only critical areas with the highest heat load are considered, urban planning measures could be optimized through targeted and combined implementation. With the application of several heat load mitigation measures such as, optimizing green spaces locations by 13%, it is possible to achieve substantial cooling benefits with heat load reduction up to 1.64°C.

The study concludes that, optimizing GI locations can decrease the temperature effect in the study area probably due to the increase in the rate of transpiration and/or evapotranspiration. This result show that, more GI should be developed as new urban parks and urban trees because, vegetation can greatly reduce the air temperature and increase relative humidity and thereby could provide thermal comfort to people. The developed framework can be further applied to assess different land arrangements for various cooling considerations. The findings help to address the growing environmental problem of extreme temperatures challenging urban areas.

5.2. Recommendations

The result of the study implies few suggestions for practical utilization, in order to maximize the cooling benefits of green infrastructure. These suggestions/recommendations may be considered in the process of urban planning GI design and management.

- One of the negative consequences of rapid urbanization is reduction and replacements of vegetation by other impervious surfaces which causes extreme hotspots in the City. Stakeholders should promote protecting and utilizing the proper LCLU policy, which benefit citizen's well-being through various ecosystem services of GI and to overcome unexpected changes in climate of the City. Therefore, urban planning measures could be optimized through targeting this critical areas or highest heat load areas.

- Urban GI can be considered as an ecologic measure to alleviate UHI by providing the cooling benefits, but the existing green infrastructure in the City is not good enough to reduce temperature, for instance the City has only one urban park. The results also showed that, the LST in the surrounding areas of the urban park declined as the distance to the park decreased. Therefore, the study recommends that the City Administration should improve the capacity of to implement sound plans at local level for improvement of strategic placements of new green infrastructures and constructing more parks, street trees in the City.

- The results imply that optimizing the locations of green infrastructure on hotspot areas can provides significant cooling benefit. The study recommends that, paying attention to optimizing the locations of GI which increases the configurations of vegetation, should be underlined to mitigate LST effects by providing the cooling benefits in the City.

REFERENCES

Ahmed.M (2015). Climate risks in megacities of the global south: Focus on Dhaka, Bangladesh. In The "State ofDRR at the Local Level" A Report on the Patterns of Disaster Risk Reduction at Local Level. Geneva, Switzerland, pp, (43),121–234.

Akbari. (2005, sep. 07). Potentials of urban heat island mitigation. International Conference "Passive and Low Energy Cooling for the Built Environment", Santorini, Greece. Retrieved 2019, from Available online at: Inive: *http://www.inive.org pp, (11),*285–394.

Amani-Beni; Zhang. (2018). Impact of urban park's tree, grass and waterbody onmicroclimate in hot summer days: A case study of Olympic Park in Beijing, China. Urban For. Urban Green., doi: ug.2018.03.016. pp, 32, 1–6.

Andrew. (2012). Exploring the relationship between land surface temperature and vegetation abundance for urban heat island mitigation in Seville, Spain. Division of Physical Geography and Ecosystem Analysis, pp, (29), 307–324.

Arnfield, A. J. (2003). International Journal of Climatology, . A review of turbulenc exchanges of energy and water, and the urban heat island., 1–26.

Arrau and Pena. (2010). The Urban Heat Island (UHI) Effect. Available online at *http://www.ur*banheatislands.com (accessed 20 October 2010), pp, 113-137.

Artis and Carnahan. (1982). Survey of Emissivity Variability in Thermography of Urban Areas. Remote Sensing of Environment, pp.(12), 313-329.

Asubonteng, K.. (2007). Identification of land use/cover transfer hotspots in the Ejisu-Juabeng.

Belete,T.(2017).Impact of land-use/land-cover changes on LST in adama zuria woreda,ethiopia, using geospatial toolS. Addis Ababa University, pp,37-47.

Billah, M., and Rahman, G. (2004). Land-cover mapping of Khulna city applying remote sensing technique. In Proceedings of the 12th International Conference on. Geospatial Information Research:Pacific and Atlantic, University of Gävl , pp. 705–714.

Bolund.(2015). Rotterdam Programme on Sustainability and Climate Change 2015-2018; City of Rotterdam:. Rotterdam, The Netherlands, 2015, 1-12.

Burgan, R. E., and Hartford, R. A. (1993). Monitoring vegetation greenness with satellite data. Geospatial Information & Remote Sensing, 11(3), 369–393.

Chaobin,2017 & UN. (2018). World Urbanization Prospects: The 2014 Revision; United Nations Department of Economics and Population: New York, NY, USA, 8-153.

Chang and Akpina,2014; Kun, (2017). Effects of urban parks on the local urban thermal environment. Urban For. Urban Green. Urban For. Urban Green13, 672–681, 1-19.

Charlesworth. (2010). A review of the adaptation and mitigation of global climate change using sustainable drainage in cities. Journal of Climate Change,volume 1 (3): 165- 180.

Chen, X. (2000). Using RS and GIS to analyze land-cover change and its impacts on the Regional able Development. International Journal Remote Sensing. (23), 107–113.

Connors, J.P., Galletti, C.S., Chow, W.T.L., (2013). Landscape configuration and urban heat island effects: assessing the relationship between landscape characteristics and land surface temperature in Phoenix, Arizona. Landscape Ecol. 28, 271–283.

Coppin and Bauer. (1996). Digital change detection in forest ecosystems with remote sensing imagery. Remote sensing reviews, 13(3-4), 207–234.

D.D.E.P.A. (2019). Dire Dawa Environmental Protection Authority; National Meteorological Agency; Dire Dawa.

DDCA. (2018). Dire Dawa Administrative Council Water Mines & Energy Office. Dire Dawa Administrative Council Integrated Resource Development Master Plan Study Project. Addis Ababa, Ethiopia.

Deepthi, J. G. (2010). Identification of Accident Hot Spots: A GIS Based Implementation for Kannur District, Kerala Implementation for Kannur District, Kerala. *International Journal of Geomatics and Geosciences, 1*(1).

Dire Dawa Adminstration Statistical Bureau. (2019). Dire Dawa Finance Economy and Development Bureau. Dire Dawa Adminstration Statistical Abstract 2015-2019.

Doan and Kusaka. (2016). Numerical study on regional climate change due to the rapid urbanization of greater Ho Chi Minh City's. .Int. J. Climatol, 36, 3633–3650.

Elvik, R. (2002). Optimal Speed Limits: The Limits of Optimality Models. *Transportation Research Record, 1818,* 32-38.

EPA. (2010). Reducing Urban Heat Islands: Compendium of Strategies –Urban Heat Island Basics.Available;online,at:http://www.epa.gov/heatisland/resources/pdf/BasicsCompendium.pdf (accessed 22 augest, 2019).

ESRI. (2016). Environmental Systems Research Institute; ArcGIS Desktop Help 10.4. Redlands, CA.

Ferreira, J. F. (2011). Geo-referencing road accidents with Google. *The electronic journal information systems evaluation, 14,* 27-36.

FAO, (1999).Terminology for integrated resources planning and management Food and agriculture organization/UN Env program, Rome, Italy and Nairobi, Kenya.

FAO. (2006). Problem Posed by the Introduction of Prosopis Spp in Selected Countries.Italy.

Fei, Z. (2016). Dynamics of land surface temperature (LST) in response to land use and land cover (LULC) changes in the Weigan and Kuqa river oasis, Xinjiang, China. Arabian Journal of Geosciences, June 2016.DOI: 10.1007/s12517-016-2521-8, 11-23.

Feyisa, G. Dons, K. & Meilby, H. (2014). Efficiency of parks in mitigating urban heat island effect: An example from Addis Ababa. Landscape and Urban Planning, 123, 87–95.

Forman,1995;Zhou,2011 and Dikman. (2019). Landscape Mosaic: The Ecology of Landscape and Regions; The Sensitivity of Urban Heat Island to Urban Green space. Cambridge University Press: New York, NY, USA, 1995, 54–63.

Fortuniak. (2009). Global environmental change and urban climate in Central European cities. International Conference on Climate Change, The environmental and socio-economic response in the southern Baltic region, Szczecin, Poland.

Gandhi and Christy . (2015). Ndvi:Vegetation change detection using remote sensing and GIS–A case studyof Vellore district. . Procedia Computer Science 57, 1199-1210.

Gebrekidan, W. (2016). Modeling land surface temperature from satellite data, the case of Addis Ababa. ES RI, Eastern Africa Education GIS conference. Held at Africa hall, United . Nations conference center from23-24 sept. 2016, Addis Ababa.

Geer, I. (1996). Glossary of Weather and Climate, with Related Oceanic and Hydrolic Terms. American Meteorological Society., 15-25.

Gill and Pauleit. (2007). Adapting cities for climate change: the role of the green infrastructure. Built Environment, 33(1), 115-133.

Gilbert, K.C., Holmes, D., and Rosenthal, R.E. (1985), "A multi-objective Optimization model for land allocation", *Management Science,* 31(12), pp.1509-1522.

Hamada, S. and Ohta, T. . (2010). Seasonal variations in the cooling effect of urban green areas on surrounding urban areas. Urban Green, 9,, doi:10.1016/j.ufug10, 15–24.

Hondula D. Vanos J. & Gosling S. (2014). The SSC: A decade of climate–health research and future directions. International Journal of Biometeorology, 58(2), 109–120.

Honjo, T. and Takakura, T. (1990). Simulation of Thermal Effects of Urban reen Areas on Their Surrounding Areas. Energy Build. doi:10.1016/1212-F, 16, 443–446.

Huang, G., Cadenasso, Zhou, W., M.L. (2011). Does spatial configuration matter? Understanding the effects of land cover pattern on land surface temperature in urban landscapes. Landscape Urban Plan. 102, 54–63.

Hunhammar. (1999). Ecosystem services in urban areas.Econ. 1999, 29, 293-301.

Josh and Ashley. (2011). The value of green infrastructure for urban climate adaptation. The Center for Clean Air Policy February 2011, 1-52.

Juntao Tan and Hung. (2018). Assessment with satellite data of the urban heat island effectsin Asian mega cities. Int. J. Appl. Earth Obs. Geoinf. 2006, 34–48.

Kalkstein, L. (1991). A New Approach to Evaluate the Impact of Climate on Human Mortality. . Environmental Health Perspectives, 96, , 145-150.

Kathry and Dr.Ana. (2019). Integrating green and blue spaces into our cities. Grantham Institute Briefing paper No 30.

Klok, L., Zwart, S., Verhagen, H., & Mauri, E. (2012). The surface heat island of Rotterdam and its relationship with urban surface characteristics. Resources, 64, 23–29.

Kong, F.; Yin, H.; James, P.; Hutyra, L.R.; He, H.S. Effects of spatial pattern of green space on urban cooling in a large metropolitan area of eastern China. Land sc. Urban Plan.2014, 128, 35–47, doi:10.1016/j.landurbplan.2014.04.018.

Kovats and Osborn. (2016). UK Climate Change Risk Assessment Evidence Report; Chapter 5, People and the Built Environment. London. Report prepared for the Adaptation Sub-Committee of the Committee on Climate Change, London.

Landsat Project Science Office. (2019). USGS. Retrieved augest 15 , 2019, from Available online at:Landsat7 Science Data User's Handbook (Goddard Space Flight Center).: http://Landsathandbook.gsfc.nasa.gov/handbook_htmls/chapter11.

Lee and Maheswaran. (2011). The health benefits of urban green spaces: a review of the evidence. Journal of Public Health, 33, 212-222.

Legates, D. R., and Willmott, C. J. (1990). Mean seasonal and spatial variability in global surface air temperature. Theoretical and applied climatology, 41(1), 11–21.

Liu,2011; and Hongbo. (2018). Urban heat island analysis using the Landsat TM data and ASTER data: A case study in Hong Kong. Remote Sens. 3, 1535–1552.

Li, X., Ouyang, Z., Xu, W., Zheng, H. (2012). Spatial pattern of green space affects LST: evidence from the heavily urbanized Beijing, China. Landscape Ecol. 27, 887–898.

Manepalli, U. A. (2011). Crash Prediction: Evaluation of Empirical Bayes and Kriging Methods. *3rd International Conference on Road Safety and Simulation.*

Matiwos, B. (2018). Detection of Land Surface Temperature in Relation to Land Use Land Cover Change: Dire Dawa City, Ethiopia. Journal of Remote Sensing & GIS, 1-9.

Mohan, M. and Pathan, S. (2011). Dynamics of urbanization and its impact on LULC: a casestudy of megacity Delhi. Journal of Environmental Protection 2: 1274-1283.

Myint, S., Zheng, B., Talen, E., Fan, (2015). The urban landscape urban warming and cooling in Phoenix and Las Vegas, Ecosystem Health and Sustainability, 1(4), 1–15.

Neema & Ohiga. (2013). Multitype green-space modeling for urban planningmodeling for urban planningusing GA and GIS. Environment Planning and Design, 40(3), 447–473.

Nichol, J.E., (1996). High-resolution LST patterns related to urban morphology in a tropical city: A satellite-based study. Journal of Applied Meteorology, 35(1), pp.135-146.

NMA. (2019). Ethiopian National Meteorological Agency. Meteorological Agency located at Dire Dawa City and Jigjiga.

Nunez, M. and Oke, T.R, (1977), the energy balance of an urban canyon Journal of Applied Meteorology, 16(1), pp.11-19.

Nyoni, R. (2017). A GIS Based Approach To Identify t Hotspots In The Greater Durban City from 2011 - 2015. University of KwaZulu-Natal, Westville campus.

Pansi, O., 2013 and Yang, L. (2015). Monitoring land use and land-cover change in the Eastern Gulf Coastal Plain using multi tempora Landsat imagery. J Geophys Remote Sens, 9-14.

Parry and Hanson. (2007). Contribution of Working Group II to the Fourth Assessment Report of the Intergovernmental Panel on Climate Change. (Cambridge University Press).

Peng, J., Xie, P., Liu, Y. and Ma, J., (2016). Urban thermal environment dynamics: A case study in the Beijing RS. Journal of environment, 173, pp.145-155.

Philip, G. M., and D. F. Watson., (1982) "A Precise Method for Determining Contoured Surfaces." Australian Petroleum Exploration Association Journal 22: 205–212.

Prata .A. (1999). Thermal remote sensing of land surface temperature fromsatellites: status and future prospects. . Remote sensing rev., 12, 175–223.

Quattrochi and Luvall,1997; Rose and Devada. (2009). Application of high-resolution thermal infrared remote sensing and GIS to assess the urban heat island effect. International Journal of Remote Sensing, (18), 287-304.

Rizwan, A.M., Dennis, L.Y., Liu, C., (2008). A review on the determination and mitigation of Urban Heat Island. Environ. Sci. 20, 120–128.

Rose and Devada. (2009). Analysis of and LST and LULC, Using RS. Imagery in Chennai City, India. Seventh International Conference on Urban Climate, Yokohama, Japan.

Roth. (2008). Urban Climate Considerations for the Development of Sustainable Cities. Available:online,at:http://www.sde.nus.edu.sg.pdf (accessed 20 augest, 2019).

Roy; Becker F & Anderson. (2014). Landsat-8: Science and product visionfor terrestrial global change research. Remote Sens Environ. Remote Sens. Environ. 2014, 85, 154–172.

Santamouris,2001; Chaobin. (2017). The role of green spaces In Energy and Climate in the Urban Built Environment. USA, 2001; Northeast Institute of Geography and Agroecology, Chinese Academy of Sciences, Changchun 130102,MDPI, 1-19.

Santana, L. (2007). Landsat ETM+ image applications to extract information for environmental planning in a Colombian city. International Journal of Remote Sensing, 28, 422-442.

Simonds J.O. (2007). Landscape Architecture: A Manual of Site Planning and Design; . McGraw-Hill Professional: NewYork, NY, USA.

Suryandari and Widyatmant. (2018). Utilization of remote sensing and GIS to identify radius of urban cool island for planning open green area in urban area (case study of Yogyakarta). IOP Conf. Series: Earth and Environmental Science 169 (2018) 012005, 2-9.

Stewart, I.D. and Oke, T.R., (2012). Local climate zones for urban temperature studies. Bulletin of the American Meteorological *Society*, 93(12), pp.1879-1900

Spronken-Smith, R. A., Oke, T. R., & Lowry, W. P. (2001). Advection and the surface energy balance across an irrigated urban park. Inter. Journal of Climatology, 20(9), 1033–1047.

Stoll, M. J., & Brazel, A. J. (1992). Surface-air temperature relationships in the urban environment.PhysicalGeography, 13(2), 160–179.

Tendayi, G., 2014; and DDCA. (2015). Spatial Planning and Open Space Integration in Urban Ethiopia. Limpopo Province, South Africa,University of Venda, Private Bag X5050.

Tessema, (2012) and Zeray. (2017). Ecological and economic dimensions of the paradoxical invasive species-Prosopis juliflora and policy challenges in Ethiopia. Journal of Economics and Sustainable Development , 3: 62-71.

Tong and XuCheng . (2018). Heat wave and health events: A systematic evaluation of different temperature indicators, heatwave intensities. Sci. Total Environ. 630,679–689.

UN-Habitat, 2015; CSA. (2017). Dire Dawa Environmental Protection Authority. DIRE DAWA: international journal.

University of Manchester. (2007). Build Parks To Climate Proof Our Cities. Retrieved augest 15, 2019, from ScienceDaily 14101534.htm: http://www.sciencedaily.com.

USGS. (2018). Landsat. http://landsat.usgs.gov/ band designations landsat satellites diakses tanggal 27 November 2018.

Voogt, J. A. (2002). Urban Heat Island. In munchester: Wiley : Munn, T., ed. Encyclopedia of Global Environmental Change, 3, 650-662.

Weng. (2017). Responses of urban heat island in Atlanta to different land-use scenarios. . Theor. Appl. Climatol., 1–13.

Whitford, V. E. (2001). City form and natural processes indicators for the ecological performance of urban areas and their application to Merseyside, UK. Landscape and Urban Planning 57 (2001), 91–100.

Williams, J.C., and ReVelle, C.S. (1996), “A 0 - 1 programming approach to delineating protected reserves,” *Environment and Planning B:* 23, pp.607–624.

Woreda, Ghana. International Institute for Geo-information Science and Earth ObservationEnschede, Netherlands., 369–393.

Wright, J., ReVelle, C.S., and Cohon, J. (1983), “A multiobjective Integer programming model for the land acquisition problem,” *Regional Science*, 13, pp.31–53.

Xian and Crane,2006; Arrau and Pena. (2010). An analysis of urban thermal characteristics and associated land cover in Tampa Bay and Las Vegas using Landsat satellite data. Remote Sensing of Environment, 104, 147-156.

Yuan and Bauer. (2007). Comparison of impervious surface area and NDVI as indicators of surface urban heat island effects. Remote Sensing of Environment, 106., 375-386.

Yue.,(2007). The relationship between LST and NDVI with remote sensing: application to Landsat 7 ETM+ data. International Journal of Remote Sensing, 28, 305-3226.

Zhao, W.; Liu, X., 2010 and Oke, J. (2014). Urban planning and climate indicators: A casestudy for a north-south of Beijing, China. Build. Environ.2015, 46, 1174–1183.

Zhou; Wang, J.; Cadenasso, M.L (2017). Effects of the spatial configuration of trees on urban heat mitigation: A comparative study. Remote Sens. Environ.2017, 195, 3.043.

APPENDICES

Appendix 1:

A). Monthly, maximum, minimum and mean temperature of Dire Dawa City from Meteorological station from 1999 and 2019.

1999												
Month	**Jan.**	**Feb.**	**Mar.**	**Apr.**	**May**	**Jun**	**Jul.**	**Aug.**	**Sep.**	**Oct.**	**Nov.**	**Dec.**
Min	14.5	15.9	18.5	18.9	19.3	22.4	20.4	20.2	21.1	18.5	15.1	13.8
Max	28.7	29.3	30.2	31.1	32.8	33.4	33.2	32.5	31.8	29.4	28.7	27.9
Av. Temp.	21.6	22.6	24.3	26	26.1	27.9	26.8	26.3	26.4	23.9	21.9	20.8
2019												
Month 's	**Jan.**	**Feb.**	**Mar**	**Apr.**	**May**	**Jun**	**Jul.**	**Aug.**	**Sep.**	**Oct.**	**Nov.**	**Dec.**
Min.	15.4	16.5	19.3	20	22.2	22.4	21.6	20.1	20.5	19.5	15.7	15
Max	29.6	30.9	32.9	32.7	33.1	33.9	33.8	33.8	31.9	30.7	29.6	27.9
Av. Temp.	22.5	23.2	24.6	26.3	27.65	28.2	27.2	26.9	26.2	25.1	22.6	21.4

[Source: (NMA, 2019)]

- ***Average Monthly Rainfall of Dire Dawa City Administration***

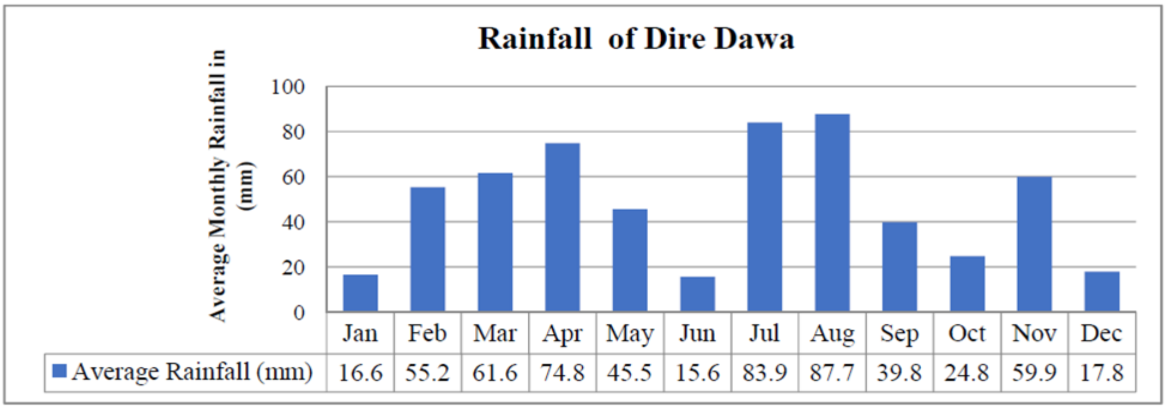

[Source: (NMA, 2019)]

B). Sample Locations of exposure and sensitive areas within Dire Dawa City

LULC	Sample Location	X	Y	LST(°C) 1999	LST(°C) 2019	Temperature (°C)
Settlement	Industrial Condominium	1064259.97	807939.28	26.38	33.89	33.9 ± 4.13
	Ture Cement Factory	1063103.85	805712.31	30.94	32.06	34.4 ± 2.51
	Cotton-Factory	1062837.15	816463.7	28.67	33.89	35.8 ± 2.56
	Sabean Area	1062780.98	811727.23	29.43	31.43	33.6 ± 2.07
	Ethio-Djibouti Rail Round	1061929.14	814108.85	24.96	27.76	29.3 ± 2.17
	Taiwan Market	1061910.37	814098.34	30.64	34.82	36.7 ± 2.57
	DDU	1064495.81	811757.41	30.64	25.82	27.7 ± 2.57
Green Infrastructure (GI)	Toni-Agriculture	1064098.92	811519.29	24.97	22.94	25.2 ± 2.41
	Millennium Park	1062712.08	813974.18	29.84	24.65	24.9 ± 1.75
	Gendegara Shrub land	1061371.93	816260.38	19.91	23.17	24.1 ± 1.29
Bare Land	Bare land	1066671.27	810268.34	33.01	36.69	39.3 ± 3.46
	Bare Land / Outskirt	1061865.03	811765.97	32.33	35.39	37.8 ± 2.26
	Dry-river	1065947.38	807207.91	30.81	34.35	36.71 ± 2.29
	Dry-River	1064456.42	814592.79	31.66	34.35	36.2 ± 2.29

C). Extent and Spatial Distribution of Existing Hot Spot Areas of 2019

FID	Name	X	Y	Z	Area (ha)
1	HS11_Industrial Condominium Area	1064259.978	807939.2029	1141	78.640652
2	HS9_Ture Cement Factory	1063103.895	805712.3132	1158	78.637994
3	HS8_Taiwan Market	1061891.297	814146.7588	1211	78.648166
4	HS10_Coca Factory	1061031.728	814135.2402	1231	78.648152
5	HS7_Abattoir	1063133.619	811313.2867	1176	78.644717
6	HS6_Sabean Area	1062780.928	811727.0842	1183	78.645219
7	HS4_Outskirt	1061865.004	811765.9717	1192	78.645266
8	HS3_Cotton Factory	1062837.154	816463.7074	1124	78.651008

9	HS1_Bare Land	1066671.274	810268.0982	1283	78.643453
10	HS2_Dry River	1065947.391	807207.9181	1127	78.639777
11	HS5_Dry River	1065981.463	813750.4012	1131	78.647681
12	HS12_Bare Land	1066933.965	805474.2174	1135	78.63771

[Sample location of Existing Hot Spot Areas collected from field,2020]

Appendix 2

A). Classification Accuracy Assessment Report for the Year 1999.

```
CLASSIFICATION ACCURACY ASSESSMENT REPORT
                ----------------------------------------
Image File : d:/2019-image/lulc-1919.img
User Name  : Amanuel Atnafu
Date       :Tue March 31 11:32:02 2020

ERROR MATRIX
-------------

ACCURACY TOTALS
----------------

          Class  Reference      Classified      Number  Producers       Users
           Name     Totals          Totals     Correct   Accuracy       Accuracy
     ---------- ----------      ----------     ------- ----------       -----
     Settlement          10             10           9     90.00%       90.00%
     Bare Land           11             11          10     90.90%       90.90%
     Dry Revers          8              8            7     87.50%       87.50%
     Shrub Land          10             11           9     90.00%       81.82%
     Sparse Vegetati     11             10           9     81.82%       90.00%

         Totals          50             50          44

Overall Classification Accuracy =      88.00%

                ----- End of Accuracy Totals -----

KAPPA (K^) STATISTICS
---------------------

Overall Kappa Statistics = 0.8575%

Conditional Kappa for each Category.
------------------------------------

         Class Name                Kappa
         ----------                -----
       Unclassified              0.0000
         Settlement              0.8879
                                 0.0000
          Bare Land              0.8801
         Dry Revers              0.8558
         Shrub Land              0.8776
                                 0.0000
  Sparse Vegetation              0.8783

                ----- End of Kappa Statistics -----
```

B). Classification Accuracy Assessment Report for the Year 2019

CLASSIFICATION ACCURACY ASSESSMENT REPORT

Image File : d:/2019-image/lulc-2019.img
User Name : Amanuel Atnafu
Date : Fri April 03 01:31:03 2020

ERROR MATRIX

ACCURACY TOTALS

Class Name	Reference Totals	Classified Totals	Number Correct	Producers Accuracy	Users Accuracy
Settlement	14	15	14	100.00%	93.33%
Bare Land	9	8	7	77.78%	87.50%
Dry Revers	4	4	4	100.00%	100.00%
Shrub Land	10	11	9	90.00%	81.81%
Sparse Vegetation	13	12	11	84.62%	91.67%
Totals	50	50	45		

Overall Classification Accuracy = 90.00%

----- End of Accuracy Totals -----

KAPPA (K^) STATISTICS

Overall Kappa Statistics = 0.8897%

Conditional Kappa for each Category.

Class Name	Kappa
Unclassified	0.0000
Settlement	0.8879
	0.0000
Bare Land	0.8901
Dry Revers	1.0000
Shrub Land	0.8558
	0.0000
Sparse Vegetation	0.8783

----- End of Kappa Statistics -----

Appendix 3:

A). the number of pixel in different land surface temperature of 1999 and 2019

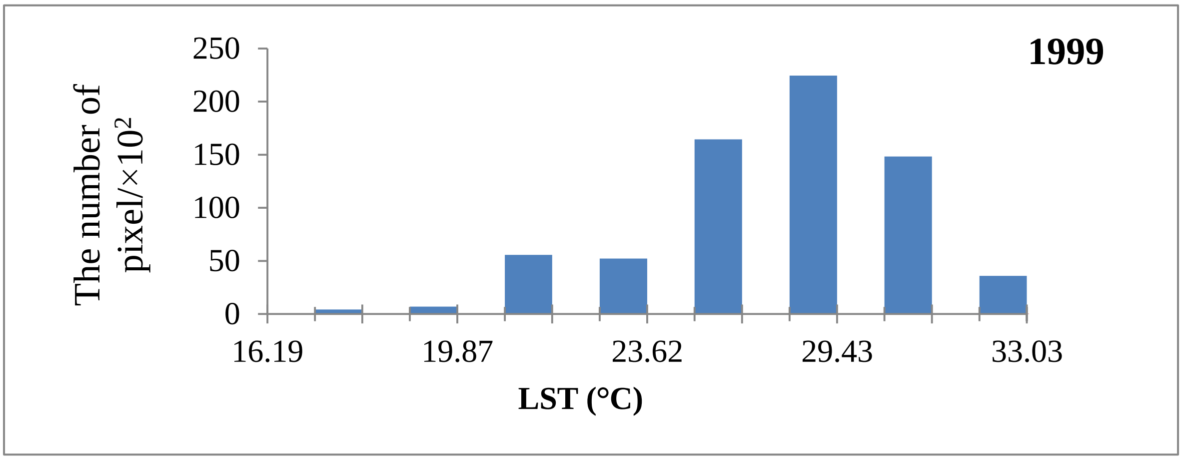

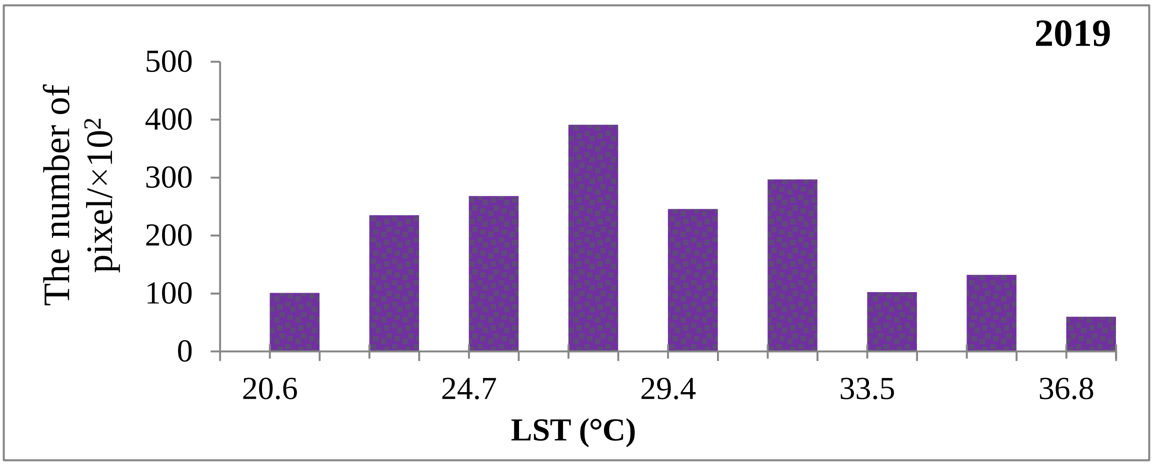

B). LST Classification by Standard deviation method 2019

No.	Zones	Class Rang	LST (°C)
1	Low/Cold spot	T <= Tmean - 1.5 STD	<=26.2
2	Medium	Tmean - 1.5 STD <T <= Tmean – STD	26.2_30.2
3	High	Tmean - STD < T <= Tmean + 1.5 STD	30.2_32.5
4	Higher/ Hotspot	Tmean + STD < T <= Tmean + 1.5 STD	>=32.5

Appendix 4:

A) Spatial Distribution of Existing Hot Spot Areas of 2019

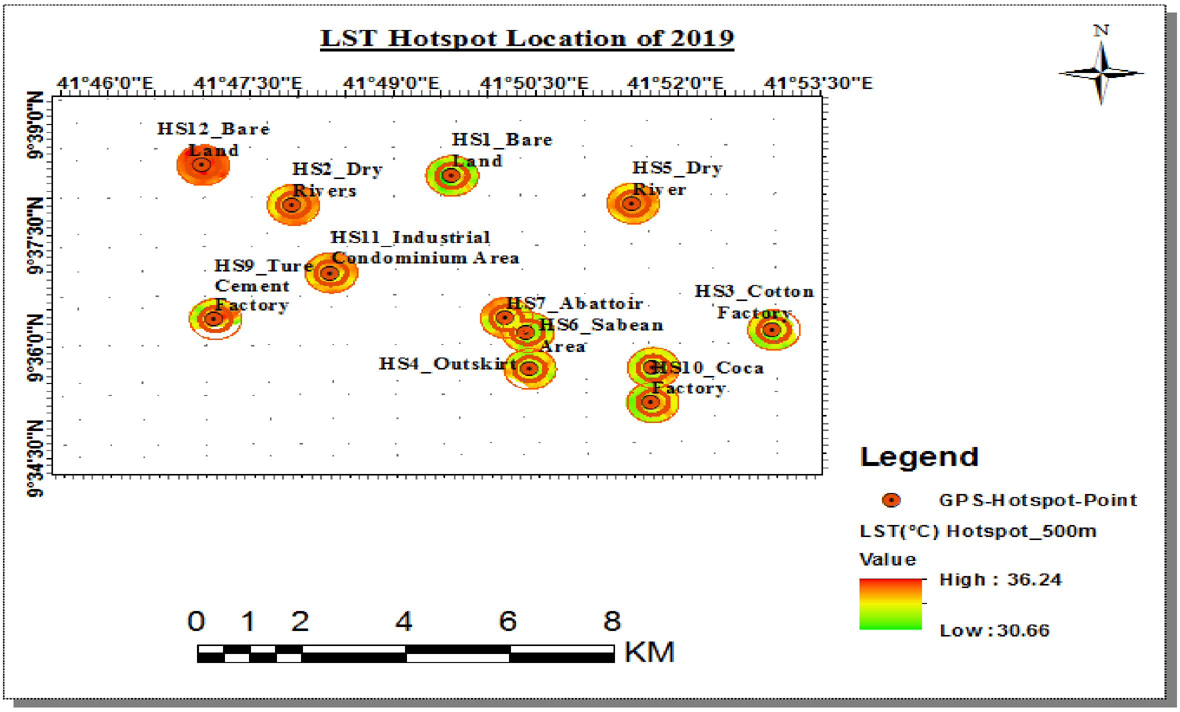

B). Spatial Autocorrelation Report

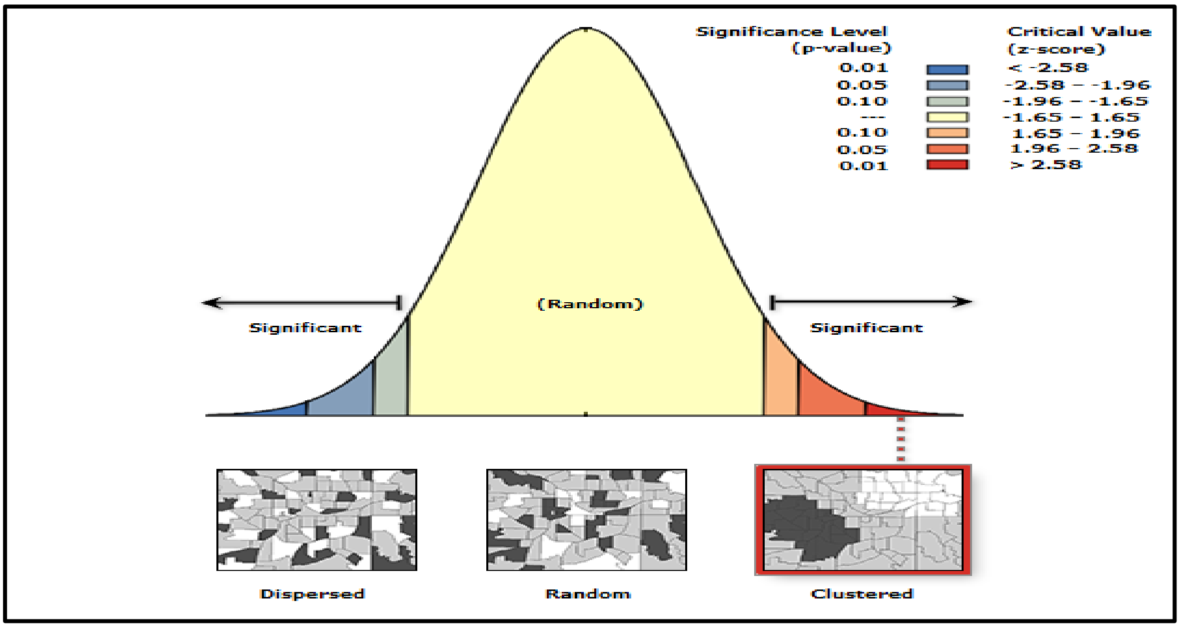

Table : Spatial Autocorrelation Moran's I Result of LST

Year	Moran's Index(I)	z-score	p-value
MAY, 1999	0.611705	225.6	0.0000
MAY, 2019	0.7261171	275.51	0.0000

Appendix 5:

A). List of identified indicators and their relationship with study by vulnerability components in Ethiopia

Components	Indicators		Layers in Sullivan Definition	Data Source
Sensitivity Layers	LULC Change	Vegetation cover	Environment	Extracted from Landsat
		Impervious surface	Environment	Extracted from Landsat
		Population density	Environment	CSA
Exposure Layers	Temperature Change	Mean air temperature change	Geospatial	NMA
		Mean LST Change	Geospatial	Extracted from Landsat

[Adopted from, Nyoni., (2017)]

A. Land surface temperature change from the year 1999 to 2019 of study area

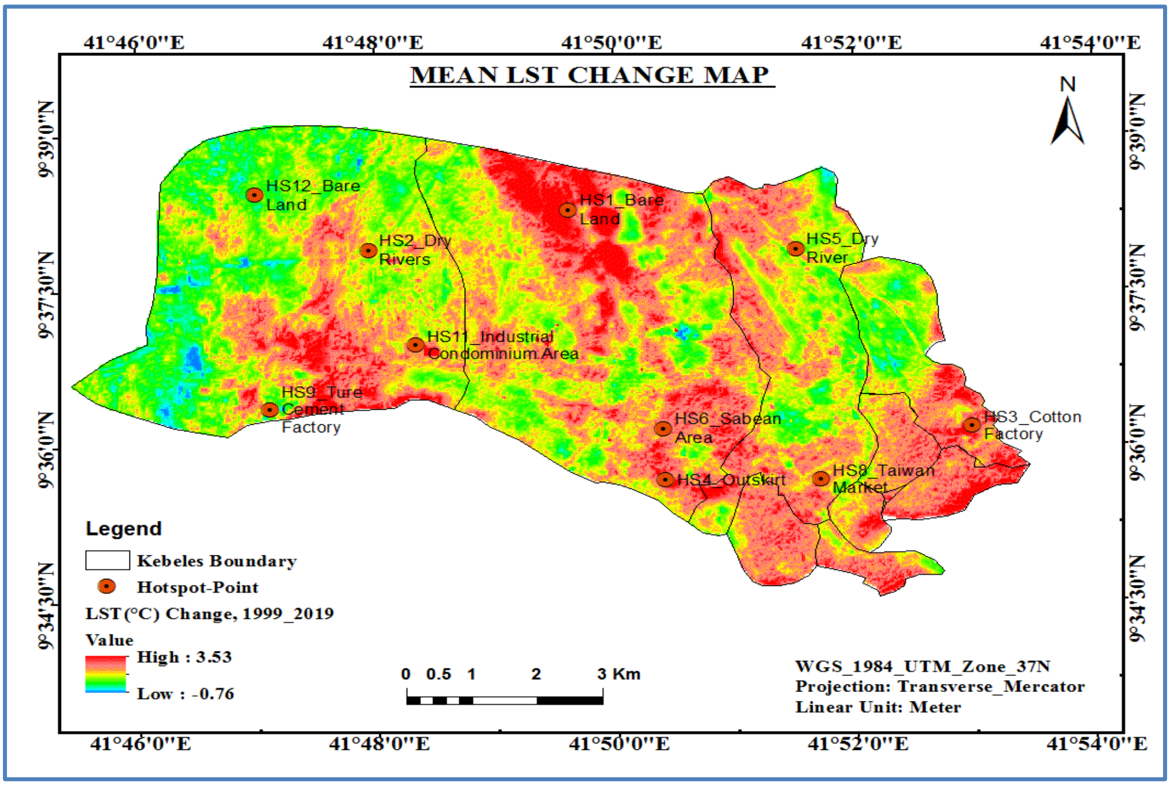

B. The trend of expansion of settlement area from the year 1999 to 2019 of study area